



TECHNISCHE
UNIVERSITÄT
WIEN
Vienna University of Technology

DISSERTATION

Characterization of extracellular carbohydrate-binding proteins unique in fungi

ausgeführt zum Zwecke der Erlangung des akademischen Grades

Doktor der Technischen Chemie

unter der Leitung von
Univ.Prof. Dipl.-Ing. Dr.techn. Christian P. Kubicek
und der Betreuung durch
Dipl.-Ing. Dr.techn. Verena Seidl-Seiboth

am

Institut für Verfahrenstechnik, Umwelttechnik und Technische Biowissenschaften
Abteilung Gentechnik und Angewandte Biochemie (E166-5)

Eingereicht an der Technischen Universität Wien
Fakultät für Technische Chemie
von

Dipl.-Ing. Simone Zach

Matrikelnummer 0030077
Kutschkergasse 29, 1180 Wien

Wien, am 11. Juni 2012

.....

Dipl.-Ing. Simone Zach

Kurzfassung der Dissertation

Der filamentöse Bodenzpilz *Trichoderma atroviride* wird in der Landwirtschaft als biologisches Pflanzenschutzmittel gegen pflanzenpathogene Pilze verwendet.

Mykoparasitismus- die Attacke und das Töten von anderen Pilzen- ist einer der Mechanismen, der für die schützenden Eigenschaften von *T. atroviride* gegenüber Pflanzen verantwortlich ist. Dabei profitiert *T. atroviride* von einer mächtigen enzymatischen Maschinerie bestehend aus Zellwand abbauenden Enzymen, einschließlich Chitinasen und Glukanasen, die in mykoparasitische Aktivitäten als auch in Prozesse zur Neugestaltung der Zellwand involviert sind.

Die Chitinasen von Pilzen können in drei Untergruppen (A, B und C) eingeteilt werden. Chitinasen der Untergruppe C besitzen zwei verschiedene Typen von Kohlehydrat-Bindungsdomänen (carbohydrate-binding modules; CBMs)- CBM18 und CBM50 (LysM Motive)- die nicht in vielen anderen Enzymen von Pilzen vorkommen.

In dieser Arbeit lag der Fokus auf TAL6, einem Protein das aus 6 LysM Motiven besteht, jedoch keine katalytische Proteindomäne besitzt. Um die Funktionen dieses Proteins zu untersuchen wurden eine vollständige Version des Proteins, bestehend aus allen 6 LysM Motiven (TAL6₆) als auch eine verkürzte Version von TAL6 (TAL6₄), nur bestehend aus den vier stark konservierten LysM Motiven der C-terminalen Region von TAL6 charakterisiert. Untersuchungen der Fähigkeit dieser Proteine an Kohlenhydrate zu binden wurden sowohl mit verschiedenen Kohlenhydrat-Polymeren, als auch mit chitin-hältigen Zellwänden von *Trichoderma*-Arten und der pflanzenpathogenen *Rhizoctonia solani* und *Botrytis cinerea* durchgeführt. Es zeigte sich eine Affinität der Proteine für hochprozessierte Formen von Chitin, jedoch konnte keine Bindung an die Zellwände der Pflanzenpathogenen festgestellt werden. Weiters wurde der Einfluß von TAL6₆ and TAL6₄ auf die Sporenkeimung von *T. atroviride* und nahe verwandten Gattungen als auch von *Aspergillus niger* und *Neurospora crassa* untersucht. Dabei wurde ein stark inhibierender Effekt von TAL6₆ auf die Sporenkeimung von *Trichoderma*-Arten beobachtet. Dieser Effekt konnte jedoch nicht bei TAL6₄ beobachtet werden, was darauf hinweist, dass die zwei N-terminalen LysM Motive von TAL6₆, die mit bisher bekannten LysM Motiven eher weitläufig verwandt sind, essentiell für die Funktion von TAL6 sind. Die beobachtete Inhibierung der Keimung war auf die Gattung *Trichoderma* begrenzt. Diese Ergebnisse zeigten klar, dass TAL6 eine biologische Funktion besitzt, die nicht mit dem Mykoparasitismus verbunden ist, sondern eher auf einen selbst-regulierenden Effekt während der Sporenkeimung hinweist.

Kürzlich durchgeführte Analysen des Genoms von *T. atroviride* zeigten, dass dieser Pilz nicht nur Chitin-abbauende Enzyme besitzt, sondern auch ein Arsenal an verschiedenen Cysteinreichen Proteinen, die möglicherweise an der Protektion der eigenen Pilz-Zellwand gegenüber hydrolytischen Enzymen beteiligt sind. Zusätzlich wurde gezeigt, dass einige *Trichoderma* spp. fähig sind Abwehrreaktionen in der Pflanze zu induzieren und das Pflanzenwachstum zu fördern. Eine Vielzahl an verschiedenen Proteinen, die diese Effekte verursachen, wurden bereits für solche Systeme beschrieben, dazu gehören Cerato-Platanin Proteine (CPPs) und Hydrophobine, aber auch Enzyme wie z.B. Xylanasen und Polygalakturonasen. Das EPL1 Protein von *T. atroviride* gehört zu der Cerato-Platanin Proteinfamilie, deren Mitglieder viele verschiedene Funktionen wie Zellwandummantelung und Zellwandprotektion aufweisen und von denen gezeigt wurde, dass sie als Auslöser für Abwehrreaktionen in Pflanzen agieren. Untersuchungen der Fähigkeit von EPL1 an Kohlenhydrate zu binden zeigten, dass EPL1 an flockiges Chitin in unterschiedlicher Größe und an kolloidales Chitin binden kann, jedoch zeigte sich keine Bindeaffinität für Chitin Beads oder für die Zellwände von *T. atroviride*.

In dieser Arbeit wurden erste Schritte zur Aufklärung der Funktion verschiedener Chitinbindender Proteine gemacht. Darüber hinaus wird ein besseres Verständnis der Interaktionen und Mechanismen während des Wachstums und der Entwicklung der Spezies *Trichoderma* als auch deren Interaktion mit anderen Organismen hilfreich für die Entwicklung verbesserter Rezepturen von Pflanzenschutzmittel sein. Die gewonnenen Erkenntnisse sind wichtig in Bezug auf den existierenden Bedarf an ökologischeren Lösungen im Pflanzenschutz um einen umweltfreundlicheren Nutzen unserer natürlichen Ressourcen in Zukunft zu gewährleisten.

Summary of the thesis

The filamentous soil fungus *Trichoderma atroviride* is applied in agriculture as a biocontrol agent (biological pesticide) against plant pathogenic fungi. Mycoparasitism – the attack and killing of other fungi – is one of the mechanisms that are responsible for the plant protection properties of *T. atroviride*. Thereby, *T. atroviride* benefits from a potent enzymatic machinery of cell wall degrading enzymes including chitinases and glucanases, which are involved in the events during mycoparasitism as well as in cell wall remodeling processes.

Fungal chitinases can be divided into three different subgroups, based on differences in their amino acid sequences and structural compositions.

Chitinases of subgroup C have two different types of carbohydrate-binding modules (CBMs) - CBM18 and CBM50 (LysM motifs) - that are not found in many other fungal enzymes. This thesis was focused on TAL6, a protein that contains 6 LysM motifs but no catalytic module. In order to be able to investigate the functions of this protein a full-length version of TAL6 containing all six LysM motifs (TAL6₆) and a truncated version of TAL6 (TAL6₄) that consists only of the four strongly conserved LysM motifs from the C-terminal region of TAL6 were characterized. Carbohydrate-binding assays using different carbon sources as well as cell walls of plant pathogenic *Rhizoctonia solani* and *Botrytis cinerea* were conducted and revealed an affinity of TAL6 for chitin beads and colloidal chitin, but no binding behavior toward the cell walls of the plant pathogens could be observed.

Further the effects of TAL6₆ and TAL6₄ on spore germination of *T. atroviride* and close relatives, as well as of *Aspergillus niger* and *Neurospora crassa* were examined. A strong inhibitory effect for TAL6₆ but not for TAL6₄ on *Trichoderma* spp. but not on other tested fungi was observed. This suggests that the two N-terminal LysM motifs of TAL6₆, which are rather distantly related to so far characterized LysMs, are essential for the function of TAL6. These results showed clearly that TAL6 has a biological function which is not connected to mycoparasitism but is rather directed toward a self-regulatory effect during spore germination.

Recent analysis of the genome of *T. atroviride* showed that this fungus has not only chitin-degrading enzymes but also an arsenal of different cysteine-rich proteins that possibly participate in protection of the own fungal cell wall against hydrolytic enzymes. In addition it was shown that several *Trichoderma* spp. are able to induce plant defense responses and enhance plant growth. A number of different elicitor proteins have already been described for

these systems, ranging from cerato-platanin proteins (CPPs) and hydrophobins to xylanases and polygalacturonases.

The protein EPL1 from *T. atroviride* belongs to the cerato-platanin protein family, of which members display various different functions like cell wall coating and protection and have been demonstrated to act as elicitors of plant defense responses. Carbohydrate-binding analysis revealed that EPL1 is able to bind to flaked chitin in different sizes and to colloidal chitin but exhibited no binding affinity to chitin beads or to cell walls of *T. atroviride*.

In this thesis first steps were made to elucidate the function of different types of chitin-binding proteins. Further, a better understanding of the interactions and mechanisms of the growth and development of *Trichoderma* spp. and its interaction with other organisms will aid in developing improved formulations for biocontrol agents. This will be important toward the existing demand for more ecological solutions with respect to crop protection to achieve a more environmentally friendly use of our natural resources in the future.

Contents

KURZFASSUNG DER DISSERTATION	I
SUMMARY OF THE THESIS	III
CONTENTS	V
1. INTRODUCTION	1
1.1 THE GENUS <i>HYPOCREA</i> / <i>TRICHODERMA</i>	1
1.1.1 THE <i>TRICHODERMA</i> CHRONOLOGY- FROM PAST TILL PRESENT	1
1.1.2 <i>TRICHODERMA ATROVIRIDE</i>	3
1.2 CROP PROTECTION- BIOLOGICAL CONTROL	4
1.2.1 BIOCONTROL OF <i>TRICHODERMA</i>	7
1.3 THE LYTIC ENZYME MACHINERY OF <i>TRICHODERMA</i>	9
1.3.1 ENZYMES INVOLVED IN CELL WALL DEGRADATION AND REMODELING	10
1.3.1.1 GLUCANASES	10
1.3.1.2 PROTEASES	11
1.3.1.3 CHITIN-DEGRADING ENZYMES	11
1.3.2 CLASSIFICATION OF FUNGAL CHITINASES INTO SUBGROUPS	13
1.4 CARBOHYDRATE-BINDING MODULES (CBMS)	14
1.5 LYSIN MOTIF (LYSM)	15
1.6 EPLs (ELICITING PLANT RESPONSE-LIKE PROTEINS) IN <i>T. ATROVIRIDE</i>	17
2. AIMS OF THIS THESIS	19
3. MATERIALS AND METHODS	20
3.1 INSTRUMENTS, CHEMICALS AND DEVICES	20
3.2 ENZYMES	24
3.3 STRAINS, CULTIVATION CONDITIONS IN APPROPRIATE MEDIA	25
3.3.1 <i>ESCHERICHIA COLI</i> STRAINS	25
3.3.1.1 CULTIVATION OF <i>E. COLI</i> STRAINS	26
3.3.1.2 <i>E. COLI</i> TRANSFORMATION PROTOCOLS	27
3.3.1.2.1 <i>E. COLI</i> TRANSFORMATION USING CHEMICAL COMPETENT CELLS	27
3.3.1.2.2 <i>E. COLI</i> TRANSFORMATION USING ONE SHOT TOP10 CHEMICAL COMPETENT CELLS	27
3.3.1.3 DNA EXTRACTION FROM <i>E. COLI</i>	27
3.3.2 <i>PICHIA PASTORIS</i> STRAINS	29
3.3.2.1 CULTIVATION OF <i>P. PASTORIS</i> STRAINS	29
3.3.2.1.1 SHAKE FLASK CULTURE OF <i>P. PASTORIS</i>	30
3.3.2.1.2 FREEZING MEDIUM	31
3.3.2.3 COLONY PCR	31
3.3.2.4 TRANSCRIPT ANALYSIS	32
3.3.3 FUNGAL STRAINS	33
3.3.3.1 CULTIVATION OF FUNGAL STRAINS	33
3.3.3.1.1 SHAKE FLASK CULTURES OF <i>T. REESEI</i>	33
3.3.3.2 TRANSFORMATION OF <i>TRICHODERMA</i> SPP.	33

3.3.3.2.1 PROTOPLASTING	33
3.3.3.2.2 TRANSFORMATION	34
3.3.3.2.3 SINGE SPORE ISOLATION	37
3.3.3.3 FUNGAL DNA ISOLATION	37
3.4 PLASMIDS AND DELETION CASSETTES	38
3.4.1 CONSTRUCTION OF THE PLASMIDS	39
3.4.1.1 CONSTRUCTION OF THE PLASMID pTAL6 ₆	39
3.4.1.2 CONSTRUCTION OF THE PLASMID pTAL6 ₄	40
3.4.1.3 CONSTRUCTION OF THE PLASMID pTAL6 ₆ Tr	41
3.4.2 PCR DETAILS TO THE SECTION 3.4.1	43
3.4.3 DELETION CASSETTES FOR GENERATION OF <i>EPL1</i> AND <i>EPL2</i> KNOCKOUT STRAINS IN <i>T. ATROVIRIDE</i> .	44
3.4.3.1 CONSTRUCTION OF THE <i>EPL1</i> DELETION CASSETTE	44
3.4.3.1.1 PCR DETAILS TO SECTION 3.4.3.1	47
3.4.3.1.2 VERIFICATION OF <i>EPL1</i> -KNOCKOUT STRAINS IN <i>T. ATROVIRIDE</i>	48
3.4.3.2 CONSTRUCTION OF THE <i>EPL2</i> DELETION CASSETTE	49
3.4.3.2.1 PCR DETAILS TO SECTION 3.4.3.2	51
3.4.3.2.2 <i>EPL2</i> -KNOCKOUT VERIFICATION	52
3.5 FERMENTATION SETUP OF <i>P. PASTORIS</i> TAL6 ₆ AND TAL6 ₄ -EXPRESSION STRAINS	53
3.6 PROTEIN PURIFICATION OF RECOMBINANT TAL6 ₆ AND TAL6 ₄	53
3.7 PROTEIN EXTRACTION FROM THE BIOMASS	55
3.8 SDS- PAGE	55
3.8.1 CHLOROFORM/ METHANOL PRECIPITATION OF PROTEINS	55
3.9 WESTERN BLOTTING	57
3.10 PROTEIN-BINDING ASSAYS WITH INSOLUBLE CARBON SOURCES	59
3.10.1 PREPARATION OF SPECIAL CARBON SOURCES	60
3.10.1.1 PREPARATION OF COLLOIDAL CHITIN	60
3.10.1.2. PREPARATION OF FUNGAL CELL WALLS	60
3.10.1.3 ALKALINE TREATMENT OF <i>T. ATROVIRIDE</i> CELL WALLS (CW)	60
3.11 EFFECT OF TAL6 ₆ AND TAL6 ₄ ON THE SPORE GERMINATION	61
3.12 PROTEIN DEGLYCOSYLATION ASSAY	62
 4. RESULTS	 63
4.1 CHARACTERIZATION OF LYSM PROTEINS IN <i>TRICHODERMA ATROVIRIDE</i>	63
4.1.1 GENOMIC ORGANIZATION OF LYSM PROTEINS	63
4.1.2 CHARACTERISTICS OF THE OVEREXPRESSION CONSTRUCTS OF TAL6 ₆ AND TAL6 ₄	69
4.2 OVEREXPRESSION OF TAL6 ₆ AND TAL6 ₄	71
4.2.1 OVEREXPRESSION IN <i>PICHTIA PASTORIS</i>	71
4.2.2 OVEREXPRESSION OF TAL6 ₆ IN <i>TRICHODERMA REESEI</i>	75
4.3 FERMENTATION OF TAL6 ₆ AND TAL6 ₄	76
4.4 LARGE SCALE PURIFICATION OF TAL6 ₆ AND TAL6 ₄	78
4.5 CHARACTERISTICS OF TAL6 ₆ AND TAL6 ₄ ACCORDING TO N- GLYCOSYLATION AND 2D-GEL ANALYSIS	81
4.5.1 N-GLYCOSYLATION	81
4.5.1.1 N-GLYCOSYLATION PREDICTION RESULTS FOR TAL6 ₄	81
4.5.2 DEGLYCOSYLATION OF TAL6 ₆ AND TAL6 ₄	83
4.5.3 2D- GEL ELECTROPHORESIS OF TAL6 ₆ AND TAL6 ₄	83
4.6 CARBOHYDRATE-BINDING ASSAYS	85
4.6.1 CARBOHYDRATE-BINDING RESULTS FOR TAL6 ₆	86
4.6.2 CARBOHYDRATE-BINDING RESULTS FOR TAL6 ₄	91
4.7 EFFECT ON SPORE GERMINATION OF TAL6 ₆ AND TAL6 ₄	95

4.8 EPL PROTEINS OF <i>T. ATROVIRIDE</i>	105
4.8.1 OVERVIEW OF EPL PROTEINS OF <i>T. ATROVIRIDE</i> AND OTHER MEMBERS OF THE CERATO- PLATANIN FAMILY	105
4.8.2 CHARACTERIZATION OF EPL PROTEINS OF <i>T. ATROVIRIDE</i>	106
4.8.3 CONSTRUCTION OF THE <i>EPL</i> DELETION CASSETTES	108
4.8.3.1 CONSTRUCTION OF THE <i>EPL1</i> DELETION CASSETTE	108
4.8.3.2 CONSTRUCTION OF THE <i>EPL2</i> DELETION CASSETTE	110
4.8.4 BINDING ASSAY OF <i>EPL1</i>	111
 5. DISCUSSION	 113
5.1 LYSM DOMAINS IN EUKARYOTES AND PROKARYOTES	113
5.2 TAL ₆ AND TAL ₄ - LYSM DOMAINS OF <i>TRICHODERMA ATROVIRIDE</i>	114
5.2.1 PROTEIN ARCHITECTURE OF TAL ₆ AND TAL ₄	114
5.2.2 HETEROLOGOUS PROTEIN EXPRESSION IN <i>PICHIA PASTORIS</i>	114
5.2.3 PROTEIN CHARACTERISTICS OF TAL ₆ AND TAL ₄	115
5.2.4 CARBOHYDRATE-BINDING PROPERTIES OF TAL ₆ AND TAL ₄	117
5.2.5 EFFECT OF TAL ₄ AND TAL ₆ ON SPORE GERMINATION IN DIFFERENT FUNGI	119
5.2.6 CARBOHYDRATE-BINDING ANALYSIS OF <i>EPL1</i> (ELICITING PLANT RESPONSE-LIKE PROTEIN)	122
5.3 CONCLUDING REMARKS	125
 6. APPENDIX	 127
6.1 SEQUENCES	127
6.1.1 SEQUENCES OF TAC ₆ , PROT ID: 348129 , 174,8 kDA	127
6.1.1.1 CDNA SEQUENCE OF TAC ₆ (JGI HOMEPAGE)	127
6.1.1.2 PROTEIN SEQUENCE OF TAC ₆	128
6.1.2 SEQUENCES OF TAL ₆ PROT ID: 297859, 78kDA	129
6.1.2.1 CDNA SEQUENCE OF TAL ₆ (JGI HOMEPAGE)	129
6.1.2.2 PROTEIN SEQUENCE OF TAL ₆	129
6.1.3 SEQUENCES OF TAL ₆ , 77.7 kDA	130
6.1.3.1 CDNA SEQUENCE OF THE TAL ₆ INCLUDING THE HIS-TAG	130
6.1.3.2 PROTEIN SEQUENCE OF THE SECRETED TAL ₆ INCLUDING THE HIS-TAG	130
6.1.4 SEQUENCES OF TAL ₄ , 36.2 kDA	131
6.1.4.1 CDNA SEQUENCE OF TAL ₄ , INCLUDING THE HIS-TAG	131
6.1.4.2 PROTEIN SEQUENCE OF THE SECRETED TAL ₄ INCLUDING THE HIS-TAG	131
 7. REFERENCES	 132
 CURRICULUM VITAE	 141
 DANKSAGUNG	 144

1. Introduction

1.1 The genus *Hypocrea*/*Trichoderma*

1.1.1 *The Trichoderma chronology- from past till present*

Trichoderma was first recognized by Persoon in 1794 [1], during the investigation of material collected from Germany. Almost 200 years passed from the initial discovery of the fungal genus *Trichoderma* until its identification and taxonomic classification. Mis- and re-identifications of several strains were responsible for the slow progress in the exploration of *Trichoderma*. Much of this confusion can be attributed to Bisby's 1939 [2] taxonomical system, in which all strains were referred to as a single species, *Trichoderma viride*. In addition, the designation *Trichoderma harzianum*, which had been used for many different species [3], caused additional confusion. A breakthrough occurred in 1969, when Rifai, under the supervision of John Webster, published his thesis: 'A revision of the genus *Trichoderma*' [4]. In his work he described nine different 'aggregate' species, with the reservation that some might comprise two or more morphologically indistinguishable species, thereby excluding *Gliocladium virens*. The findings of Rifai, Bissett and coworkers [5] revealed four sections of the fungi, with two monographed out of the nine aggregate species. Additionally Rifai classified five subdivisions of the genus *Trichoderma*: *Trichoderma*, *Pachybasium*, *Longibrachiatum*, *Sarturnisporum* and *Hypochreanum*. At that time, taxonomy of *Trichoderma*/*Hypocrea* was rather difficult, as the identification of the species was based mainly on morphological differences. Advances in DNA based phylogenetic analysis in the past few decades enabled the reassessment of the genus *Trichoderma*. Applying these new, groundbreaking techniques revealed several aspects of the genus *Trichoderma* and its subdivision that could previously not be resolved based on morphological characterizations. Thus, it was not astonishing that *G. virens* was confirmed to be a *Trichoderma* species [6], and it was further highlighted that *Trichoderma* is phylogenetically indistinguishable from the sexual form *Hypocrea*. The relationship between *Trichoderma* and its teleomorph *Hypocrea* was already suggested in 1865 by Tulasne [7]. The DNA-based phylogenetic analysis of *Trichoderma* species was in the last decade further developed into online identification tools designed by Christian P. Kubicek and Irina Druzhinina, namely a DNA barcoding system (TrichoKEY) and a customized similarity search tool (TrichhoBLAST), offered by the website www.isth.info. This contributed to a high resolution of taxonomic entities within the

genus *Trichoderma* [8]. Based on several sequence hallmarks, including the internal transcribed spacers (ITS1 and ITS2) of rRNA gene clusters, the translation-elongation factor (EF-1 α), as well as the D1 and D2 region of 28S rDNA, the small subunit of the mitochondrial rDNA, and a fragment of *ech42*, it was possible to elucidate the biodiversity of *Trichoderma* in great detail [8].

Modern DNA sequencing technologies and automated gene prediction, annotation and analysis tools (Fgenesh, Fgenesh+ and Genewise programs) are used nowadays to analyze the complete genomes of organisms. Several fully annotated *Trichoderma* genome sequences are already available on the website of the Joint Genome Institute (JGI) of the US Department of energy. The first *Trichoderma* species that was sequenced was *Trichoderma reesei* [9], followed by the genomes of the two mycoparasites *Trichoderma atroviride* IMI206040 and *Trichoderma virens* Gv29-8. The genome size of *T. atroviride* IMI206040 was analyzed to be 36.1 Mbp and that of *T. virens* Gv29-8 38.8 Mbp, comprising 11865 gene models for *T. atroviride* and 12428 gene models for *T. virens* [10].

Currently, the list of known *Hypocrea/Trichoderma* species is composed of ~130 species (<http://www.isth.info/biodiversity/index.php>). There remains a considerable number of *Hypocrea* strains and, of course, *Trichoderma* strains that have been collected but still need to be fully identified [11].

Trichoderma spp. belonging to the *ascomycota* division are described in literature as the ecologically most widely distributed fungi. These organisms can be found in almost every latitude and habitat in climates ranging from the tundra to the tropics. *Trichoderma* spp. are in general green-spored and are able to colonize wood, herbaceous plant materials and other fungi by degrading their cell walls with hydrolytic enzymes. Further competition with other microorganisms for nutrients and living space as well as inhibition and degradation of enzymes that are essential for plant pathogenic fungi have been reported [12]. In addition, some *Trichoderma* spp. are capable of directly interacting with plants and inducing local and systemic resistance responses in plants [13].

When all of these traits are taken into account, *Trichoderma* spp. appear to be mostly beneficial to human ecology and several species, e.g. *T. virens*, *T. harzianum* and *T. atroviride*, *Trichoderma asperellum* and *T. hamatum* are known as biocontrol species applied in agricultural applications. Weindling was the first individual, who published a potential role for *Trichoderma* spp. in biological control almost 80 years ago [14]. *Trichoderma* spp. are of particular interest in both crop protection and industrial applications. For example *T. reesei* is

an important producer of cellulases, which are used in the production of second-generation biofuels from cellulosic plant waste material. Moreover, the applications of *Trichoderma* spp. in the fields of white and green biotechnology are becoming more important. In addition to these advantages of *Trichoderma* spp., some negative aspects have also been reported. *Trichoderma longibrachiatum* is capable of causing serious infections that sometimes lead to the death of immunocompromised or HIV-infected persons [15]. Strains of *Trichoderma pleurotum* and *Trichoderma pleuroticola* have been identified as pathogenic to the edible mushrooms *Pleurotus ostreatus* (oyster mushrooms) [16]. In the 1980s *Trichoderma* spp. were responsible for considerable crop loss by mushroom farms as they caused deleterious infections to the edible mushrooms [17]. The aggressive infection of edible mushrooms by these fungi became generally known as ‘green mold disease’ [18]. Thus, this highlights the variability of properties and life-styles that can be found within the genus *Trichoderma* ranging from beneficial to harmful species and underlines the importance to develop a still better understanding of the taxonomy and biology of the genus *Trichoderma*.

1.1.2 *Trichoderma atroviride*

T. atroviride was first described in 1892 by Karsten [19]. At this time *T. atroviride* was mistaken as *T. harzianum* in literature but was reintroduced and redescribed by Bisset [20] and Samuels [21], who recognized the difference between the two species. Several species have been renamed since the advent of DNA-based phylogenetic tools, including the strain P1 that is commonly used in research as a model organism for mycoparasitism and was also used in this thesis. In contrast to *T. harzianum*, when *T. atroviride* is cultivated at 25-30 °C on potato dextrose agar (PDA) it produces a specific coconut odor, that of the antifungal antibiotic 6-pentyl- α -pyrone [21]. In the nineties *T. atroviride* strains were discovered to be potent mycoparasites and play an important role in biological control, as it was then reported that *T. atroviride* antagonizes *Rhizoctonia solani* [22] when attacking field potatoes. Furthermore, the fungi also demonstrated protective activity toward wheat seeds when they are colonized by the plant pathogen *Fusarium culmorum* [23].

T. atroviride (teleomorph *Hypocrea atroviridis*) strains P1 (formerly *T. harzianum* ATCC 74058) and IMI206040, for which the genome is sequenced (JGI homepage: <http://genome.jgi-psf.org/Triat1/Triat1.home.html>) are commonly applied in the mycoparasitism research (see 1.2.1 Biocontrol of *Trichoderma*) [24].

1.2 Crop protection- Biological Control

The steadily growing world population and the accompanying increased need for food, feed and fuel has led to an increase in the demand for agricultural commodities [25]. In 2011, the production of wheat, maize, rice, soybeans, cotton and sunflowers increased in comparison to 2010 by approximately 4.2 %.

Limited acreage necessitates higher yields in crop production to meet the existing demand, which has increased the importance of the issue of crop protection (Fig. 1).

Crop Protection Market Performance 2011		
Year	Conventional Agrochemical Market (\$m)	Change from Previous Nominal
2005	31,190	1.5
2006	30,425	-2.5
2007	33,190	9.1
2008	40,475	21.2
2009	37,880	-6.4
2010	38,315	1.2
2011	45,210	18.0
Note Market value is at distribution level and Average Year exchange Rates		

Fig. 1: Crop protection market performance in 2011. Taken from www.phillipsmcdougall.com.

Based on an analysis from Phillips McDougall, the global crop protection market is estimated to have increased by 18.0 % to reach \$ 45,210 Mio in 2011.

Fulfilling the existing demand for crop protection is also an important field of financial interest and product development of the agricultural industry. Currently, crop protection is realized mainly by the application of pesticides. Pesticides are chemicals that are applied to protect plants against vermin, such as insects, fungi, bacteria and rodents. The sufficient production of good quality agricultural products at moderate costs is nowadays possible due to the application of pesticides [26].

In the 1940s *p,p'*-dichlorodiphenyltrichloroethane (DTT) was used as the active agent of chemical pesticides applied in agriculture for mosquito control and is still in use in certain third world countries [27]. More developed pesticides possess only a limited number of nervous system targets, which has resulted in widespread resistance among arthropod populations [25]. In addition, resistance has developed in other populations. Farm workers are facing serious diseases due to toxic pesticide exposure. The use of chemical fungicides on cropping farms has started to become the focus of public concern. The potential effects are of tremendous importance to human health and ecological systems. Considering the problematic situation, the focus on developing biological agents that can be successfully applied in

agriculture that function as so-called 'biological control' agents has become of utmost interest.

Biological control of plant pathogens was defined by Cook and Baker [28]: 'Biological control is the reduction of inoculum density or disease-producing activities of a pathogen or a parasite in its active or dormant state, by one or more organisms, accomplished naturally or through manipulation of the environment, host or antagonist, or by mass introduction of one or more antagonists.' In other words: 'Biological control is the reduction in the amount of inoculum or disease-producing activity of a pathogen accomplished by or through one or more organisms other than man.'

As mentioned by Hoitink as one of the first, antagonists play an important role in the implementation of biological control either directly or indirectly [29]. For indirect strategies the activity of indigenous microbial antagonists is boosted by the addition of organic amendments to the soil. This can be achieved by two mechanisms. One makes use of cross-protection, which involves the induction of resistance within the host plant against a particular pathogen. The other mechanism results in plant growth stimulation by root-colonizing bacteria [30, 31]. The direct approach includes the addition of the antagonist directly to the soil or plant material. Antagonists are described as naturally occurring, mostly soil microorganisms, which are able to interfere with the growth and/or survival of plant pathogens.

Different mechanisms are involved in biocontrol- early definitions and recent examples:

Antibiosis: Baker and Griffin [32] defined antibiosis as the inhibition or destruction of an organism due to the metabolic products of another. For example *T. atroviride* produces an antifungal compound, 6-pentyl pyrone, which is able to inhibit plant-pathogenic fungi [33].

Competition: Many plant pathogens require exogenous nutrients to successfully germinate, penetrate and infect host tissue [32]. For example strains of *Trichoderma* spp. are reported to control *Fusarium* spp. on wheat haulms and rice that may operate via competition for nutrients [34].

Mycoparasitism: An attack in which one fungus serves directly as the nutrient source for another [35]. In 1973 Barnett and Binder distinguished between two forms of mycoparasitism: the necrotrophic form, which is identified as destructive parasitism resulting in the death or

destruction of the host, and biotrophic parasitism, in which the living host supports the parasite [36]. Necrotrophic mycoparasitism is characterized by an aggressive approach where hyphal interaction is defined by the parasite growing along the host hyphae, thereby aiding in penetration of the host hyphal cell wall. This is supported by the release of hyphal cell wall-degrading enzymes or exotoxins. In a biotrophic mycoparasitic relationship, the living host supports the growth of the parasite, with the mycoparasites obtaining their nutrients directly from the living mycelium of the host [35]. *Trichoderma* spp. are necrotrophic mycoparasites.

Biological control has become important and will become even more so in the crop protection industry and its fight against soil-borne and foliar plant pathogenic fungi and oomycetes, e.g. *Rhizoctonia*, *Botrytis*, *Phytophthora*, *Phytium*, *Sclerotinia* and *Fusarium*.

Leading companies are attempting to produce crop protection products that are not harmful for the environments but remain effective against plant pathogens. Very early it was reported that companies started to employ different approaches, for example the combination of conventional pesticides and biological control agents in fields [37] and later on even the combination of two more biological agents was suggested [38] [39].

Biocontrol agents are not harmful to the environment and do not result in pathogen resistance. The lack of resistance thus does not necessitate increased and harsher use of such agents to maintain effectiveness. The agents are specific in action, are able to only attack the pathogen of interest and are effective in small quantities. Furthermore, they are able to multiply themselves but are controlled by the plant and indigenous microbial populations. Biocontrol agents decompose more quickly than conventional chemical pesticides and can also be used in conventional or integrated pest management systems [40]. Though there are many advantages, there are also disadvantages in using biopesticides in plant protection. Biological control agents are, as any other living organism, influenced by environmental conditions, such as temperature, humidity or the predominant microflora, and therefore can be strongly dependent on these factors. These reasons could lead to insufficient performance of the biological agent toward pathogens. Such a possibility has continued to lend strength to arguments for the use of chemical pesticides [41].

It has been reported that biological agents are particularly useful for application in greenhouse systems. In such systems the environmental conditions can be controlled and optimized for biocontrol agents [42]. Not all of these products are registered as biological control agents but are also known as plant growth promoters, plant strengtheners or soil conditioners. Most of the organisms used for the production of biological agents against soil-borne crop diseases

include microbes such as *Bacillus*, *Burkholderia*, *Coniothyrium*, *Fusarium*, *Gliocladium*, *Pythium*, *Streptomyces*, *Talaromyces* and *Trichoderma* [41] [43].

1.2.1 Biocontrol of *Trichoderma*

A potential mycoparasitic role for *Trichoderma* was first proposed by Weindling in 1934 [44]. He described the mycoparasitic activity of *Trichoderma lignorum* toward the plant pathogen *R. solani*. Since then, a large number of studies confirmed *Trichoderma* species as biological control agents. Several commercially available products for the protection and growth enhancement of crops are based on the characteristics of *Trichoderma* strains. Known commercial formulations include the following: RootShield® Granules, PlantShield® HC based on the *T. harzianum* strain T-22. (BioWorks Inc., USA), Supresivit™ (Borregard BioPlant, Denmark), Binab T® (Bio- Innovation, Sweden), Trichodex™ (Markhteshim, Israel) and SoilGuard™ (Thermo trilogy, USA). However, there are many more products than the aforementioned and not all products are registered as biocontrol agents but are instead advertised and promoted as plant growth promoters, plant strengtheners or soil conditioners. In comparison to chemical pesticides, the registration of biological agents and biopesticides underlies fewer regulations and is therefore less time consuming and can be performed at lower costs for the company [41].

Trichoderma strains are superior to other microorganisms for biocontrol due to their high reproductive capacity, ability to survive under unfavorable conditions, efficiency in the utilization of nutrients, capacity to modify the rhizosphere, strong aggressiveness against phytopathogenic fungi and efficiency in promoting plant growth and defense mechanisms, which enable them to develop in any living space at high population density. The most common *Trichoderma* strains that are currently used for biological control are *T. virens*, *T. viride* and *T. harzianum* [35].

Trichoderma disease control is the result of the interaction of different mechanisms. *Trichoderma* spp. are capable of establishing an unfavorable environment for the plant pathogen via competition for resources and living space as well as direct attack. Furthermore, this fungal genus is responsible for strengthening the growth of plants and even induces systemic or localized resistance.

Trichoderma spp. present higher activity in comparison to other fungi in regards to the uptake of soil nutrients and therefore can biocontrol other fungi (e.g. *Botrytis cinerea*, a known plant

pathogen) by successfully competing for soil nutrients [35]. It has been documented that *Trichoderma* produce siderophores, which are able to chelate the iron making it impossible for other fungi to metabolize it. In addition, *Trichoderma* spp. demonstrate an enhanced ability to battle for living space by producing intermediate catabolic products that can, for example, acidify the rhizosphere or by producing or resisting metabolites that either impede spore germination (fungistasis) or help the pathogen to penetrate the plant or kill the cells (antibiosis) [12].

Harman et al. have described *Trichoderma* strains as plant opportunistic symbionts and avirulent organisms that exhibit positive effects on plants such as the induction of systemic or localized resistance and the stimulation of plant growth and root development (biofertilization) [13]. This phenomenon was first described by Bigirimana et al. [45] when they discovered the resistance of leaves of bean plants against the fungal pathogen *B. cinerea* after a treatment of the soil with *T. harzianum* strain T-29. When *Trichoderma* colonizes the roots of the plants, only the first two layers of the root cells are penetrated but, further colonization of roots is observed. There, the production and release of bioactive molecules take place that induces systemic or localized resistance [45]. These bioactive compounds either belong to the family of avirulence proteins or are enzymes with other functions. There is a difference between localized- and systemic-induced resistance. While localized defense responses are restricted to the site of interaction with the fungus, systemic defense responses spread throughout the plant and are therefore effective even at sites distant from the *Trichoderma* location. The plant responds to this attack by producing defense-related plant enzymes including peroxidases, β -1,3-glucanases and the lipoxygenase-pathway hydroperoxide lyases, as well as low-molecular weight compounds that exhibit antimicrobial activity [13] [46].

Necrotrophic hyperparasitism or mycoparasitism occurs through the direct interaction between *Trichoderma* spp. and a pathogen [12].

When *Trichoderma* spp. encounter other fungi, several events have preceded the contact.

Trichoderma spp. sequentially produce cell wall degrading and sensing enzymes, which catalyze the release of cell wall fragments and possibly also peptides from cell wall proteins of the pathogen. These molecules interact with receptors such as G protein-coupled receptors or nitrogen-sensing receptors on the surface of *Trichoderma* hyphae. This initiates a signaling cascade involving G-proteins and mitogen-activated protein kinases (MAPKs), which consequently leads to the production of fungitoxic endochitinases, resulting in a direct attack

on pathogen cell walls [12] [13]. *Trichoderma* spp. recognize the pathogen and grow directly toward it. Sugar-binding proteins (lectins) of the target fungus are recognized by *Trichoderma* and induce coiling of the *Trichoderma* hyphae around the pathogen hyphae. However, it has been reported that such coiling events are not strictly dependent on mycoparasitic activity, as the hyphae of *Trichoderma* can also coil around themselves without the presence of a pathogen [12]. Through appressorium-like bodies and hyphal loops, *Trichoderma* may then invade the host and enter the lumen of the pathogen and parasitize it which ultimately leads to the death of the host hyphae [12] [13].

1.3 The lytic enzyme machinery of *Trichoderma*

The cell wall of fungi provides important protective functions against environmental stress factors, e.g. desiccation, high osmotic pressure or heat and also protects cells against mechanical injuries and hostile compounds such as toxins and lytic enzymes. The fungal cell wall consists of 90 % polysaccharides, primarily glucans and chitin [47].

Chitin, which is the second-most abundant polymer found in the biosphere, is the main structural component of cell walls and is crosslinked to a branched β -1,3-1,6-glucan via β -1,4-linkages. Two crystalline polymorphic forms can be found in nature, which are characterized according to the arrangement of their *N*-acetylglucosamine chains in α -chitin (antiparallel) and β -chitin (parallel) [48]. The exoskeleton of arthropods, yeast, insect and fungal cell walls contain α -chitin, which is composed of tightly packed sheets with alternating parallel and antiparallel chains. β -chitin, which occurs less frequently in nature and can for example be found in squid pens, is organized in parallel chains [49].

Chitin synthases are large membrane-bound proteins that are responsible for the synthesis of chitin, which occurs at the hyphal tips from UDP-activated *N*-acetylglucosamine sugars. In specialized vesicles, so-called chitosomes, the enzymes are transported in fungal hyphae toward the tips, where they are proteolytically activated and catalyze the synthesis of *N*-acetylglucosamine (GlcNAc) oligomers [47].

1.3.1 Enzymes involved in cell wall degradation and remodeling

Different protein families play a major role in the process of cell wall degradation during mycoparasitism including chitinases, *N*-acetylglucosaminidases, different types of β -glucanases (β -1,3; β -1,6), α -1,3- glucanases and proteases [10].

The Carbohydrate-Active Enzyme (CAZy) database, which provides information on enzymes that build and breakdown complex carbohydrates and glycoconjugates was established by Henrissat et al. [50]. This database comprises and categorizes glycoside hydrolases (GHs), glycosyl transferases (GTs), polysaccharide lyases (PLs), carbohydrate esterases (CEs) and carbohydrate-binding modules (CBMs) into different families (<http://www.cazy.org>).

CAZome (the total number of genes encoding CAZymes) analysis of the mycoparasites *T. atroviride* and *T. virens* and comparison with other already sequenced fungi revealed that the numbers of chitinases and β -1,3-glucanases are significantly higher in mycoparasitic *Trichoderma* spp. than in other filamentous fungi.

1.3.1.1 Glucanases

β -1,3-glucanases hydrolyze β -1,3-glucan, which is, in addition to chitin, a major component of the fungal cell wall. These enzymes can be further divided into *exo*- β -1,3-glucanases (EC 3.2.1.58) and *endo*- β -1,3- glucanases. The prefixes indicate the mechanism by which these enzymes degrade the *O*-glycoside bonds of β -glucan chains. *Exo*- β -1,3-glucanases cleave predominantly from the chain ends (mostly the non-reducing end), whereas the *endo*- β -1,3-glucanases cleave randomly within the glucan chains [51]. β -1,3-glucanases from *Trichoderma* were shown to inhibit spore germination or the growth of pathogens in synergistic cooperation with chitinases and antibiotics [35]. Despite the numerous β -1,3-glucanases that have been isolated, only a few genes have been cloned, e.g. *bgn13.1* from *T. harzianum*. Transformants overexpressing BGN13.1 inhibit the growth of *B. cinerea*, *R. solani* and *Phytophthora citrophthora*. BGN13.1 thereby can be classified as the major enzyme out of three β -1,3-glucanases that are expressed by *T. harzianum* and acts as an *endo*-glucanase [51].

α -1,3-glucanases (EC 3.2.1.59) are extracellular enzymes that catalyze the cleavage of α -1,3-glycosidic bonds and are known for their contributory role in the antagonistic response of *T. harzianum*. *T. harzianum* secretes α -1,3-glucanases when grown on polysaccharides and uses

fungal cell walls as a carbon source. AGN13.1 is an α -1,3-glucanase of *T. harzianum* that belongs to the *exo*-type glucanases and exhibits lytic and antifungal activities against fungal plant pathogens [52].

1.3.1.2 Proteases

Carbohydrate-active enzymes and proteases contribute to the degradation of the fungal cell wall and play a role in biocontrol. *Trichoderma* spp. proteases might be of significant importance for the mycoparasitic attack, because the fungal cell wall is covered by a layer of various cell wall bound proteins. Further, proteases have been suggested to be involved in the inactivation of extracellular proteins of phytopathogenic fungi [51]. The pathogenicity of *B. cinerea* can be decreased by the inhibitory effects of secretory proteolytic *T. harzianum* enzymes on hydrolytic enzymes of *B. cinerea*. The germination of conidia of *B. cinerea* can also be inhibited via such mechanisms [53]. Several protease-encoding genes have been cloned from *Trichoderma* spp. The subtilisin-like serine protease from *T. atroviride* PRB1 appears to be a key element in the parasitic process. The corresponding gene *prb1* is transcriptionally regulated in response to nitrogen availability [54]. As it is unlikely that the fungus experiences a real nitrogen limitation at this stage, Seidl et al. further hypothesized that the expression of proteolytic enzymes during the onset of mycoparasitism is dependent on the formation of peptides as a signal for nitrogen deficiency [55]. A serine-protease with trypsin activity (PRA1) was isolated from *T. harzianum* CECT 2413 and was found to reduce the number of hatched eggs of root-knot nematodes after incubation with pure PRA1 preparations [56].

1.3.1.3 Chitin-degrading enzymes

Chitinolytic enzymes can be divided into *N*-acetylglucosaminidases (EC 3.2.1.52) and chitinases (EC 3.2.1.14). The difference between these enzymes is the mode of action by which they exhibit chitin degradation. *N*-acetylglucosaminidases (NAGases) catalyze the hydrolytic release of terminal non-reducing *N*-acetylglucosamine (GlcNAc) units but exhibit the highest substrate affinity toward the dimer *N,N'*-diacetylchitobiose (GlcNAc)₂, which is degraded into two GlcNAc monomers [57].

Chitinases hydrolyze the β -1,4-linkages in chitin and chitooligomers into short-chain chitooligomers. According to the CAZy classification, *N*-acetylglucosaminidases belong to

the glycoside hydrolase (GH) family 20, whereas chitinases are members of GH family 18 and 19 according to their amino acid homology. Another classification scheme also exists, where GH family 19 chitinases, which can be found in higher plants, can be subdivided into three different classes (class I, II and IV). Class III and class V chitinases exhibit no sequence homology with class I, II and IV enzymes and belong to the GH family 18 chitinases. Fungal chitinases exclusively belong to GH family 18. GH family 18 also includes chitinases of bacterial, animal, viral and plant origin.

The substrate binding pockets of class III and class V enzymes differ completely. While class III enzymes have plain, open substrate-binding grooves, class V enzymes exhibit a deep, tunnel-shaped substrate-binding groove. The structure of GH family 18 enzymes typically are characterized by an $(\alpha/\beta)_8$ -barrel structure composed of eight α -helices and an eight-stranded β -sheet. Additionally, the structure possesses an N-terminal β -strand-rich domain and a small $(\alpha+\beta)$ domain. In contrast to family 18, the structural features of family 19 enzymes are totally different. They are arranged in two lobes, which are predominantly composed of α -helices and the substrate binding cleft is assumed to lie in between [58] [59] [60].

In analogy to other lytic enzymes chitinases can also be divided into *endo*- and *exo*-chitinases based on their cleavage patterns. With the *exo*-mechanism, the degradation initiates from one of the chain ends, whereas the starting point in the *endo*-mechanism can be elsewhere along the polymer chain. However, it should be noted that this classification is not always so clear-cut. An additional aspect shown in details for chitinases of the bacterium *Serratia marcescens*, is processivity of enzymes. The above mentioned *exo*- and *endo*- type cleavage of enzymes can occur in combination with either a processive or a non-processive mode of action. Therefore, processive chitinases do not release the substrate after hydrolytic cleavage but slide it through the active-site tunnel for the next cleavage to occur. Non-processive chitinases dissociate completely from the substrate after hydrolysis. This leads for non-processive enzymes to different substrate degradation patterns with a homogenous distribution of medium chain (6-30mer) products and for processive enzymes to remnants of the polymeric substrate and only 2-8mer short chain degradation products [61] [62].

1.3.2 Classification of fungal chitinases into subgroups

According to the results of a phylogenetic analysis of fungal genomes, chitinases were further differentiated into 3 subgroups [60].

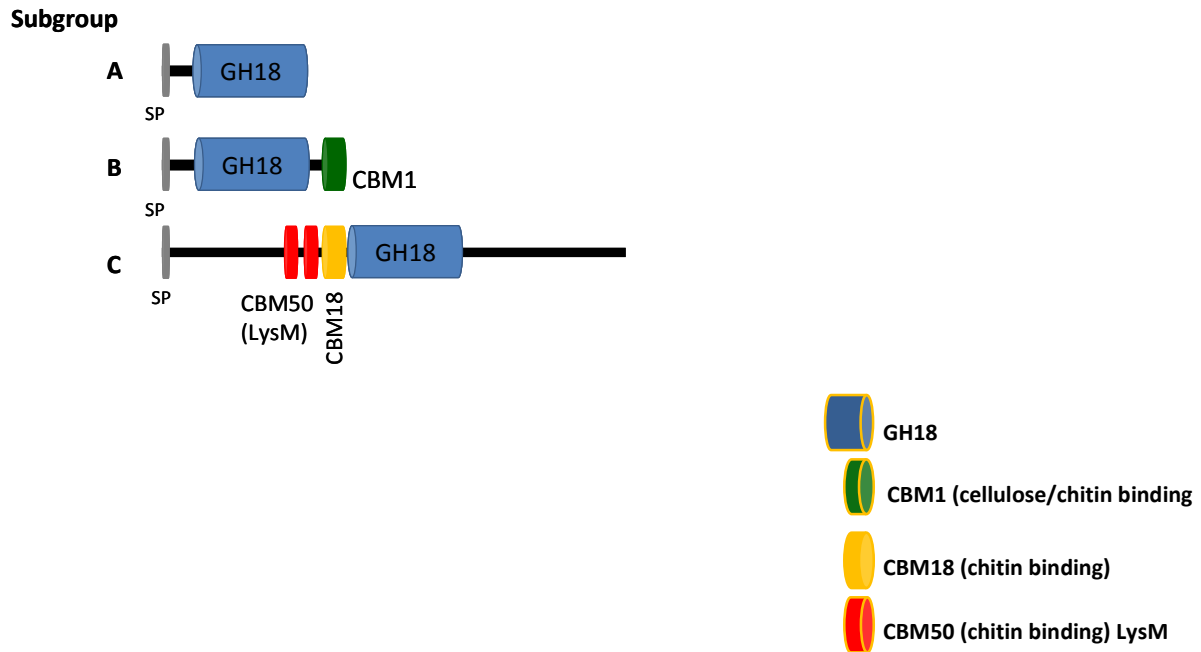


Fig. 2: Domain organization of the three subgroups of fungal chitinases: SP, signal peptide; GH 18, glycoside hydrolase family 18; Taken from: Gruber 2011 [63].

Subgroup A chitinases have on average a molecular mass of 40-50 kDa, and many of these proteins exhibit an N-terminal signal peptide and thus are mostly extracellular proteins. These chitinases mostly do not have a carbohydrate-binding domain (CBM).

Subgroup B chitinases vary in molecular size from 30-90 kDa and are dependent on the occurrence of CBMs. They are grouped as small subgroup B chitinases (30-45 kDa) or appear as proteins that are attached to serine/threonine-rich domains and/or a GPI-anchoring signal. They are plasma-bound proteins with 90 kDa in size. The CBMs of subgroup B are located at their C-terminal ends. In *Trichoderma* spp., the CBMs of subgroup B chitinases belong exclusively to the CBM1 family, designated as possessing cellulose- and chitin-binding properties [64].

Subgroup C chitinases are a novel class of fungal chitinases that comprise proteins larger than those in subgroup A and B. The molecular mass of these proteins varies between 140-170 kDa. These proteins contain an N-terminal signal peptide, which targets them to the secretory pathway. Furthermore, subgroup C chitinases possess a chitin-binding domain (CBM 18) and multiple LysM domains, which are short domains characterized by the ability to bind to

peptidoglycans [61]. There are further substrate binding differences between these three subgroups.

Subgroup A and subgroup C chitinase structures correspond to class V, which exhibit tunnel-shaped substrate binding clefts that account for their *exo*-activity, while subgroup B enzyme structures correspond to a class III- possessing plain, open substrate-binding groove, indicative of *endo*-activity [62].

1.4 Carbohydrate-binding modules (CBMs)

Recent analysis of *Trichoderma* spp. genomes have revealed that the cell wall degrading enzyme machinery is an even more complex system than previously anticipated [10].

Subgroup C chitinases have particularly interesting features. They contain CBM 18 (chitin-binding) and CBM 50 (LysM) domains and their predicted open reading frames encode proteins with a size of approximately 150 kDa. In comparison, the size of subgroup A and B chitinases is, on average, 35-45 kDa [61]. In general, carbohydrate-binding modules are attached to glycoside hydrolases to associate them with insoluble polysaccharides and facilitate their degradation. CBMs are reported to fulfill three main functions: 1) a proximity effect, 2) a targeting function and 3) a disruptive function [65].

- 1) The concentration of the enzyme on the surface of the substrate increases in order to enhance the degradation of the polysaccharide.
- 2) Damaged regions of plant cell walls are recognized and distinct regions are detected by the enzymes.
- 3) The disruptive effect enhances the degradative capacity of the catalytic module; this effect is uncertain.

CBMs can be classified into three types according to structural and functional similarities: surface-binding CBMs (Type A), glycan-chain-binding CBMs (Type B) and small sugar-binding CBMs (Type C).

CBM 18 can be referred to as a small sugar-binding CBM (Type C). This class is notable because of the ability to bind optimally to mono-, di- or trisaccharides [65]. In the CAZy database CBMs are – in analogy to glycoside hydrolases - grouped into different families.

1.5 Lysin motif (LysM)

Lysin motifs (LysM modules, LysMs) are carbohydrate-binding protein modules classified in the CAZy database as CBM family 50. They were first detected in 1986 in bacteria as 44-amino acid domains that bind to the peptidoglycan (PG) of bacterial cell walls [66].

Later, it was reported that these domains also occur in bacterial PG hydrolases, peptidases, chitinases, esterases, reductases and nucleosidases, as well as in certain eukaryote proteins. Nowadays based on the wealth of genome data from many different organisms, more than 4000 proteins among the prokaryotes and eukaryotes are known that contain LysM motifs. As this motif was originally identified in bacterial lysins, it was designed the lysin motif, short LysM [67]. The LysM domain is one of the most common modules in bacterial cell surface proteins. For example, *Staphylococci* produce IgG-binding proteins to deactivate the host immune response. The C-terminal part of the protein binds to the bacterial cell wall and contains a LysM domain [68]. In bacteria, the LysM seems to have evolved into a general peptidoglycan-binding motif, whereas in eukaryotes it is a chitin-binding motif [69].

LysM motifs have also been recognized in plants. In *Arabidopsis*, the LysM-containing chitin elicitor receptor kinase 1 (CERK1) has been shown to be essential for perception of the fungal cell wall component chitin and for resistance to fungal pathogens. However, LysM motifs in plants can also have completely different functions as in *Medicago truncatula*, the receptor is responsible for the mediation of the symbiotic interaction of the plant with nitrogen-fixing bacteria. The receptor is localized in the plasma membrane and has three LysM motifs in the extracellular domain as well as the intracellular kinase domain [70] [71]. This expands the function of LysM motifs in plants from recognition systems for defense purposes to cell-cell communication systems.

The first identified fungal protein with a LysM motif was a chitinase from the yeast *Kluyveromyces lactis* that is part of the so-called killer toxin system, which inhibits the growth of other, susceptible yeast cells [72]. In addition, it has been reported that the protein Ecp6, which contains multiple LysM motifs and is a virulence factor, is responsible for the disabled immune response of *Solanum lycopersicum* (tomato), which is attacked by the plant pathogen *Cladosporium fulvum*. During infection, plant chitinases release chitin oligomers from the fungal cell wall. Ecp6 binds these chitin-oligosaccharides and thereby prevents recognition of these molecules by the tomato plant, which otherwise would elicit its defense responses. It has been hypothesized that this may represent a common strategy of host

immune suppression by fungal pathogens because LysM effectors are found quite often in the fungal kingdom [73].

A classification of fungal LysM proteins was established by Ronnie de Jonge and Bart Thomma (2009), resulting in five distinguishable types that differ among their overall domain architecture. Type A contains proteins that solely consist of a varying number of LysMs. A representative for this type is Ecp6 from *Cladosporium fulvum*, which contains three LysMs. Members of the second group possess not only LysMs but also a cysteine-rich, chitin-binding domain. They are characterized because of their homology to chitinases. The third group proteins resemble the carbohydrate-binding antiviral protein cyanovirin-N (CV-N), in addition to a nested LysM. The last two groups exhibit LysM proteins recombined with a variety of different domains.

Sequence analysis reveals that a LysM motif in its currently recognized form consists of 44 amino acids (aa), of which the first 16 and the last 10 are the most conserved. In Fig. 3 conserved aa of LysMs from *T. atroviride*, *T. virens* and *T. reesei* are shown. Height of the letters reflects the degree of conservation. This shows that a considerable degree of variation can be found in these protein motifs, which possibly infers additional functions or a greater variety of binding properties than so far anticipated.

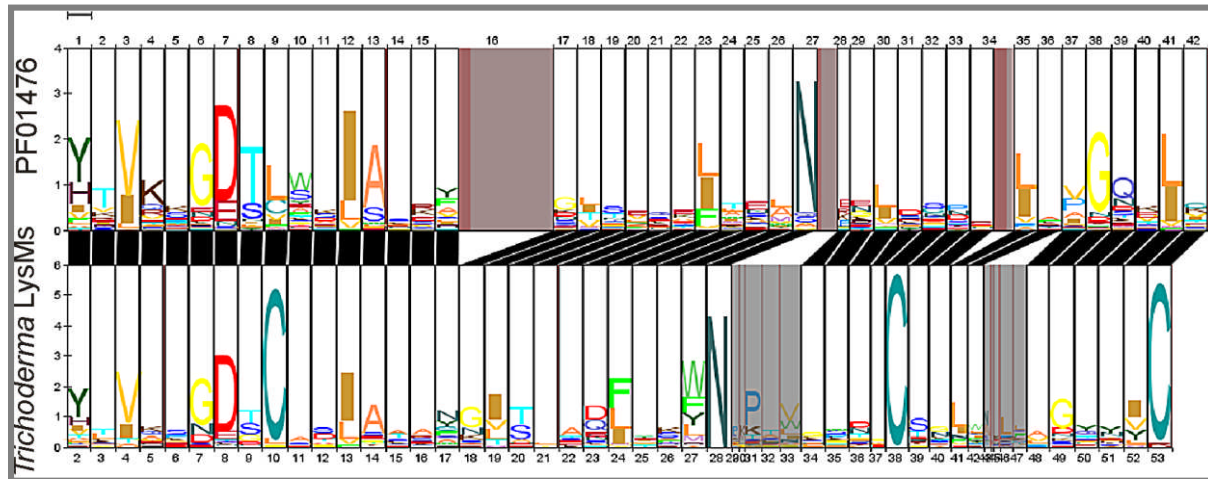


Fig. 3: Pairwise HMM logo comparison of the PFAM LysM logo (PF01476, upper panel) and a multiple alignment of LysMs (SM00257) from *T. atroviride*, *T. virens* and *T. reesei* (lower panel), created with LogoMat-P. Taken from: Gruber et al 2011 [63].

Prokaryotic LysMs comprise extensive secondary structures and hydrogen bonding networks that establish tertiary structures but do not contain any disulfide bridges, as can be found in eukaryotic LysMs [69]. The LysM motif has a $\alpha\beta\alpha$ -secondary structure with the two α -helices packed on the same side of the two-stranded antiparallel sheet. The presence of two

highly conserved glycine residues were listed as one of the features of this sequence motif, but these residues do not appear to be strongly conserved in fungal LysM motifs (Fig. 3) [68]. Genome analysis revealed that in the *Trichoderma* genomes the genes upstream or downstream of genes encoding subgroup C chitinases, which themselves contain LysM motifs, or in close proximity to these chitinase genes often contain LysM motifs. This incidence suggests a connected function of LysM proteins and subgroup C chitinases. For some of these proteins also EST (expressed sequence tag)- sequences are available, which indicates that they are functional proteins and not remnants from genomic recombination events [63].

In the following LysM domains of *T. atroviride* are referred to as TAL proteins. *Trichoderma* TAL proteins consist of a signal peptide and between 2 and 6 LysM domains. They are secreted proteins that are composed solely of carbohydrate-binding domains. TAL6 (protein ID: 297859) consists of 6 LysM modules, of which four are highly similar but that do not present high similarity with the other two modules. Gene expression of *tal6* revealed that this gene is coregulated with *tac6*, which encodes a chitinase of subgroup C. Expression of TAC6 was found to be induced during hyphal network formation in contrast to other chitinases of subgroup C, which are expressed during mycoparasitism or are induced by chitin or fungal cell walls [63].

1.6 EPLs (eliciting plant response-like proteins) in *T. atroviride*

Cerato-platanin (CP) a phytotoxic protein of 12.4 kDa has first been reported in the culture filtrates of the ascomycete *Ceratocystis fimbriata* f. sp. *platani*, the causal agent of canker stain disease [74]. Members of the cerato-platanin (CP) family are small secreted proteins containing four conserved cysteine residues that form disulfide bonds characterized by high sequence homology and it is a stable component of the fungal cell wall [74] [75]. Cerato-platanin shares some structural and functional characteristics with the hydrophobin family, but differs from the hydrophobins in having only four cysteines instead of eight [76]. Proteins of the cerato-platanin family (CPP) are reported to act as phytotoxins, elicit defense responses in plants and allergic reactions in humans and further are involved in the crosstalk activities in host fungus interactions [75] [77] [78]. The genomes of *Trichoderma* spp. contain three genes that encode protein members of the cerato-platanin family, named EPLs (eliciting plant response-like proteins) in *T. atroviride* [75] [78]. The EPL1 protein of *T. atroviride* was

reported to be the major secreted protein during growth on glucose, but was also shown to be expressed under all growth conditions tested, which included further carbon sources like glycerol, L-arabinose, D-xylose, colloidal chitin and cell walls of the plant pathogen *R. solani*. The function of members of the cerato-platanin family in fungal growth is not fully understood until now. In contrast the involvement of these proteins in the induction of plant defense responses has been well documented for several fungal species. EPL1 could be detected in its monomeric and dimeric form [75] [78]. SM1 is the *T. virens* homologue of EPL1 and it was shown that this protein efficiently induced plant defense responses in cotton and in maize plants [77]. Further, it was shown that only the monomeric form of these proteins were able to induce plant defense responses and that the dimerization was dependent on two double oxidized tryptophane residues and a single glycosylation, which was found in SM1, while EPL1 is not glycosylated [75] [79]. Although these studies revealed interesting functions in the interaction of *Trichoderma* with plants, the question still remains to be answered what the primary function of these proteins is. All filamentous fungi appear to have one to three cerato-platanin encoding genes and the respective orthologue of EPL1 is often found to be highly expressed under many different growth conditions. Thus, this remains to be shown if these proteins have a function in events such as e.g. fungal growth and development or cell wall protection.

2. Aims of this thesis

In plant pathogenic fungi a function of LysM effector proteins in the host-pathogen interaction was shown, but also mycoparasitic and saprobic fungi contain LysM proteins [73]. Therefore the question that arises is: what is the function of these proteins in other fungi? In this thesis a LysM protein (TAL6) from the mycoparasite *T. atroviride* was chosen for further biochemical characterization. The full-length protein containing six LysM motifs (TAL6₆) and a truncated version of this protein, containing four LysM motifs (TAL6₄) were overexpressed. The properties of the in *Pichia pastoris* heterologously expressed proteins TAL6₆ and TAL6₄ were analyzed in detail with respect to their primary protein characteristics (MW, pI, dimer formation and glycosylation). Further, a biochemical and functional analysis of these proteins was carried out, including carbohydrate-binding studies with soluble and insoluble carbon sources as well as the effect of these proteins on germination efficiency and growth of different fungi. Not only hydrolytic enzymes such as chitinases are involved in mycoparasitic events but also cerato-platanin proteins are suggested to have an influence on the host-fungal interactions. EPL proteins found in *Trichoderma atroviride* are members of the cerato-platanin family. Although some of the features of this protein family such as their size, cysteine-rich amino acid sequences and cell wall location are reminiscent of hydrophobins, there exist distinct differences between these two protein families. In order to further elucidate the function of these proteins, single and double knockout strains of genes encoding the cerato-platanin proteins *epl1* and *epl2* were generated in *T. atroviride*. The protein EPL1 from *T. atroviride* was also purified from fungal cultivations and its carbohydrate-binding properties were characterized to increase our understanding of the biochemical properties of cerato-platanin proteins.

.

3. Materials and Methods

3.1 Instruments, Chemicals and Devices

The Tables 1-5a illustrate equipment, chemicals and devices, which were used in common in this thesis.

Table 1: Equipment and Devices

Instrument	Producer
Centrifuges/Rotors	
Centrifuge 5424	Eppendorf AG, Hamburg, Germany
Sigma Centrifuge 3- 18K	Sigma- Aldrich , Missouri, USA
Sigma Centrifuge 3- 30K	Sigma- Aldrich , Missouri, USA
Rotor 19976H	Sigma- Aldrich , Missouri, USA
Swing- out rotor 11390/13150	Sigma- Aldrich , Missouri, USA
Tischkühlzentrifuge 1-15 PK	Sigma- Aldrich , Missouri, USA
Rotor 12132	Sigma- Aldrich , Missouri, USA
Chromatographic Systems/Columns	
ÄKTA™ purifier	Amersham Pharmacia Biotech, NY, USA
HisTrap™ HP columns	GE Healthcare, Sweden
HiScale 16 column	GE Healthcare, Sweden
HisTrap™ FF columns	GE Healthcare, Sweden
PCR Cyclers	
MYCycler™ Thermal Cycler	Bio-Rad, California, USA
Thermocycler T 3000	Biometra GmbH, Germany
Shakers	
IKA ^R VORTEX	IKA , Germany
Thermomixer compact 5350	Eppendorf AG, Hamburg, Germany
IKA- VIBRAX-VR VX7	Janke& Kunkl GmbH& Co KG, Germany
Magnetic stirrer Hei Standard	Heidolph Instruments

Table 2: Additional instruments

Instrument	Producer
Additional Equipment and Devices	
Nanodrop ^R ND-1000 Spectrophotometer	Nanodrop Technologies, USA
GelDoc Universal HoodII	Bio-Rad, California, USA
PowerPac Basic	Bio-Rad, California, USA
Gel chamber wide mini-sub cell gt	Bio-Rad, California, USA
Gel chamber mini-sub cell gt	Bio-Rad, California, USA
Electrophoresis Power Supply- EPS 300	Pharmacia Biotech, Switzerland
Waterbath	Fischer Scientific Inc., England
PHM 82 Standard pH Meter	Radiometer Copenhagen
Balance SARB-OT300 2B	Sartorius AG, Germany
Semi- Phor TM TE70	HOEFER Scientific Instruments, San Francisco
CERTOclav Type CVII/1600	KELOMAT Haushaltsgeräte Traun, Austria
Sanyo Incubator MIR-153	Sanyo Electric Co., Ltd. Japan
Incubator Infors HT Multitron	Infors HT, Switzerland
Mini Hybridization Oven OV1	Biometra GmbH, Germany
Incubator B5060E	Heraeus, Germany
Waterbath for incubating	Gesellschaft für Labortechnik mbH, Germany
Protean IEF Cell	Bio-Rad, California, USA
Microscope TR 500	VWR International Belgium
MicroPulser	Bio-Rad, California, USA
Gene Pulser Cuvette 165-2086	Bio-Rad, California, USA
Lab-Tek [®] II Chambered Coverclass	NALGE-NUNC International Corp., USA
Lyophilizer freeZone 2.5	Labcono, Kansas City, USA
Labfors S- 000115999	Infors HAT, Switzerland
EmulsiFlex-C3 Homogenizer	AVESTIN, Mannheim, Germany

Table 3: Liquid handling

Instrument	Producer
Pipetman Neo P10N, 1–10 µL	Gilson, Wisconsin, USA
Pipetman Neo P20N, 2–20 µL	Gilson, Wisconsin, USA
Pipetman Neo P200N, 20–200 µL	Gilson, Wisconsin, USA
Pipetman Neo P1000N, 100–1000 µL	Gilson, Wisconsin, USA

Table 4: Membranes and Gels

Membranes/Filters	Article No.	Producer
Whatman blotting paper	3030917	Whatman International Ltd., England
Miracloth	475855	VWR(Calbiochem)
Hybond- C Extra Nitrocellulose	RPN303E	Amersham Biosciences
Membrane 45 Micron		
Ready Strip IPG Strips pH3-10, 7 cm	163-2000	Bio-Rad, California, USA
Amicon Ultra centrifugal filter units	Z717185-8EA	Sigma- Aldrich , Missouri, USA
Steritop- GP Filter Unit (150 mL)	SCGPT01RE	Millipore
Sterile Syringe Filter 0.20 µm	2052-025	Asahi Glass Co., LTD., Japan
Sterile Syringe Filter 0.45 µm	2053-025	Asahi Glass Co., LTD., Japan

Table 5: Special chemicals

Chemicals	Producer	Article No.
5- Brom-4-chloro-3-indoyl phosphate p- toluidin salt	Sigma -Aldrich Chemie GmbH, Germany	B6777
Imidazole ACS reagent	Sigma -Aldrich Chemie GmbH, Germany	I2399
Nitrotetrazolium blue chloride approx.98%	Sigma -Aldrich Chemie GmbH, Germany	N6876
Water for Molecular Biology	Merck GmbH, Germany	T143.4
Sodium dithionite	Sigma -Aldrich Chemie GmbH, Germany	28-2925
Anti-His(C-term) Antibody	Invitrogen , Austria	R93025
Hygromycin B	VWR (Calbiochem), Austria	400051-1
Coomassie Brilliant blue G250	Merck GmbH, Germany	1154440025
1,4- Dithiothreitol	Carl Roth GmbH, Germany	6908.1
Anti- Mouse IgG(H+L), AP Conjugate	Promega, Austria	S3721
N- acetyl- D- Glucosamine	Sigma -Aldrich Chemie GmbH, Germany	A8625
Ethanol	Merck GmbH, Germany	1009712500
Methanol	Merck GmbH, Germany	1060092500
Sulfuric acid	Merck GmbH, Germany	1007312500
D-(-)- Quinonic acid	Sigma -Aldrich Chemie GmbH, Germany	22580
Tween 80	Merck GmbH, Germany	8221870500
Triton X-100	Merck GmbH, Germany	1086031000
Phosphoric acid 85%	Merck GmbH, Germany	8150580010
Hydrochloric acid	Carl Roth GmbH, Germany	X942.2
Isoamyl alcohol	Merck GmbH, Germany	100979
Acetic acid	Carl Roth GmbH, Germany	3738.1
Sodium hydroxide	Carl Roth GmbH, Germany	6771.2
Tris	Carl Roth GmbH, Germany	4855.3
2- propanol	Sigma -Aldrich Chemie GmbH, Germany	650447

Table 5a: Special chemicals continued

Chemicals	Producer	Article No.
Sodium acetate	Merck GmbH, Germany	1062640500
D- Sorbitol	VWR (Calbiochem), Austria	ALFA36404A3
Ammonium persulphate	Sigma -Aldrich Chemie GmbH, Germany	A3678
N,N- dimethyl formamide	Carl Roth GmbH, Germany	T921.1
Trichloromethane/Chloroform	Carl Roth GmbH, Germany	3313.2
Lysing Enzyme from <i>Trichoderma harzianum</i>	Sigma -Aldrich Chemie GmbH, Germany	L1412
Potao Dextrose Agar	Difco, USA	213400
Lauryldimethylamine-oxide	Sigma -Aldrich Chemie GmbH, Germany	40234
2-(4-(2-Hydroxyethyl)- 1-piperazinyl)-ethansulfonic acid	Sigma -Aldrich Chemie GmbH, Germany	H3375
Protease Inhibitor Cocktail	Sigma -Aldrich Chemie GmbH, Germany	P8215
Phenol	VWR (Calbiochem), Austria	A1578.0500
Ribonuclease A from bovine pancreas	SERVA	34388.02
PIPES	Sigma -Aldrich Chemie GmbH, Germany	P-1851
Potato Dextrose Broth	Difco, USA	254920
Polyethylene glycol 6000	Merck GmbH, Germany	8074911000
Chitin from crab shells	Sigma -Aldrich Chemie GmbH, Germany	C7170
Bicine BioUltra	Fluka Chemie AG, Austria	14871
Bio-Rad Protein Assay Dye Reagent Concentrate	Bio- Rad	500- 0006
Bis- Tris	Carl Roth GmbH, Germany	9140.1
ARBOCEL cellulose fibre	J. Rettmayer& Söhne GmbH, Germany	B800
(3-[(3-Cholamidopropyl)-dimethylammonio]-propane- sulfonate	Merck GmbH, Germany	111662
Nickel(II)- chloro-hexahydride	Merck GmbH, Germany	B300417
Glass perls 0,75-1,0 mm	Carl Roth GmbH, Germany	A554.1
Glass perls 0,25- 0,50 mm	Carl Roth GmbH, Germany	A553.1
Chitin beads	BIOLABS	S6651
D- Histidine	Sigma -Aldrich Chemie GmbH, Germany	H3751
α- Mannosidase from <i>Canavalia ensiformis</i> (Jack bean)	Sigma -Aldrich Chemie GmbH, Germany	M7257
Iodacetamid	Sigma -Aldrich Chemie GmbH, Germany	16125
Bio- Lyte 3/10 Ampholyte	Bio- Rad	163-1112
EndoH streptomycetes	New England Biolabs	P07025

3.2 Enzymes

The enzymes, which were used for DNA manipulation are listed in Table 6, 7, 8, and 9, respectively.

Table 6: Restriction Enzymes

Enzyme	Conc.	Restriction site	Buffer	Article No.
BamHI	10u/μL	5'-G [^] GA T C C-3'	10X Buffer BamHI	ER0051
Acc65I	10u/μL	5'- [^] GA [^] G T A C C-3'	10X Buffer O	ER0901
BcuI (SpeI)	10u/μL	5'-A [^] C T A G T-3'	10X Buffer Tango™	ER1251
BstXI	10u/μL	5'-C C A N N N N [^] N T G G-3'	10X Buffer O	ER1021
BglI	10u/μL	5'-G C C N N N N [^] N G G C-3'	10X Buffer O	ER0071
EcoRI	10u/μL	5'-G [^] AA T T C-3'	10X Buffer EcoRI	ER0271
HindIII	10u/μL	5'-A [^] AG C T T-3'	10X Buffer R	ER0501
KpnI	10u/μL	5'-G G T A C [^] C-3'	10X Buffer KpnI	ER0521
NdeI	10u/μL	5'-C A [^] T A T G-3'	10X Buffer O	ER0581
NotI	10u/μL	5'-G C [^] AG C C C G C-3'	10X Buffer O	ER0591
XbaI	10u/μL	5'-T [^] AC T A G A-3'	10X Buffer Tango™	ER0681
XhoI	10u/μL	5'-C [^] AT C G A G-3'	10X Buffer R	ER0691
BglII	10u/μL	5'-A [^] GA T C T-3'	10X Buffer O	ER0081
Cfr9I (XmaI)	10u/μL	5'-C [^] CC G G G-3'	10X Buffer Cfr9I	ER0171
Eco32I (EcoRV)	10u/μL	5'-G A T [^] A T C-3'	10X Buffer R	ER0301
SacI	10u/μL	5'-G A G C T [^] C-3'	10X Buffer SacI	ER1131
SalI	10u/μL	5'-G [^] AT C G A C-3'	10X Buffer O	ER0641
SmaI	10u/μL	5'-C C C [^] AG G G-3'	10X Buffer Tango™	ER0661
PstI	10u/μL	5'-C T G C A [^] -3'	10X Buffer O	ER0611
XmaJI (AvrII)	10u/μL	5'-C [^] AT A G G-3'	10X Buffer Tango™	ER1561

Restriction was performed as recommended by the producer. All these enzymes were purchased from Fermentas, Germany.

Table 7: Alkaline Phosphatases

Enzyme	Buffer	Article No.	Producer
FastAP™ Thermosensitive Alkaline Phosphatase	10X FastAP™ Buffer	EF0651	Fermentas, Germany
Calf Intestine Alkaline Phosphatase	10X Reaction Buffer	EF0341	Fermentas, Germany

Alkaline Phosphatases were used for dephosphorylation of the prepared vectors to prevent religation. The two different Alkaline Phosphatases worked without differencing the result.

Table 8: DNA modifying enzymes

Enzyme	Buffer	Article No.	Producer
T4 DNA Ligase DNA Ligation Kit Ver.2.1	10X T4 DNA Ligase Buffer	EL0011 6022	Fermentas, Germany Takara Bio Europe S.A.S., Austria

For implementing PCR- reactions the following DNA polymerases were used.

Table 9: DNA Polymerases

Polymerase	Article No.	Producer
Phusion™ High- Fidelity DNA Polymerase	F-530S	Biozym, Germany
GoTaq® DNA Polymerase	M8301	Promega GmbH, Germany
Roche Expand Long Template PCR System	11681834001	Roche, Austria

3.3 Strains, cultivation conditions in appropriate media

In this chapter all the strains and their cultivation conditions and required media and buffers are listed.

3.3.1 *Escherichia coli* strains

E. coli strains JM109 were used for plasmid propagation. For cloning of DNA fragments into vectors the In-Fusion Advantage PCR Cloning Kit w/Cloning Enhancer (Eubio, Austria) was used and commercially available chemically competent cells were purchased from Invitrogen (One Shot TOP10 Chemically Competent *E. coli*- C4040-03).

3.3.1.1 Cultivation of *E. coli* strains

E. coli cultures were grown at 37 °C. For incubation and regeneration after transformation different media were used as can be seen in Table 10 and Table 11, respectively.

Table 10: Composition of *E. coli* growth medium

Lysogenic Broth (LB) Medium	
Ingredients	10 g/L Tryptone 5 g/L Yeast Extract 10 g/L NaCl

LB agar plates were obtained by adding 15 g/L agar (Oxoid) to the components of the LB medium before autoclaving.

Antibiotics, if needed, were added after sterilizing and cooling down of the LB medium to a temperature of 50 °C. Thereby the final concentration of Ampicillin was 100 µg/mL.

Agar plates were stored at + 4 °C.

Table 11: Composition of *E. coli* growth medium used for the transformation of *Pichia pastoris* transformants

Low Salt Lysogenic Broth (LB) Medium	
Ingredients	10 g/L Tryptone 5 g/L Yeast Extract 5 g/L NaCl dissolve the components and adjust the pH to 7.5

Table 12: Composition of *E. coli* regeneration medium

SOC Medium	
Ingredients	20 g/L Bacto™ Tryptone 0.58 g/L NaCl 5 g/L Bacto™ Yeast Extract 2 g/L MgCl ₂ 0.18 g/L KCl 2.46 g/L MgSO ₄ 3.81 g/L α- D(+)- Glucose monohydrate

3.3.1.2 *E. coli* Transformation Protocols

3.3.1.2.1 *E. coli* transformation using chemical competent cells

100 µL of the chemical competent cells were thawed on ice. Then 1-3 µL of DNA were pipetted to the cells, mixed by gently stirring with a pipette tip. The preparation was incubated on ice for 30 minutes. The cells were heat shocked by placing them in the thermocycler at 42 °C for 2 minutes. They were put back on ice for a short time and 500 µL of LB medium without selection marker were added immediately. The cells were regenerated in a thermocycler at 37 °C and 700 g for 30 minutes. After the regeneration, aliquots of the cell suspension were plated on selection agar plates and were incubated at 37 °C over night.

3.3.1.2.2 *E. coli* transformation using one shot TOP10 chemical competent cells

The chemical competent cells, which were used in this doctoral thesis, were purchased from Invitrogen. 100 µL of the chemical competent cells were thawed on ice. Then 1-3 µL of DNA were pipetted to the cells, mixed by gently stirring with a pipette tip. The preparation was incubated on ice for 30 minutes. The cells were heat shocked by placing them in the thermocycler at 42 °C for 50 seconds. They were put back on ice for a short time and 200 µL of SOC medium were added immediately. The cells were regenerated in a thermocycler at 37 °C and 700 g for 60 minutes. After the regeneration, aliquots of the cell suspension were plated on selection agar plates and were incubated at 37 °C over night.

E. coli cells containing the appropriate plasmid were used to inoculate 4 mL LB- medium for mini-preps (or 50 mL LB- medium for midi-preps) using a sterile toothpick. The eprouvettes/ flasks were incubated at 37 °C, 170 g for 18 hours. The cells were harvested by centrifuging at 3000 g for 5 minutes.

The supernatant was discarded and the DNA was extracted from the pellet.

3.3.1.3 DNA extraction from *E. coli*

Plasmid DNA was extracted from *E. coli* using the buffers P1, P2 and P3 (preparation given in Tables 13, 14 and 15). For this an overnight culture of *E. coli* was incubated at 37°C and 150 g shaking.

On the following day 1.5 mL of the culture were centrifuged at 13000 g and RT for 5 minutes. 100 µL of buffer P1 were added to the pellet and vortexed until the pellet had been dissolved. Cell lysis was achieved by adding 200 µL of buffer P2, the sample was then mixed by gently inverting the tube several times and afterwards buffer P3 was added to neutralize the solution and precipitate SDS and genomic DNA in white flakes.

The sample then was centrifuged to get rid of the white particles (denatured cell contents) at 13000 g and +4 °C for 15 minutes. The supernatant was transferred into a fresh tube. For further precipitation 500 µl of isopropanol were added and the solution was centrifuged at high speed and +4 °C for 30 minutes. The supernatant was discarded and the pellet was washed with 500 µL of 75 % (v/v) EtOH and centrifuged again at high speed and +4 °C for 5 minutes. The pellet was air-dried and then resolved in 30 µL of dH₂O and stored at -20 °C.

Solutions for DNA isolation of plasmids from *E. coli*:

Table 13: SolutionP1

P1	
Preparation	6.06 g/L Tris 3.72 g/L Na ₂ EDTA.H ₂ O dissolve in 800 mL dH ₂ O and adjust the pH to 8.0 prior to use add 500 µL RNase to 50 mL of total volume

Table 14: Solution P2

P2	
Preparation	8.0 g/L NaOH 100 mL SDS 10% (v/v) adjust to pH 5.5 using glacial acetic acid (~ 110 mL)

Table 15: Solution P3

P3	
Preparation	8.0 g/L NaOH 100 mL SDS 10% (v/v) adjust to pH 5.5 using glacial acetic acid (~ 110 mL)

DNA preparation and purification steps were performed according to the supplied manuals and additional application of the following kits.

Table 16: DNA preparation and purification kits

Kit	Producer
QIAquick Gel Extraction Kit (250)	Quiagen, Germany
QIAquick PCR Purification Kit (250)	Quiagen, Germany
In-Fusion Advantage PCR Cloning Kit w/Cloning Enhancer	Eubio, Austria

3.3.2 *Pichia pastoris* strains

P. pastoris strain X33 referred to as wild type, was used in this doctoral thesis and was provided by the Institute of Molecular Biotechnology at Graz University of Technology.

3.3.2.1 Cultivation of *P. pastoris* strains

For incubation and cultivation of these two strains of *P. pastoris* containing the right plasmids the Yeast Extract Peptone Dextrose (YPD) medium without additional antibiotics was used, as mentioned in Table 17.

Table 17: Composition of the YPD medium used for the cultivation of *P. pastoris* X33

YPD medium	
Ingredients	20 g/L Bacto peptone 10 g/L Bacto yeast extract D- Glucose Monohydrate 20 % (w/v)

For the preparation of the YPD medium peptone and yeast extract were dissolved in 900 mL of water and after autoclaving 100 mL of sterile 20 % (w/v) D- Glucose Monohydrate solution were added.

YPD agar plates were obtained by adding 15 g/L agar (Oxoid) additionally to the components of the YPD medium before autoclaving.

Antibiotics, if needed, were added at a temperature of 50 °C after sterilizing and cooling down the YPD medium. Thereby the final concentration of Zeocin was 100 µg/mL.

Agar plates were stored at + 4 °C.

For cultivating positive mini-preps (positive colonies were identified by colony PCR, see section 3.3.2.3) the final volume of the YPD medium was 50 mL with an end concentration of Zeocin of 25 µg/mL. This was necessary, because otherwise the cells were not able to grow.

P. pastoris strains were grown on 28 °C. Baffled shake flask cultures of *P. pastoris* containing the right plasmids were grown on 28 °C at 250 g for optimal oxygen intake.

For optimal expression of the protein domains every 24 hours 20 g/L D- Glucose were added to the medium.

3.3.2.1.1 Shake flask culture of *P. pastoris*

P. pastoris cells containing the appropriate plasmid were used to inoculate 100 mL YPD-media, The flasks were incubated at 28 °C, 250 g for 16-18 hours until the culture reached an OD₆₀₀ (optical density) of 2-6. The cells were harvested by centrifugation at 3000 g for 5 minutes at room temperature. The supernatant was discarded and the cell pellet was resuspended to an OD₆₀₀ of 1.0 in YPD medium. This solution was used to induce expression in 200 mL of YPD medium. Every 24 hours the GAP promoter was induced again by adding 20 g/L Glucose. After 96 hours the recombinant *P. pastoris* cells were removed from the growth medium by pelleting at low speed centrifugation (3000 g, 5 minutes at RT). The supernatant was then concentrated 10-fold with Amicon Ultra centrifugal filter units Ultra-15, MWCO 50 kDa in a swing- out rotor 11390/13150 (Sigma Laborzentrifugen, Germany) for 30 minutes at 4 °C.

The supernatant were analyzed for protein expression by colloidal Coomassie stained SDS-PAGE and Western Blot.

3.3.2.1.2 Freezing medium

For storing harvested *P. pastoris* cultures containing the appropriate plasmids safe at – 80 °C a freezing medium was generated. 500 µL overnight culture were added to 500 µL of 50 % (v/v) glycerine.

3.3.2.2 Preparation of competent cells of *Pichia pastoris* and Transformation

The preparation of the competent cells of *P. pastoris* X33 and the transformation was performed according to the ‘Condensed Protocol’ for competent cell preparation and transformation of the methylotrophic yeast *P. pastoris* [80].

A *P. pastoris* X33 culture was grown overnight in 50 mL YPD medium in a 28 °C shaking incubator. The yeast was grown to an OD₆₀₀: 0.8-1.0 and afterwards centrifuged at 500 g for 5 minutes. The resulting pellet was resuspended in 9 mL of ice-cold BEDS solution containing 100 mM DTT. Then the cell suspension was held tightly in hands at gently shaking for 5 minutes. The culture again was centrifuged at 500 g for 5 minutes and the pellet was resuspended in 1 mL of BEDS solution without DTT. Aliquots of the competent cells of 80 µL were prepared.

For transformation 800 ng of linearized plasmid DNA were mixed with 80 µL of competent cells in an electroporation cuvette (2.0 mm, BioRad) and kept on ice for 5 minutes.

The samples were electroporated using the following parameters: charging voltage 2.5 kV; number of pulses: 1.

After electroporation 0.5 mL of 1.0 M sorbitol and 0.5 mL YPD medium were added and the cells were regenerated in a thermocycler at 28 °C and 110 g for 120 minutes. 100 µL of the cell suspension were plated on YPD Agar plates containing 100 µg/mL Zeocin.

3.3.2.3 Colony PCR

To verify if the appropriate plasmid have been inserted, a colony PCR from the grown colonies was done. The rapid colony PCR method was performed to verify the presence of transformed DNA following the protocol of Thor et al. [81].

For this determination the oligos: 5'-GTA CCT GCA GCA TCA AAG CTA GGC GTA CCC-3' and 5'-GTA CGC GGC CGC TCC TGT AAC ACG AGC AGC G-3' were used for the amplification of the *tal6₆* gene and for the amplification of the *tal6₄* gene the primer pair 5'-

GTA CCT GCA GAC AGC ATC CCA TCT ATT TCG C-3' and 5'-GTA CTC TAG AGC TCC TGT AAC ACG AGC AGC GG-3' were used.

3.3.2.4 Transcript Analysis

RNA isolation from *P. pastoris* was done according to the manual of the EasySelect™ Pichia Expression Kit (Invitrogen). For the synthesis of the cDNA the Quick Protocol from Fermentas was used. 5 µg of the template RNA were used. The timepoints which had been investigated were 0, 24, and 48 hours.

Reverse transcription polymerase chain reaction (RT-PCR) of the genes *tal6₆* and *tal6₄* was carried out using the following oligos:

6LysM-fw: 5'-GTA CCT GCA GCA TCA AAG CTA GGC GTA CCC-3' and 6LysMRT-Rv: 5'-GGT TTC GTT GTA GCC GTA GGT AA-3'

4LysM-fw: 5'-GTA CCT GCA GAC AGC ATC CCA TCT ATT TCG C-3' and 4LysMRT-Rv: 5'-GGC TTA GAT GTA GTG GTG GGT AG-3'.

Table 18: Oligos which have been used for Real time PCR

Primer name	Sequence	Annealing Temperature [C°]	Fragment length [bp]
6LysM-fw 6LysMRT-Rv	5'-GTA CCT GCA GCA TCA AAG CTA GGC GTA CCC-3' 5'-GGT TTC GTT GTA GCC GTA GGT AA-3'	60.6	515
4LysM-fw 4LysMRT-Rv	5'-GTA CCT GCA GAC AGC ATC CCA TCT ATT TCG C-3' 5'-GGC TTA GAT GTA GTG GTG GGT AG-3'	60.3	557

3.3.3 Fungal strains

Trichoderma atroviride (teleomorph *Hypocrea atroviridis*) strains P1 (formerly *Trichoderma harzianum* ATCC 74058) and IMI 206040 were used in this thesis. Furthermore *Trichoderma reesei* (teleomorph *Hypocrea jecorina* QM 9414, *T. virens* Gv29-8, *Neurospora crassa* ATCC N402 and *Aspergillus niger* N402 were used in this doctoral thesis.

Fungal strains were provided by the Institute of Chemical Engineering, Research Area Gene Technology and Applied Biochemistry, Working Group Gene Technology at the Vienna University of Technology.

3.3.3.1 Cultivation of fungal strains

For cultivation of *T. atroviride*, Potato Dextrose Agar (PDA) and Potato Dextrose Broth (PDB) (both purchased from Difco, USA) were used. Fungi, except *A. niger*, were grown on 25 °C 12 hours at light/dark cycle. *A. niger* was grown on 28 °C. The cultivation of *N. crassa* was performed in eprouvettes with tilted agar.

For the transformation *T. atroviride* was grown on PDA plates covered with cellophane discs.

3.3.3.1.1 Shake flask cultures of *T. reesei*

T. reesei was grown in Mandels-Andreotti medium with glucose as carbon source [82]. Samples were taken after 24 and 48 hours and 15 mL of the supernatant were concentrated 10-fold with Amicon Ultra centrifugal filter units Ultra-15, MWCO 50 kDa in a swing-out rotor 11390/13150 (Sigma- Aldrich, Missouri, USA) for 30 minutes at 4000 g and 4 °C. Afterwards 250 µL of the concentrated supernatant were precipitated using the chloroform/methanol precipitation method for proteins (see Material and Methods 3.8.1). The proteins were analyzed by SDS- PAGE and Western blotting.

3.3.3.2 Transformation of *Trichoderma* spp.

3.3.3.2.1 Protoplasting

For transformation of fungal strains spore solutions were prepared by harvesting the spores with 6 mL of 0.8 % (w/v) NaCl and 0.09 % (v/v) Tween. The spores were removed from the

agar plate using a Drigalsky spatula and were then filtered through a glass wool Eppendorf tube with a small hole in the bottom. The spores were counted and diluted with the physiological salt solution to a final concentration of $\sim 10^7$ spores per 100 μL .

10 PDA plates with cellophane discs were prepared and 10^7 spores per plate were streaked out. The plates were incubated for 18 hours at 28 °C.

The next day the protoplasting solution was prepared. 0.2 g of Lysing Enzymes (*T. harzianum*) were added to 30 mL of solution A (Table 19). The solution was sterilized by filtration into a sterile 15 mL falcon tube. 2-3 mL of this enzyme solution were then pipetted into a sterile petri dish and covered with one cellophane disc with the germinated spores using sterile tweezers, again 2-3 mL of lysing solution were added and then a cellophane disc was added once again. This was repeated for five cellophane discs. Then the petri dishes with the cellophane discs were incubated for 90 minutes at 28 °C and 80 g. Every 30 minutes the petri dishes were taken out and the mycelium was gently pulled apart with sterile tweezers to guarantee complete moistening of the mycelium with the protoplasting solution. Additionally mycelial clumps were dispersed by gentle pipetting with a 1 mL tip which had the end cut off (in order to reduce shearing forces).

After incubation the protoplasts were harvested by filtering the protoplast suspension through a thin layer of glass wool, which had been plugged in a sterile glass funnel, into a sterile 50 mL falcon tube. Afterwards the glass wool was washed with a few mL of solution A. All steps concerning the harvesting and work with protoplasts were done on ice!

The protoplast solution was centrifuged for 10 minutes, 2000 g and at 4 °C in a swing-out rotor. Then the supernatant was removed cautiously and the pellet was resuspended in 4 mL of solution B (see Table 20). After a second centrifugation for 10 minutes, 2000 g at 4 °C, the protoplasts were resuspended in minimum of 400 μL of solution B and kept on ice.

3.3.3.2.2 Transformation

The transformation mixture was prepared by adding 10 μL of purified DNA (1 $\mu\text{g}/\mu\text{L}$) and 50 μL of PEG solution (Table 21) to 200 μL of protoplast suspension. The solution was mixed gently to dissolve the PEG and incubated for 20 minutes on ice. Then another 2 mL of PEG solution were added, again the solution was mixed gently and then was incubated for 5 minutes at room temperature. After 4 mL of solution B had been added, 800 μL of the transformation solution were pipetted to 4 mL of tempered overlay medium (see Table 22),

mixed shortly and then poured onto the bottom medium (see Table 23). The plates then were incubated at 28°C for 3- 4 days.

After 3- 4 days transformants were cut out with a needle and were transferred to agar plates containing the selective growth media. Transformants, which showed growth on these selection plates, were purified by single spore isolation and correct integration of the DNA was verified by PCR.

For transformations of the *epII* deletion cassette the selection marker *amdS* (Acetamid) was used. Therefore another medium was used for transformation and selection of single spores. For transformation the bottom and overlay medium containing *amdS* were used (see Table 24 and Table 25). The solutions used for transformation of *T. atroviride* and *T. reesei* are given in Tables 19, 20 and 21.

Table 19: Composition of Solution A

Solution A (200mL)	
Preparation	43.72 g Sorbitol (1.2 M) 2.72 g KH ₂ PO ₄ (0.1 M) adjust the pH to 5.6

Table 20: Composition of Solution B

Solution B (100mL)	
Preparation	18.22 g Sorbitol (1 M) 0.73 g CaCl ₂ (50 mM) adjust the pH to 7.5 by 1 mL 1 M TrisHCl (pH 7.5)

Table 21: Composition of PEG Solution

PEG Solution (100mL)	
Preparation	25 g PEG 6000 0.73 g CaCl ₂ (50 mM) adjust the pH to 7.5 by 1 mL 1 M TrisHCl (pH 7.5)

Table 22: Composition of the Overlay Medium

Overlay Medium	
Ingredients	Agarose 2 % (w/v) 182.17 g/L 1 M Sorbitol dissolve the components in dH ₂ O to a final volume of 1 L and add after autoclaving Hygromycin to a final concentration of 100 µg/ mL

Table 23: Composition of Bottom Medium

Bottom Medium	
Ingredients	37 g/L PDA 182.17 g/L 1 M Sorbitol dissolve the components in dH ₂ O to a final volume of 1 L and add after autoclaving Hygromycin to a final concentration of 100 µg/ mL

Table 24: Composition of *amdS* Medium (Bottom medium)

<i>amdS</i> containing Medium	
Ingredients	1 g MgSO ₄ 10 g KH ₂ PO ₄ 10 g Glucose 20 mL Trace element solution 15 g Agar Noble 182.17 g Sorbitol dissolve the components in dH ₂ O to a final volume of 1 L and add after autoclaving 10 mL of Acetamid (1 M)

Table 25: Composition of *amdS* Medium (Overlay medium)

<i>amdS</i> containing Medium (overlay medium)	
Ingredients	1 g MgSO ₄ 10 g KH ₂ PO ₄ 10 g Glucose 20 mL Trace element solution Agarose 2 % (w/v) 182.17 g Sorbitol dissolve the components in dH ₂ O to a final volume of 1 L and add after autoclaving 10 mL of Acetamid (1 M)

3.3.3.2.3 *Singe spore isolation*

Fungal transformants were picked by cutting small mycelial pieces (ca. 3 x 3 mm) from the transformation plates with a sterile needle and transferring them to PDA plates with 100 µg/mL hygromycin. For purifying the spores, which had grown on *amdS* containing medium the isolated single spores were kept on *amdS* medium (see Table 24) without sorbitol.

The transformants were consequently purified by two rounds of single spore isolation. This was achieved by gently pipetting 10 µL of 0.8 % (w/v) NaCl and 0.09 % (v/v) Tween solution on sporulated agar plates. The solution was mixed with the spores by pipetting the solution up and down, and then the 10 µL were plated out on a selection agar plate containing 0.1 % (v/v) Triton, which restricts colony growth. Fungal colonies growing in these agar plates from single spores were picked by cutting out small mycelial pieces with a sterile needle, and transferred to PDA plates without any selection marker and afterwards from these agar plates a sporulated, mycelial piece was transferred to PDA plates containing 100 µg/mL hygromycin.

3.3.3.3 *Fungal DNA isolation*

The fungal DNA isolation in this thesis was performed according to the protocol of the DNA Quick isolation method interpreted by Rita Linke and Andre Schuster from our research division.

With a sterile needle a little piece of the mycelium grown on an agar plate was cut out and transferred into a Eppendorf tube that contained glass beads 0.75-1.0 mm and glass perls 0.25-0.50 mm (Carl Roth GmbH, Germany) and 500 µL lysis buffer (Table 26). The tubes were immediately vortexed and incubated on a thermomixer compact 5350 at 68 °C for 30 minutes. 150 µL of solution P3, which is also used for the DNA isolation of *E. coli* (Table 15), were added and the tubes were vortexed again. The samples were centrifuged at 13000 *g* for 30 minutes at 4 °C. The supernatant was transferred into a new tube and 500 µL of isopropanol were added to each tube and vortexed. For optimal precipitation of the DNA the samples were stored for 2 hours at – 20 °C and were afterwards centrifuged at maximum speed at 4 °C. Then the pellets were washed with 500 µL of 75 % (v/v) EtOH and were air-dried for about 10 minutes and afterwards dissolved in 30 µL dH₂O.

For RNA degradation the samples were treated with RNase. 3 µL of RNase (10 mg/mL) were pipetted to each tube and were incubated at 37 °C für 2 hours.

Table 26: Preparation of the Lysis buffer of *T. atroviride*

Lysis buffer for <i>T. atroviride</i>	
Preparation	48.45 g/L Tris 17.53 g/L EDTA 8.76 g/L NaCl dissolve all components and adjust the pH to 8.0 then add 10 g/L SDS

3.4 Plasmids and deletion cassettes

Plasmids and construction of vectors which have been used for the overexpression of TAL₆ and TAL₄ in *P. pastoris* are shown in this section. For the overexpression the manipulated expression plasmids were used. Starting material pPICZB α and pPICZB (Fig. 3 and Fig. 4) were purchased from Invitrogen. Secretion of the desired protein is provided by the alpha factor sequence of *P. pastoris*, which is included in pPICZB α .

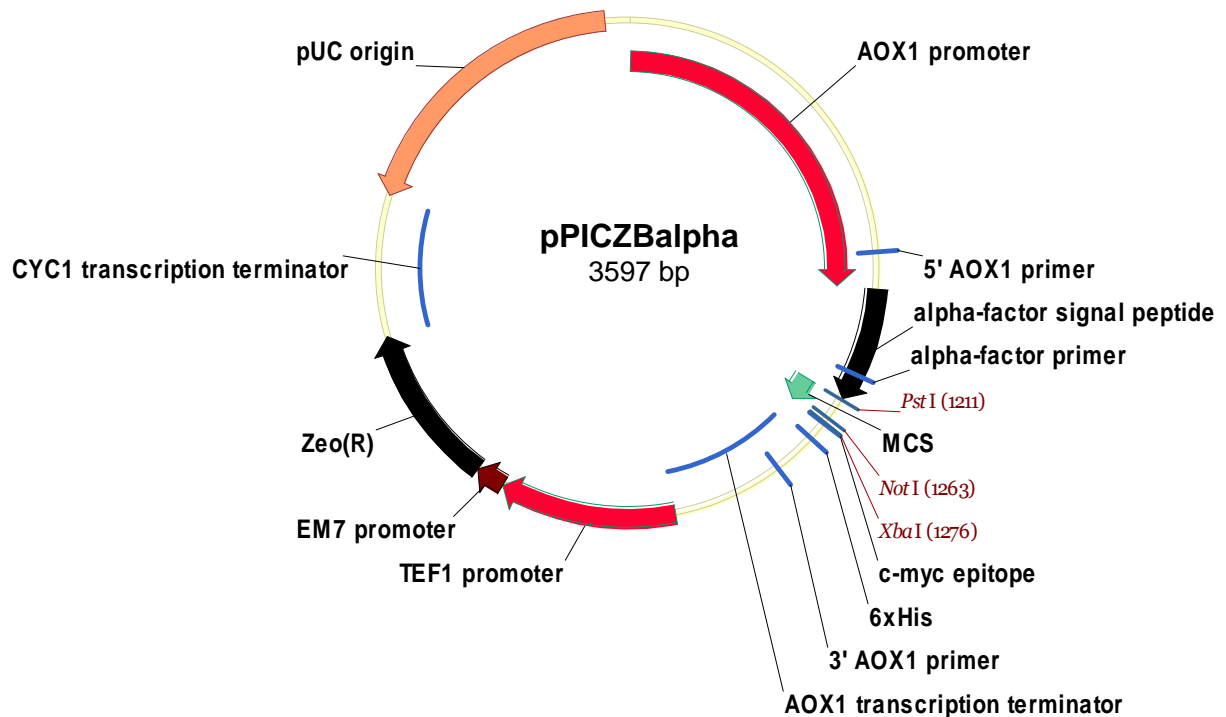


Fig. 3: pPICZB α is commercially available from Invitrogen. The expression vector contains the AOX₁ promoter (alcohol oxidase), the alpha factor, Zeo(R) Zeocin resistance gene, pUC origin for *E.coli* and the Polyhistidine (6xHis) tag.

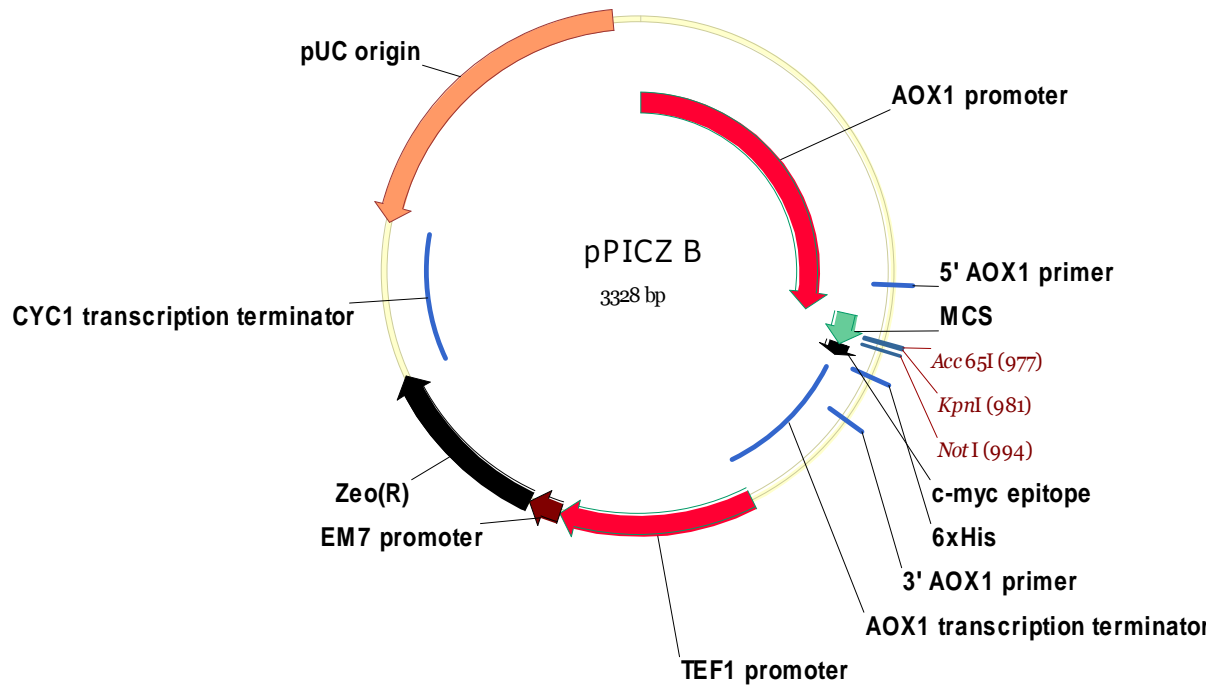


Fig. 4: pPICZB is commercially available from Invitrogen. The expression vector contains the AOX₁ promoter (alcohol oxidase), Zeo(R) Zeocin resistance gene, pUC origin for *E. coli* and the Polyhistidine (6xHis) tag.

3.4.1 Construction of the plasmids

3.4.1.1 Construction of the plasmid pTAL6₆

All the mentioned PCR reactions were carried out by using the GoTaq® DNA Polymerase (Promega GmbH, Germany). In common the PCR reactions are performed according to the supplier's recommendation.

First the genes coding for the protein domains were amplified by polymerase chain reaction (PCR) using the following primer pair for *tal6₆*: 6LysM-Fw: 5'-GTA CCT GCA GCA TCA AAG CTA GGC GTA CCC-3' and 6LysM-Rv: 5'-GTA CGC GGC CGC TCC TGT AAC ACG AGC AGC G-3' with flanking *Pst*I and *Not*I restriction sites. This PCR fragment was cloned into the corresponding sites of the pPICZB α transformed into *E. coli* JM109 cells, which were selected positively for Zeocin resistance. Since no efficient protein production could be achieved with this plasmid, the AOX₁ (alcohol oxidase) promoter was exchanged with the constitutive GAP (glyceraldehyde-3-phosphate dehydrogenase) promoter (pGAP). For this the oligos GAPBglII_Fw: 5'-GAT AGA TCT GAT CTT TTT TGT AGA AAT GTC TTG GTG-3' and AlphaPstI_Rv : 5'-GAT CCT CGA AGC TTC GGC CTC TCT CTT CTC GA-3' were used to amplify the coding sequence from pGemTGAP (TU Graz) with flanking

*Bgl*III and *Pst*I restriction sites. This PCR fragment was then cloned into the corresponding sites of the pPICZBa transformed into the JM109 cells, which were selected for Zeocin resistance. The resulting plasmid was named pTAL6₆ (Fig. 5).

The plasmid was linearized with *Bst*XI and transformed into *P. pastoris* (see transformation into *P. pastoris* 3.3.2.2).

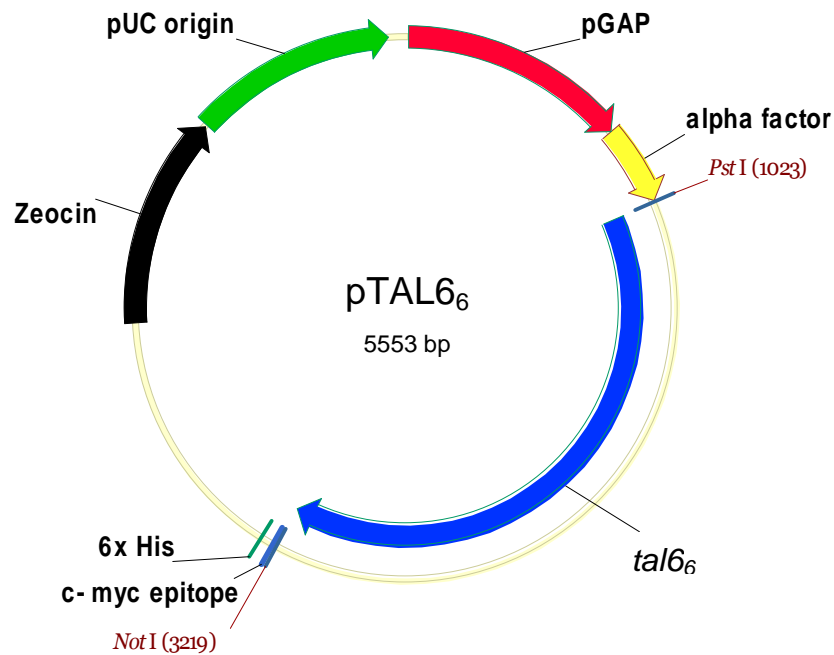


Fig. 5: Plasmid pTAL6₆, which was constructed in this thesis. The expression vector contains the constitutive GAP (glyceraldehyde-3-phosphate dehydrogenase) promoter (pGAP), the *tal6*₆ gene (2193bp), the alpha factor for secreted expression, Zeo(R) Zeocin resistance gene, pUC origin for *E. coli*, and the Polyhistidine (6xHis) tag.

3.4.1.2 Construction of the plasmid pTAL6₄

In analogy to what was described above for pTAL6₆, plasmid pTAL6₄ was constructed. The *tal6*₄ gene was amplified by PCR using the oligos: 4LysM-Fw: 5'-GTA CCT GCA GAC AGC ATC CCA TCT ATT TCG C-3' and 4LysM-R: 5'-GTA CTC TAG AGC TCC TGT AAC ACG AGC AGC GG-3' with flanking restriction sites *Pst*I and *Xba*I. This PCR fragment was then cloned into the corresponding sites of the pPICZBa transformed into the JM109 cells, which were selected positively for Zeocin resistance using low salt LB medium (ref Invitrogen handbook). Since no efficient protein production could be achieved with this plasmid, the AOX1 (alcohol oxidase) promoter was exchanged with the constitutive GAP

(glyceraldehyde-3-phosphate dehydrogenase) promoter (pGAP). For this the oligos GAPBglII_Fw: 5'-GAT AGA TCT GAT CTT TTT TGT AGA AAT GTC TTG GTG-3' and AlphaPstI_Rv : 5'-GAT CCT CGA AGC TTC GGC CTC TCT CTT CTC GA-3' were used to amplify the coding sequence from pGemTGAP (TU Graz) with flanking *Bgl*II and *Pst*I restriction sites. This PCR fragment was then cloned into the corresponding sites of the pPICZB α transformed into *E. coli* JM109 cells, which were selected for Zeocin resistance. The plasmid was linearized with *Bst*XI and transformed into *P. pastoris* (see transformation of *P. pastoris* 3.3.2.2).

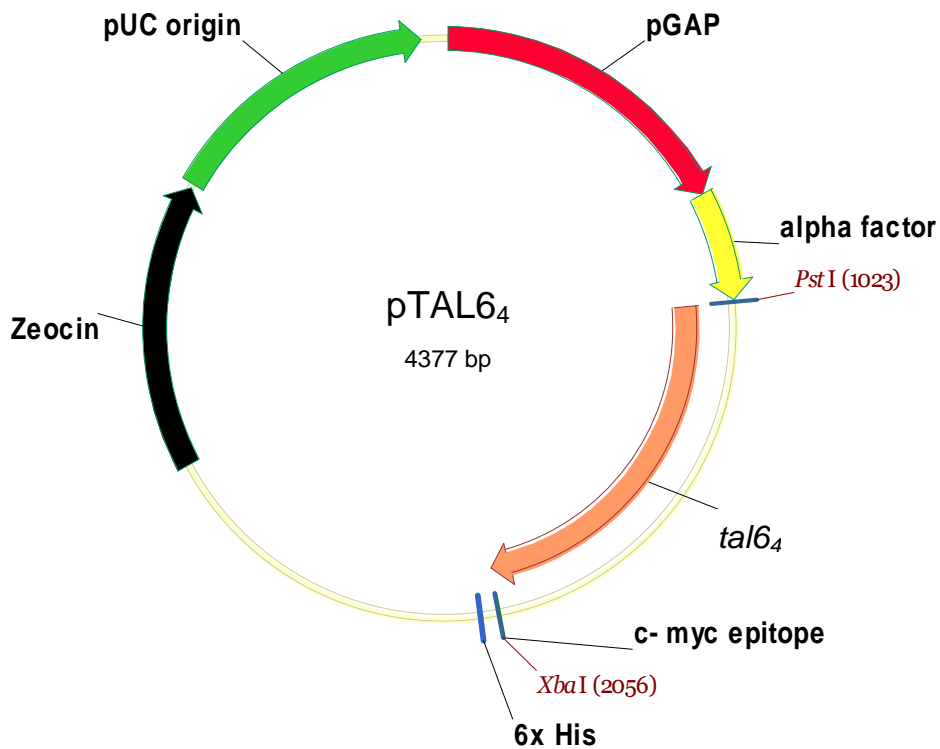


Fig. 6: Plasmid pTAL6₄, constructed in this thesis. The expression vector contains constitutive GAP (glyceraldehyde-3-phosphate dehydrogenase) promoter (pGAP), the *tal*6₄ gene (1030bp), the alpha factor for secreted expression, Zeo(R) Zeocin resistance gene, pUC origin for *E. coli*, and the Polyhistidine (6xHis) tag.

3.4.1.3 Construction of the plasmid pTAL6₆Tr

For expression of TAL6₆ in *T. reesei* a plasmid containing the genomic DNA (with introns) of *tal*6₆ was constructed (pTAL6₆Tr). The construction of pTAL6₆Tr was carried out using the oligos 6LysMAcc65I_Fw: 5'-GTA CCT GGT ACC TCA AAG CTA GGC GTA CCC-3' and 6LysM-Rv: 5'-GTA CGC GGC CGC TCC TGT AAC ACG AGC AGC G-3' to amplify the

tal6₆ gene with introns and with the flanking *Acc65I* and *NotI* restriction sites. This PCR fragment was then cloned into the corresponding sites of the pPICZB and transformed into the *E. coli* JM109 cells, which were selected positively for Zeocin resistance.

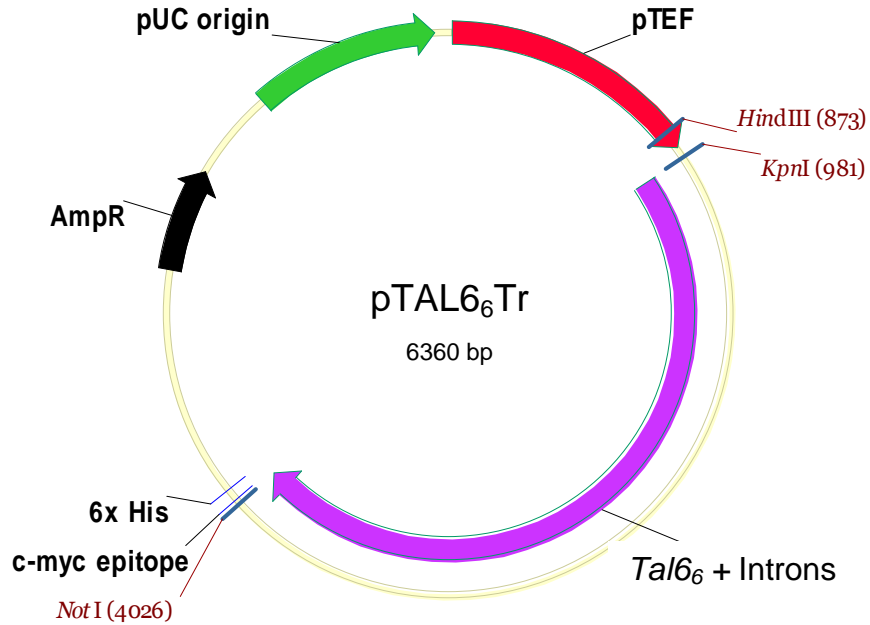


Fig. 7: Plasmid pTAL6₆Tr constructed in this thesis. The expression vector contains the TEF (translation elongation factor 1 alpha) *t6l* gene including introns (2700bp), Amp^R Ampicillin resistance gene, pUC origin for *E. coli*, and the Polyhistidine (6xHis) tag

3.4.2 PCR details to the section 3.4.1

In the following details of the PCRs used in this section are listed.

Table 27: Oligos which have been used for the amplification of *tal6₆* and *tal6₄*

Primer name	Sequence	Annealing Temperature [C°]	Fragment length [bp]
6LysM-Fw	5'-GTA CCT GCA GCA TCA AAG CTA GGC GTA CCC-3'	59	2193
6LysM-Rv	5'-GTA CGC GGC CGC TCC TGT AAC ACG AGC AGC G-3'		
4LysM-Fw	5'-GTA CCT GCA GAC AGC ATC CCA TCT ATT TCG C-3'	60	1030
4LysM-Rv	5'-GTA CTC TAG AGC TCC TGT AAC ACG AGC AGC GG-3'		
6LysMAcc65IFw	5'-GTA CCT GGT ACC TCA AAG CTA GGC GTA CCC-3'	64	2700
6LysM-Rv	5'-GTA CGC GGC CGC TCC TGT AAC ACG AGC AGC G-3'		

Table 28: Components which were used for the setup of the PCR reaction done with the GoTaq® DNA Polymerase.

PCR Ingredients GoTaq® DNA Polymerase	
Ingredients	Volume [µL]
5X Green reaction buffer	10
MgCl ₂ (25 mM)	5
dNTP's 10mM	1
forward primer	1
reverse primer	1
GoTaq® DNA Polymerase	0.5
dH ₂ O	31.5
Total	50

Table 29: Cycling conditions using the GoTaq® DNA Polymerase

Thermal cycling conditions GoTaq® DNA Polymerase			
Step	Temperature	Time	Number of cycles
Initial denaturation	95 °C	1 min	1
Denaturation	95 °C	1 min	
Annealing	50-65 °C	1 min	30
Extension	72 °C	1 min/kb	
Final extension	72 °C	5 min	1
	16 °C	hold	1

3.4.3 Deletion cassettes for generation of *epl*- and *epl2*-knockout strains in *T. atroviride*.

In order to be able to generate *epl*- and *epl2*-knockout strains in *T. atroviride*, the respective genes were deleted by targeted gene replacement. For the *epl1* deletion cassette the selection marker was the *amds* gene, which enables growth on acetamide as the sole nitrogen source and for the *epl2* deletion cassette the selection marker used was *hph* (hygromycin phosphotransferase).

The target gene is replaced by a selection marker cassette (containing the selection marker gene with a promoter and a terminator) by a double cross over mechanism. In order to achieve homologous recombination, the knockout cassette must contain the up- and downstream flanking regions of the target gene. These flanking regions consist of fragments of 500 – 1000 bp of the DNA regions that are upstream of the coding region (= promoter, 5'-flanking region) and downstream of the coding region (= terminator, 3'-flanking region) of the target gene. These regions had to be cloned into the vector containing the selection marker gene near the beginning/ end of the selection marker cassette.

3.4.3.1 Construction of the *epl1* deletion cassette

In Fig. 8 the native *epl1* gene and the *epl1*-knockout cassette are shown. The promoter and the terminator of the *amds* gene the original ones isolated from *Aspergillus*.

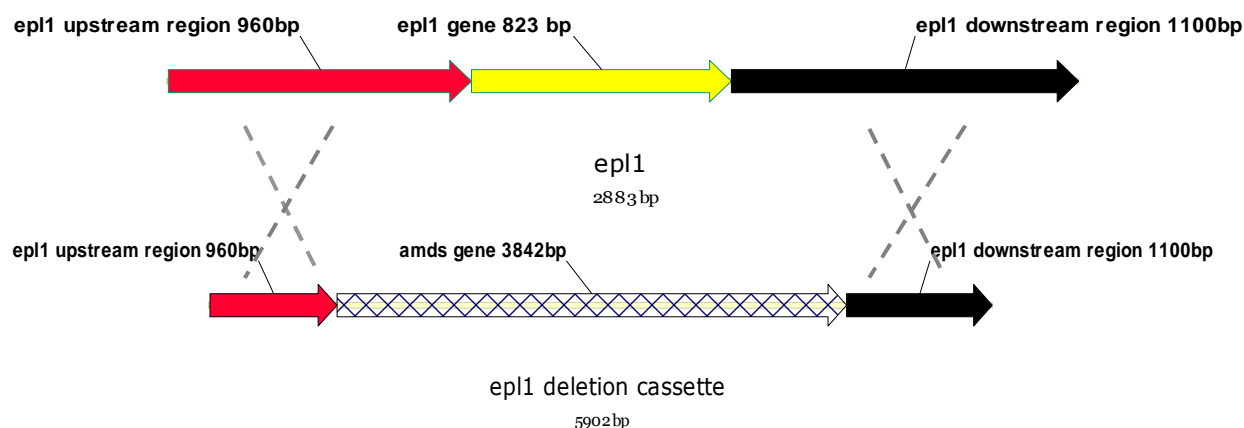


Fig. 8: Schematic illustration of double cross over mechanism to create the *epl1* deletion cassette. The *amds* gene, which is regulated by the original promoter and terminator of *Aspergillus* replaces the *epl1* gene.

A pBlueScript SK⁺ containing the *amds* gene was generated. This was done by excising the *amds* gene from the p3SH2 vector with *SalI* and *Acc65I* and inserting into the same sites of the pBlueScript SK⁺ (Fig. 9).

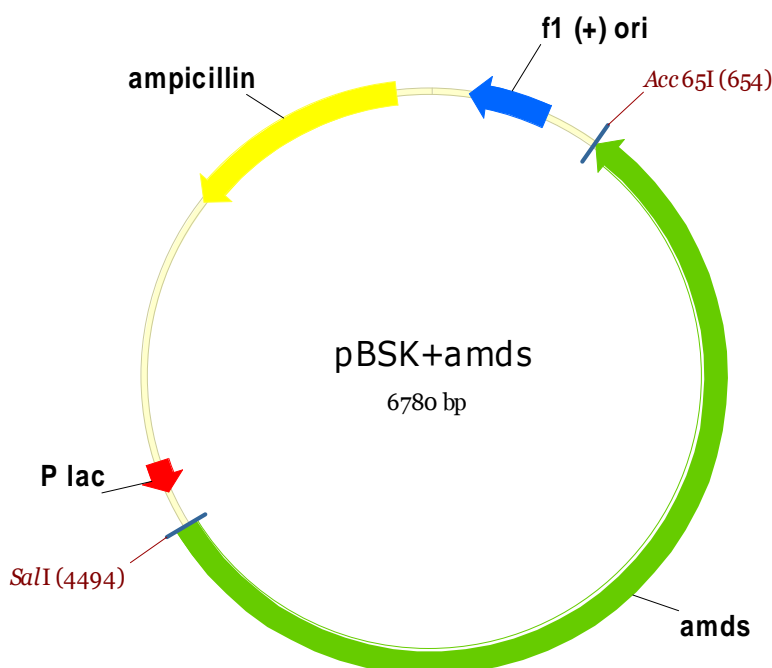


Fig. 9: Vector map of pBlueScript SK⁺ containing the *amds* gene (3842bp), P (lac): promoter of the *E. coli* lac operon, Ampicillin: Ampicillin resistance gene, f1 (-) ori: f1 origin of replication.

For the construction of the *epl1* deletion cassette 1 kb of the up- and downstream non-coding region of the *T. atroviride* P1 *epl1* were amplified using the primer pairs *epl1amdSProm_Fw* and *epl1amdSProm_Rv*, respectively.

The promoter fragment in the size of 960 bp and a terminator fragment in the size of 1100bp, were amplified using the GoTaq® DNA Polymerase and the following oligos: *epl1amdSProm_Fw*: 5'-TAT CGA TAC CGT CGA CGC TGC TAG CAA GAA GAA CT-3' and *epl1amdSProm_Rv* 5'-TAC TCA AGA CGT CGA CAA GCT GAG TAG TAG TGA AGC GAA-3' and for the terminator fragment the oligos: *epl1amdSTerm_F* 5'-CTC AAC CAT GGT ACC GAC CAT TAT GGA ATT GCA TCG-3' and *epl1amdSTerm_R* 5'-GGG CGA ATT GGG TAC CAC AGT CGT CGA TGT AAG T-3' were used. Thereby the sequence of the forward primer contained a 15 bp sequence with the *SalI* restriction site of the pBSK⁺ *amds* vector followed by the sequence of the 5' region of the upstream flanking region of the *epl1* gene. The sequence of the reverse primer contained a 16 bp region of the *amds* selection cassette containing a *SalI* restriction site, which had been inserted into the pBSK⁺ *amds* vector followed by the sequence of the 3' region of the upstream flanking region of the *epl1* gene. Similarly, for amplification of the terminator fragment the primer contained a 16 bp region of the *amds* selection cassette containing the *Acc65I* restriction site followed by the sequence of the 5' region of the downstream flanking region of the *epl1* gene, and the reverse primer contained a sequence with the *Acc65I* restriction site of the pBSK⁺ *amds* vector followed by the sequence of the 3' region of the downstream flanking region of the *epl1* gene. These 'overlapping' primers enabled the insertion of the respective DNA fragments into the vector that was first linearized using the respective restriction sites using the In-Fusion Advantage PCR Cloning Kit w/Cloning Enhancer (Eubio, Austria). The 960 bp *epl1* promoter fragment and the linearized pBSK⁺ *amds* vector were first recombined and transformed into One Shot TOP10 Chemically Competent *E. coli*- C4040-03 cells (Invitrogen).

Grown colonies were verified by digesting with *SalI*. Positive colonies were digested with *Acc65I*. In a second step the terminator region was recombined to the promoter- pBSK⁺ *amds* fragment using again the In-Fusion Advantage PCR Cloning Kit w/Cloning Enhancer (Eubio, Austria). The transformation was carried out in One Shot TOP10 Chemically Competent *E. coli* cells C4040-03 (Invitrogen) according to the instructions of the supplied manual. Grown colonies were verified as positive by digesting with *Acc65I*.

The *eplI* deletion cassette was amplified using the Roche Expand Long Template PCR System (Roche, Austria) according to the manual and the outer primer pair: *eplIamdSProm_Fw* 5'-TAT CGA TAC CGT CGA CGC TGC TAG CAA GAA GAA CT-3' and *eplIamdSTerm_Rv* 5'-GGG CGA ATT GGG TAC CAC AGT CGT CGA TGT AAG T-3'. The *eplI* deletion cassette was then transformed into *T. atroviride*. (see section 3.3.3.2.)

3.4.3.1.1 PCR details to section 3.4.3.1

In the following details of the PCRs used in this section are listed.

Table 30: Oligos that were used for the amplification of *eplI* deletion cassette

Primer name	Sequence	Annealing Temperature [C°]	Fragment length [bp]
<i>eplIamdSProm_Fw</i>	5'-TAT CGA TAC CGT CGA CGC TGC TAG CAA GAA GAA CT-3'	55.3	960
<i>eplIamdSProm_Rv</i>	5'-TAC TCA AGA CGT CGA CAA GCT GAG TAG TAG TGA AGC GAA-3'		
<i>eplIamdSTerm_Fw</i>	5'-CTC AAC CAT GGT ACC GAC CAT TAT GGA ATT GCA TCG-3'	54.5	1100
<i>eplIamdSTerm_Rv</i>	5'-GGG CGA ATT GGG TAC CAC AGT CGT CGA TGT AAG T-3'		
<i>eplIamdSProm_Fw</i>	5'-TAT CGA TAC CGT CGA CGC TGC TAG CAA GAA GAA CT-3'	54.5	5902
<i>eplIamdSTerm_Rv</i>	5'-GGG CGA ATT GGG TAC CAC AGT CGT CGA TGT AAG T-3'		

Table 31: Components that were used for the setup of the PCR reaction carried out with the Roche Expand Long Template PCR System

PCR Ingredients Roche Expand Long Template PCR System	
Ingredients	Volume [μL]
10x PCR Buffer	5
10 mM dNTP's	1.75
upstream primer	1.5
downstream primer	1.5
Expand Long Template PCR mix	0.5
dH ₂ O	39.75
Total	50

Table 32: Cycling conditions using the Expand Long Template PCR mix

Thermal cycling conditions Roche Expand Long Template PCR System			
Step	Temperature	Time	Number of cycles
Initial denaturation	94 °C	2 min	1
Denaturation	94 °C	10 sec	10
Annealing	40-65 °C	30 sec	
Extension	68 °C	2 min	
Denaturation	94 °C	10 sec	25
Annealing	40-65 °C	30 sec	
Extension	68 °C	2 min +20 sec	
Final extension	68 °C	7 min	1
	4 °C	hold	1

3.4.3.1.2 Verification of *epl1*-knockout strains in *T. atroviride*

Fungal transformants were checked for homologous (gene knockout) vs. heterologous integration by PCR using the GoTaq® DNA Polymerase (Promega, Germany) using two primer combinations given in Table 33:

Table 33: Oligos that were used for verification of *epl1*-knockout strains

Primer name	Sequence	Annealing Temperature [C°]	Fragment length [bp]
epl1 trafo-check_Fw	5'-ACA TCC TAC TCG TAC ATG CA-3'	55.3	WT: 2100 KO: 5942
epl1trafo-check_Rv	5'-CCA TTT CTC GGC TAG TAT TG-3'		
epl1 trafo-check_Fw	5'-ACA TCC TAC TCG TAC ATG CA-3'	55.3	3756
amds RV	5'-CCA GAG CTC GTT CAT GTT AAC AGC-3'		

Components, which were used for the PCR setup and the adequate cycling conditions, can be seen in Table 31 and Table 32, respectively.

3.4.3.2 Construction of the *epl2* deletion cassette

For the construction of the *epl2* deletion cassette no In-Fusion Advantage PCR Cloning Kit w/Cloning Enhancer has been used.

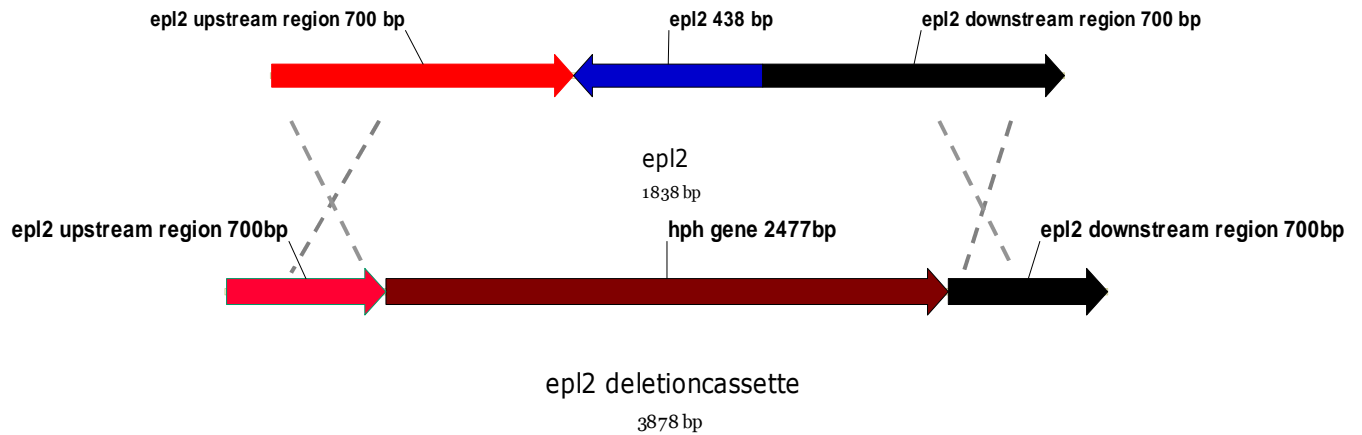


Fig. 10: Schematic illustration of the double cross over mechanism of *epl2* to create the *epl2* deletion cassette.

For the construction of the *epl2* deletion cassette the pJHepI2 vector (see Fig. 11) was constructed, which was part of the bachelor project of Jasmin Hauzenberger.

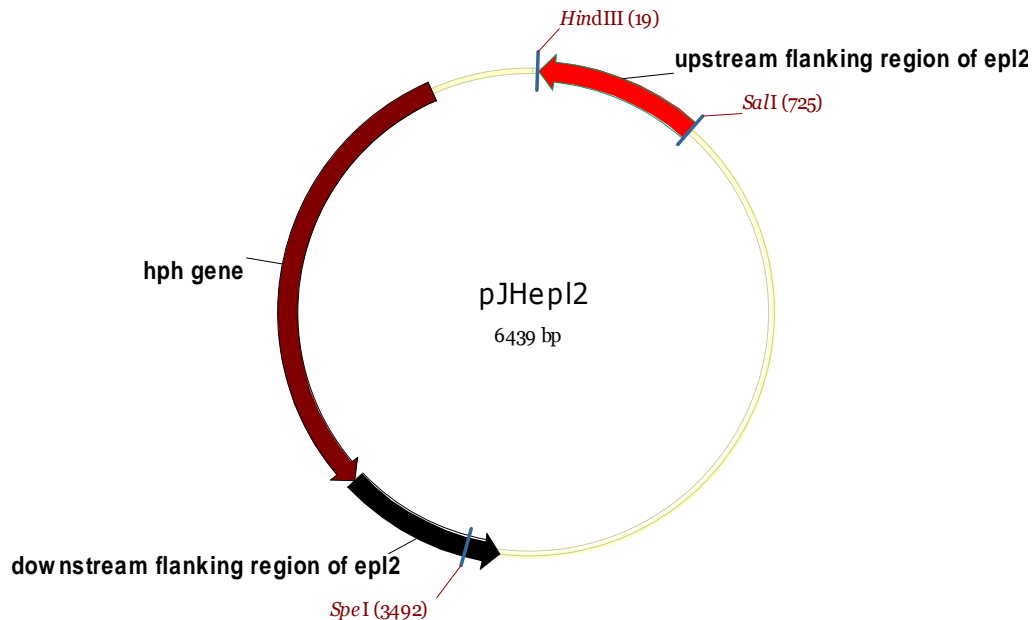


Fig. 11: Schematic illustration of the pJHepI2 vector. The vector contains the *hph* gene (hygromycin-phosphotransferase gene), flanked by the promoter and the terminator region of *epl2*.

The pJHepl2 vector was constructed to contain a fungal selection marker, the *hph* gene (regulated by the *T. reesei pki* promoter and *T. reesei cbh2* terminator), and to be able to conduct the double cross over mechanism, the up- and downstream non coding regions of the *epl2* gene of *T. atroviride*.

For that the pLOX vector, which included the hygromycin-phosphotransferase gene (*hph*) was double digested with *HindIII* and *SalI*. At the same time the up- and downstream non coding regions of the *epl2* gene were amplified by PCR using the GoTaq® DNA Polymerase (Promega, Germany) and the following primer pairs. For the upstream non flanking region of the *epl2* gene, which functions as promoter, the oligos: epl2HindIII_Fw 5'- GTA CAA GCT TGC TGG CTG TCA ACT GCA TGT C-3' and epl2SalI_Rv 5'- GTA CGT CGA CGT ATG AGA AGC GTC GAA GAG G-3' were used. The downstream non coding region of the *epl2* gene which functions as terminator was amplified by using the oligos: epl2SpeI_Fw 5'- GTA CAC TAG TCT TTG CGG CCG TTT TCT C-3' and epl2SpeI_Rv 5'- : GTA CAC TAG TTT TCC ATG TGC TCG ACT TAC-3'. The promoter fragment was double digested using the *HindIII* and the *SalI* enzymes and then ligated into the pLOX vector. The pLOX vector containing the promoter fragment was then digested with *SpeI* and dephosphorylated. Prior to the ligation of the terminator fragment into the pLOX vector containing the promoter fragment, the terminator fragment was also *SpeI* digested and then ligated.

Then the *epl2* deletion cassette was amplified using the GoTaq® DNA Polymerase (Promega, Germany) according to user's manual and the outer primer pair: epl2HindIII_Fw 5'-GTACAA GCT TGC TGG CTG TCA ACT GCA TGT C-3' and epl2SpeI_Rv 5'-GTA CAC TAG TTT TCC ATG TGC TCG ACT TAC G-3'. The *epl2* deletion cassette was then transformed into *T. atroviride* (see section 3.3.3.2).

3.4.3.2.1 PCR details to section 3.4.3.2

In the following details of the PCRs used in this section are listed.

Table 34: oligos which have been used for the amplification of *epl2* deletion cassette

Primer name	Sequence	Annealing Temperature [C°]	Fragment length [bp]
epl2HindIII_Fw	5'- GTA CAA GCT TGC TGG CTG TCA ACT GCA TGT C-3'	59.8	700
epl2SalI_Rv	5'- GTA CGT CGA CGT ATG AGA AGC GTC GAA GAG G-3'		
epl2SpeI_Fw	5'- GTA CAC TAG TCT TTG CGG CCG TTT TCT C-3'	55.2	700
epl2SpeI_Rv	5'- : GTA CAC TAG TTT TCC ATG TGC TCG ACT TAC-3'		
epl2HindIII_Fw	5'-GTACAA GCT TGC TGG CTG TCA ACT GCA TGT C-3'	57.9	1901
epl2SpeI_Rv	5'-GTA CAC TAG TTT TCC ATG TGC TCG ACT TAC G-3'		

Table 35: Components which were used for the setup of the PCR reaction done with the GoTaq® DNA Polymerase.

PCR Ingredients GoTaq® DNA Polymerase	
Ingredients	Volume [µL]
5X Green reaction buffer	10
MgCl ₂ (25 mM)	5
dNTP's 10mM	1
upstream primer	1
downstream primer	1
GoTaq® DNA Polymerase	0.5
dH ₂ O	31.5
Total	50

Table 36: Cycling conditions using the GoTaq® DNA Polymerase

Thermal cycling conditions GoTaq® DNA Polymerase			
Step	Temperature	Time	Number of cycles
Initial denaturation	95°C	1 min	1
Denaturation	95°C	1 min	
Annealing	50-65°C	1 min	30
Extension	72°C	1 min/kb	
Final extension	72°C	5 min	1
Soak	4°C	indefinite	1

3.4.3.2.2 *epl2*-knockout verification

Potentially knock- outs were identified by PCR using the GoTaq® DNA Polymerase (Promega, Germany) by using two primer combinations as can be seen in table 31.

Table 37: oligos which have been used for the verification of *epl2* knockout

Primer name	Sequence	Annealing Temperature [C°]	Fragment length [bp]
epl2 trafo-check_Fw	5'-GCA GCA GTG TGT CTC AGT TG-3'	58.8	WT: 1501
epl2trafo-check_Rv	5'-GCT AAT GAT GTA TGT GAC CCA-3'		KO: 3621
hphSG_Fw	5'-CGC AAG GAA TCG GTC AAT AC-3'	55.2	2517
epl2trafo-check_Rv	5'-ATC CTG CTG TTA CGG CCT G-3'		

Components, which have been used for the PCR setup and the adequate cycling conditions, can be seen in Table 35 and Table 36, respectively.

3.5 Fermentation setup of *P. pastoris* TAL6₆- and TAL6₄-expression strains

Fermentations were performed in a stirred Labfors S- 000115999 bioreactor (Infors HAT, Switzerland) with a working volume of 2 L and a total volume of 3 L. The reactor was started at 28 °C and 1200 g with 500 mL of 4- fold concentrated YPD medium. The airflow was kept constant at the maximum of the system (2 L/min) and the pH was maintained at 5.0 by 30 % (v/v) NH₄OH. The dissolved oxygen (dO₂) was higher than 40 % during the whole fermentation to avoid oxygen limitation. The flask inoculum (100 mL of YPD medium) was inoculated with a single colony of positive transformants of TAL6₆ and TAL6₄ and cultured in an Incubator Infors HT Multitron (Infors HT, Switzerland) for 20 hours at 28 °C, 250 g. 100 mL of the preculture were used to seed the medium in the bioreactor. The end of the batch was indicated by a sharp decrease of CO₂ in the offgas. Afterwards, a pulse of 500 mL 4- fold concentrated YPD media containing 80 g/L glucose was carried out to further increase the biomass concentration and concomitantly the product content. The fermentation was carried out for about 72 hours. Then the protein broth was centrifuged in a RC-3B centrifuge (Sorvall Instruments) for 2 hours at 10000 g.

3.6 Protein purification of recombinant TAL6₆ and TAL6₄

For purification of the overexpressed TAL6₆ and TAL6₄ proteins containing His-tags, the ÄKTATM purifier (Amersham Pharmacia Biotech, NY, USA) was used. The culture supernatants from *P. pastoris* fermentations of the respective strains (see above) were harvested and filtered through SteritopTM Filter Units 0.22 µm (Millipore). 250 mL of the filtered supernatant were concentrated in Amicon Ultra centrifugal filter units Ultra-15, MWCO 50 kDa in a swing- out rotor 11390/13150 (Sigma Laborzentrifugen, Germany) for 30 minutes at 4000 g and 4°C and the buffer changed into 20 mM Tris- HCl buffer pH 7.5 using these devices.

For protein purification a HiScale16 column 30 mL (GE Healthcare, Sweden) and HisTrapTM HP columns 1 mL (GE Healthcare, Sweden) were used. The HiScale16 column was packed manually with a ProBondTM Nickel-Chelating Resin (Invitrogen, Austria) while the HisTrapTM HP columns were purchased ready to use. HisTrap HP 1 ml columns are designed

for simple, one-step purification of histidine-tagged proteins. The columns were used according to the supplied manual of the HisTrap™ HP column.

Detection was performed by an online conductivity meter and a UV detector adjusted at 280 nm. The software controlling and creating the individual methods were performed with the programs Unicorn 4.11 and MODDE 7.0.

The method included a gradient consisting of a buffer (A), which had a low concentration of imidazole (2 mM) and buffer (B) containing a high concentration of imidazole (500 mM). For buffer preparation the composition can be seen in Table 38 and 39. The application was designed to start with a low salt concentration in solvent A and a higher salt concentration in solvent B.

10 mL of concentrated and buffer changed supernatant of the proteins were loaded manually on the column by using a 10 mL Superloop™ (GE Healthcare). Prior to the purification started a washing step using 5 column volumes (CV) with buffer A was implemented until the absorbance reached the baseline. Fractions which showed a peak at 280 nm were collected and long term stored at -20 °C.

In the following tables the compositions of buffers are listed that were used for purification of recombinant TAL6₆- and TAL6₄ containing His-tags. All buffers which were used for ÄKTA purification were filtered sterile before use.

Table 38: Preparation of the Binding buffer

Binding Buffer	
Preparation	12.12 g/L Tris 29.22 g/L NaCl 0.14 g/L Imidazole dissolve all components and adjust the pH to 7.5

Table 39: Preparation of the Elution buffer

Elution Buffer	
Preparation	12.12 g/L Tris 29.22 g/L NaCl 34.04 g/L Imidazole dissolve all components and adjust the pH to 7.5

3.7 Protein extraction from the biomass

To verify that the TAL6₆ and TAL6₄ are secreted proteins, total intracellular and cell wall bound proteins from the biomass were also extracted and checked on SDS-gels. 2 g of the harvested biomass was resuspended in 20 mL of 20 mM Tris HCl buffer pH 7.5. The cells were lysed using an EmulsiFlex-C3 Homogenizer (AVESTIN, Mannheim, Germany). Cell debris was removed by centrifugation for 20 minutes, 13000 g at +4 °C. Afterwards the cell debris were consecutively extracted with different detergents: 1 % (v/v) Triton, 2 % (w/v) CHAPS, 1 % (v/v) Tween and the protein extracts were analyzed by SDS- PAGE and Western blot analysis.

3.8 SDS- PAGE

Prior to performing SDS- PAGE or Western blot analysis the proteins were concentrated by using a Chloroform and Methanol precipitation.

3.8.1 Chloroform/ methanol precipitation of proteins

Using 250 µL from the supernatant (either from shake flasks or from purified Äkta fractions) a chloroform and methanol precipitation was performed according to the protocol of Wessel et al. [83]. The resulting pellets were dissolved in 30 µL of Tris HCl buffer pH 7.5.

For protein electrophoresis 10 % polyacrylamid gels were generated for preparation see (Table 40- 42) [84].

Preparation of the protein samples was done by mixing 30 µg of supernatant with the sample loading buffer (Table 44) and incubating them at 95 °C for 5 minutes. Then the samples were centrifuged for 1 minute at high speed (13000 g). 30 µL of each sample were loaded on SDS-gels.

PageRuler™ Prestained Protein Ladder SM0671 (Fermentas) was used as protein size marker. The electrophoresis was performed at 200 V using BioRad Mini-PROTEAN devices. Afterwards the SDS- gels were stained with colloidal Coomassie overnight and destained with dH₂O on the following day.

In the Tables 40- 45 the preparation of the buffers used for the SDS- Page are described.

Table 40: Preparation of the Acrylamid- Stock 30 % (w/v)

Acrylamid Stock, 30 % (w/v) 500mL	
Preparation	146 g Acrylamid 4 g Bisacrylamid dissolve in 500 mL dH ₂ O, store in the dark at +4 °C

Table 41: Preparation of the Separating Gel Buffer

Separating Gel Buffer 500mL	
Preparation	90.75 g Tris 2 g SDS dissolve in 500 mL dH ₂ O and adjust the pH to 8.8, store at +4 °C

Table 42: Preparation of the Stacking Gel Buffer

Stacking Gel Buffer 500mL	
Preparation	30.25 g Tris 2 g SDS dissolve in 500 mL dH ₂ O and adjust the pH to 6.8, store at +4 °C

Table 43: Preparation of the 10x Running Buffer

10x Running Buffer	
Preparation	30 g/L Tris 144 g/L Glycine 10 g/L SDS

Table 44: Preparation of the Sample Loading buffer

Sample Loading Buffer for Western blot analysis (10 mL)	
Preparation	1.25 mL of 0.5 M HCl pH 6.8 2.5 mL Glycerol 2.0 mL 10% SDS (w/v) 0.2 mL Bromphenolblau 0.5 mL β - Mercaptoethanol 3.55 mL dH ₂ O

Table 45: Preparation of the Staining buffer for SDS-Gels

Colloidal Coomassie staining Buffer	
Preparation	- Dissolve 8 g (NH ₄) ₂ SO ₄ in 78.1 mL dH ₂ O and add 1.9 mL 85% H ₃ PO ₄ (v/v) - Dissolve 0.08 g Colloidal Coomassie G250 in 1.6 mL dH ₂ O and vortex - mix the two solutions and before use add 20 mL of Methanol

Gels were stained over night in a closed box to prevent evaporation of the methanol and afterwards destained with water for a few hours.

3.9 Western blotting

For further performing Western blot analysis, proteins from unstained SDS-gels were transferred to a nitrocellulose membrane Hybond- C Extra, 45 Micron GE Healthcare by electroblotting in a Semi- PhorTM TE70 (HOEFER Scientific Instruments, San Francisco) using the Blotting buffer (Table 47). After the blotting was finished the membrane was washed two times 10 minutes in TBST buffer (Table 46), then was blocked 20 minutes in TBST buffer and finally the proteins were probed 60 minutes with the primary Anti-His (C-term) Antibody (Invitrogen, Austria) at 1:5000 dilution. Then the membrane was again washed four times 10 minutes in TBST buffer and incubated 40 minutes with Anti- Mouse IgG (H+L), AP Conjugate (Promega, Austria) to detect bound antibody. After washing (four times 10 minutes in TBST buffer) and equilibrating the membrane in staining buffer (Table 48) the signals were visualized by incubating the membranes in 15 mL BCIP[®]/NBT solution (Table 49). To stop the reaction, the membrane was rinsed with dH₂O.

In the following the composition of all buffers and solutions which had been used for Western blotting are listed below:

Table 46: Preparation of the TBST buffer

TBST Buffer	
Preparation	2.42 g/L Tris 8.77 g/L NaCl Tween 80 0.1% (v/v) dissolve in 1 L dH ₂ O and adjust the pH to 7.4, store at +4 °C

Table 47: Composition of the Blotting Buffer

Blotting Buffer	
Preparation	2.42 g/L Tris 11.27 g/L Glycine dissolve in 800 mL dH ₂ O and 200 mL MeOH adjust the pH to 8.9, store at +4 °C

Table 48: Composition of the Staining Buffer

Staining Buffer	
Preparation	12.11 g/L Tris 15.5 g/L NaCl 1.017 g/L MgCl ₂ · 6H ₂ O dissolve in 1 L dH ₂ O and adjust the pH to 7.4, store at +4 °C

Table 49: Preparation of the Staining Solution

Staining Solution 15mL	
Preparation	15 mL Staining Buffer + 56 μ L Chromogen 5 % (w/v) dissolved in DMF:dH ₂ O 70:30 + 28.1 μ L BCIP 5 % (w/v) dissolved in dH ₂ O use the staining solution right after preparation

3.10 Protein binding assays with insoluble carbon sources

Protein binding assays were performed using different insoluble carbon sources. 10 mg of fungal cell walls (preparation given in the section below ‘Preparation of special carbon sources’) were used in an autoclaved and non-autoclaved form. 10 mg of colloidal chitin (preparation given in the section below: 3.10.1 ‘Preparation of special carbon sources’), chitin from crab shells fine and crude (Sigma -Aldrich Chemie GmbH, Germany), ARBOCEL cellulose fibre (J. Rettmayer& Söhne GmbH, Germany) and 250 μ L of chitin beads (New England Biolabs) were also used for the binding studies. Prior to use the chitin beads were washed 3- times with 20 mM Tris-HCl buffer pH 7.5.

200 μ g (2.6 pmol of TAL6₆ and 5.5 pmol of TAL6₄) of proteins respectively were added to the different carbon sources. With 20 mM Tris- HCl buffer a total volume of 1 mL was reached. The samples were incubated for 4 hours at room temperature with gentle agitation. The samples were then centrifuged for 5 minutes at high speed. The supernatant was transferred into a new Eppendorf tube and the pellets were washed 3 times with 20 mM Tris-HCl buffer pH 7.5. The pellet was then suspended in 20 mM Tris- HCl puffer pH 7.4 containing 1 % (w/v) SDS and incubated for 10 minutes at 99 °C. After centrifuging the samples again for 5 minutes at high speed the supernatant was transferred into a new Eppendorf tube.

250 μ L of the supernatants were precipitated using the chloroform and methanol precipitation to be further investigated using SDS- PAGE (see 3.8) and Western blotting (see 3.9).

3.10.1 Preparation of special carbon sources

3.10.1.1 Preparation of colloidal chitin

Colloidal chitin was prepared as described by Roberts et al. [85].

20 g crab shell chitin (Sigma, Austria) were suspended in 400 mL conc. HCl, stirred over night at 4 °C and filtered through glass wool. Then the filtrate was precipitated by adding 2 L of ethanol and washed with distilled water until a pH of 5.0 was reached. Then colloidal chitin was freeze dried over night in the Lyophilizer freeZone 2.5 (Labcono, Kansas City, USA).

3.10.1.2 Preparation of fungal cell walls

Cell walls of *Botrytis Cinerea*, *Rhizoctonia solani*, *T. atroviride* and *T. reesei* were prepared by growing the fungi in PDB broth for 24 and 48 hours. The mycelia were harvested by filtering through miracloth (Calbiochem, Germany) and washed with distilled water containing 0.1 % (w/v) SDS. The mycelia were grinded in liquid nitrogen and suspended in distilled water containing 1 % (w/v) SDS. The mycelia then were washed 3 times with distilled water containing 1 % (w/v) SDS and were afterwards lyophilized over night.

3.10.1.3 Alkaline treatment of T. atroviride cell walls (CW)

Cell walls were grown as mentioned above (preparation of different carbon sources) and harvested by filtering through miracloth (Calbiochem, Germany) and washed with distilled water containing 0.1 % (w/v) SDS. The mycelia were grinded in liquid nitrogen. 10 mg of the frozen cell walls were transferred into Eppendorf tubes and then were washed 3- times with distilled water containing 1 % (w/v) SDS afterwards 3- times with distilled water and centrifuged 10 minutes at 3000 g. The pellet was resuspended in 1 mL of buffer 1 (Table 50) and heated for 30 minutes at 100 °C and then washed 5- times with distilled water. The pellet was then resuspended in 1mL of buffer 2 (Table 51) and was incubated at 65 °C for 2 hours and afterwards centrifuged for 10 minutes at 3000 g. The pellet was washed 3- times with dH₂O and freeze- dried for 3 days.

Table 50: Preparation of the buffers for alkaline treatment of the cell walls of *T. atroviride*

Alkaline treatment buffer 1, 200mL pH 7.5	
Preparation	1.21 g Tris 4.00 g SDS 0.63 g β -Mercaptoethanol 2.92 g EDTA adjust the pH to 7.5 with conc. HCl

Table 51: Preparation of the buffers for alkaline treatment of the cell walls of *T. atroviride*

Alkaline treatment buffer 2, 200mL	
Preparation	3.78 g NaBO ₄ 7.99 g NaOH mix the two components

3.11 Effect of TAL6₆ and TAL6₄ on the spore germination

The effect of TAL6₆ and TAL6₄ on spore germination and fungal growth was analyzed by microscopy. For the imaging experiment spore solutions of *T. atroviride*, *T. reesei*, *Aspergillus niger* and *Neurospora crassa* were prepared by harvesting half of a sporulated petri dish plate of *T. atroviride*, *T. reesei* and *A. niger* and two eprouvettes with tilted agar of *N. crassa* each with 3 mL of PDB medium. Final concentration of the spore solutions was between 5×10^5 - 1×10^6 spores per mL. In a Lab-Tek® II Chambered Coverclass (NALGE-NUNC International Corp., USA) different conditions of the experiment were carried out.

The total volume in one chamber was 200 μ L. 170 μ L of the spore suspension was pipetted into one chamber and different concentrations of the TAL6₆- and TAL6₄ protein (in 20 mM Tris HCl buffer pH 7.5) were added: 30 μ g, 15 μ g and 5 μ g. The volume difference to 200 μ L was filled up with 20 mM Tris HCl buffer pH 7.5.

In total there were 3 different approaches which were performed: In one approach only PDB medium, in the second approach 2- times PDB medium and 1- time chitinase supernatant (culture of *Trichoderma atroviride* was harvested after 48 hours of incubation at 28 °C, 250 g and buffer changed with 20 mM Tris HCl buffer pH 7.5 and filtered with a steritop filter unit 0.22 μ M), and in the third approach 2- times PDB medium and 0.5- times chitinase

supernatant were used for the investigation of the germination efficiency of different fungi when incubated with the proteins TAL6₆ and TAL6₄.

T. atroviride, *T. reesei* and *A. niger* were incubated for 12 hours at 28 °C and *N. crassa* was incubated for 6 hours.

Germination behavior of the different spores was investigated on an inverted Nikon TE300 microscope by using differential interference contrast optics and imaged with a Nikon DXM1200F digital camera.

3.12 Protein deglycosylation assay

For protein deglycosylation assays 5 µg of the respective overexpressed proteins were used. First, 2 µL of the 10X Glycoprotein Denaturing Buffer (New England Biolabs) was added to the proteins and distilled water was added to a volume of 20 µL. The mixture was incubated for 10 minutes at 99 °C afterwards 3 µL of 10X G5 Reaction Buffer (New England Biolabs) and 2 µL of Endo H (New England Biolabs) and 2 µL of α - Mannosidase from *Canavalia ensiformis* (Jack bean) (Sigma -Aldrich Chemie GmbH, Germany) were added to each Eppendorf tube. The total volume was filled up to 30 µL with distilled water. The samples were kept on 37 °C for 6 hours. The samples were loaded on 10 % SDS-gels and analyzed by staining with colloidal Coomassie and Western blotting using an Anti-Histag antibody (Invitrogen) for detection.

4. Results

4.1 Characterization of LysM proteins in *Trichoderma atroviride*

4.1.1 Genomic organization of LysM proteins

Fungal chitinases of subgroup C contain CBM 18 (chitin binding) and CBM family 50 (LysM modules) [60] [64]. Two different types of modular architectures were recently reported for subgroup C chitinases (Fig. 12 depicts a schematic illustration of the two possible arrangements of subgroup C chitinases). They can contain either two CBM 18 domains or one CBM 18 and two CBM 50 LysM domains, located at the N-terminal end of their GH 18 module [64] [86] [63].

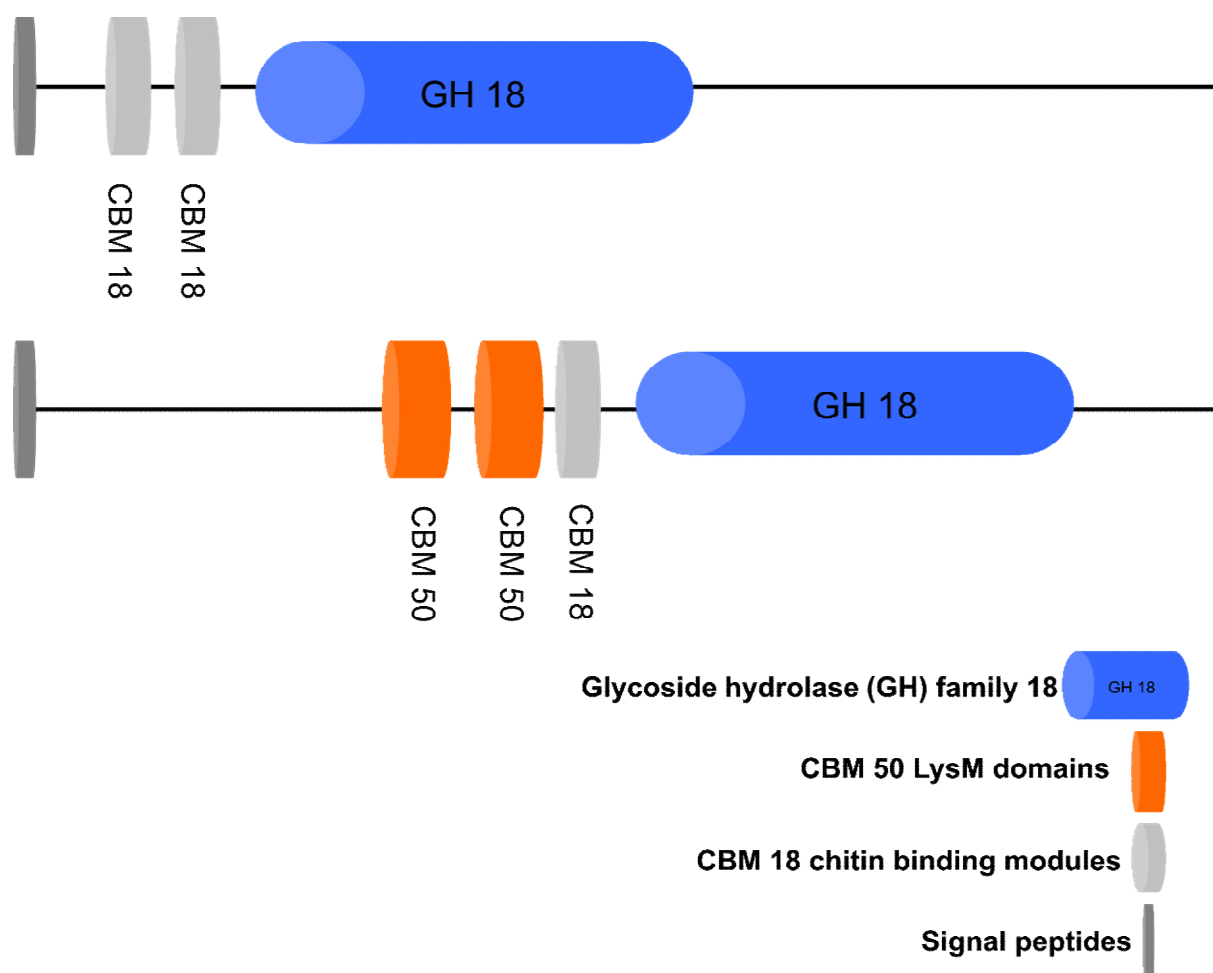


Fig. 12: Schematic illustration of either ways of modular architecture of chitinases of subgroup C. The first type contains only CBMs of family 18. The second type exhibits LysMs. Taken from Gruber et al. [63].

LysM proteins consist of a signal peptide and several LysM motifs. The genes encoding LysM proteins can frequently be found adjacent to or in the vicinity of subgroup C chitinase genes. Analysis of genomic sequence database entries for *Trichoderma* spp. revealed that in *T. atroviride* and *T. virens*, 6 out of 8 and 6 out of 10, respectively, genes encoding LysM proteins neighbor or are in close proximity to subgroup C chitinases, whereas no LysM proteins have been reported to be near subgroup A or B in *Trichoderma* genomes [63]. In addition, in some other fungi genes encoding LysM proteins are also frequently found next to subgroup C chitinase genes, e.g., *A. nidulans*, *Neurospora crassa*, whereas in other fungi this is not the case (*Magnaporthe grisea*).

Table 52 presents an overview of the overall number of subgroup C chitinases (sgC chitinases) in *Trichoderma*, their modular structures and associated LysM proteins [63]. As was shown in Fig. 12 chitinases of subgroup C have in general two different types of architecture. The first type have only CBMs of family 18 but no LysMs and the CBMs as well as the GH 18 module are located in the N-terminal part of the protein. In contrast chitinases of the second type have their GH 18 module approximately located in the middle of the protein and contain N-terminally of the GH 18 module one CBM 18 and two LysMs [63]. According to Table 52 the sgC chitinases can easily be divided in the first or the second type or represent a mixture of them as can be proposed for TVC3, TVC7, TVC8 and TVC9 of *T. virens* and for TRCHI18-1 of *T. reesei*. This means that those sg C chitinases belong to second type, which is containing LysMs and are neighbored by LysMs as well. Neighboring of LysMs is mainly observed by sgC chitinases of the first type that do not contain LysMs.

Table 52: Overview of the number of subgroup C chitinases in *T. atroviride*, *T. virens* and *T. reesei* describing the modular structure as well as the LysMs neighboring the subgroup C chitinases in the genome

	sgC chitinases	modular structure		neighboring LysMs
		containing LysMs	only CBM18	
<i>Trichoderma atroviride</i>	TAC ₁		X	4
	TAC ₂		X	2
	TAC ₃	X		
	TAC ₄		X	3
	TAC ₅		X	3
	TAC ₆		X	6
	TAC ₇	X		
	TAC ₈		X	
	TAC ₉	?	?	
	TVC ₁	X		
	TVC ₂		X	2
	TVC ₃	X		4
	TVC ₄		X	4
	TVC ₅		X	
	TVC ₆		X	4
<i>Trichoderma virens</i>	TVC ₇	X		1
	TVC ₈	X		1
	TVC ₉	X		3
	TVC ₁₀	X		
	TVC ₁₁	?	?	
	TVC ₁₂		X	
	TVC ₁₃	X		
	TVC ₁₄	X		
	TVC ₁₅	?	?	
	TRCH18-1	X		2
<i>Trichoderma reesei</i>	TRCH18-8	X		
	TRCH18-9	X		
	TRCH18-10	X		

In this thesis we were interested in the role of the LysM protein TAL6, whose gene is next to the gene of the subgroup C chitinase TAC6 (Protein ID 348129) in *T. atroviride*.

LysM motifs (LysMs) were originally described in prokaryotes as peptidoglycan-binding domains. In eukaryotes they were more recently described to have chitin-binding properties and were reported to be involved in the interaction of plants with their symbiotic, nitrogen-fixing bacteria, as well as the perception of chitooligomers during fungal infection and thus the induction of plant defense responses. Thus, these functions comprise cell-cell communication as well as defense responses [67] [69]. In fungi, for two LysM proteins from

plant pathogenic fungi a function in binding chitooligosaccharides was reported, which prevents the recognition of these chitooligosaccharides to be detected by the plant and thus masks the fungus during infection [73].

However, also non-pathogenic fungi have LysM proteins and they might therefore have other, not yet described functions. Therefore, in this thesis the protein TAL6 was selected for further investigations. The subgroup C chitinase gene *tac6* was shown to be induced during hyphal network formation of *T. atroviride* and *tal6* was reported to be transcriptionally co-regulated. This would suggest that the respective proteins are rather involved in self-communication and cell wall remodeling-related processes. Further TAL6 was also chosen for a biochemical characterization of its carbohydrate-binding properties because it contains six LysM motifs, of which four are highly similar to each other, whereas the other two are more distantly related to the current consensus pattern for LysM motifs in the SMART and PFAM databases (for details see Fig. 14).

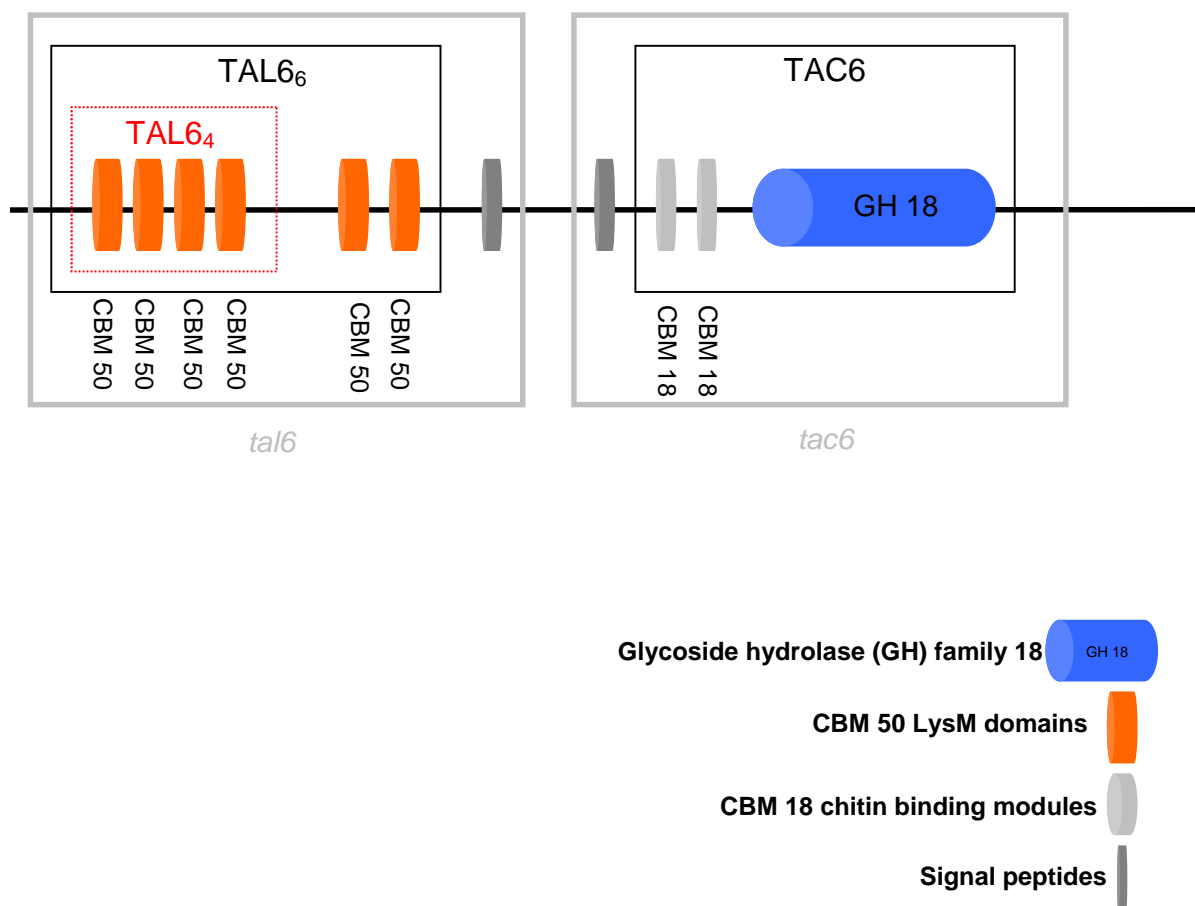


Fig. 13: Schematic illustration of the *tal6* gene and the neighboring *tac6* gene located in the genome, which are coding for the TAL6 protein and for the subgroup C chitinase TAC6, respectively.

The genomic organization of *tac6* and *tal6* and the modular architecture of the respective proteins are shown in Fig. 13. As can be seen in this figure two versions of TAL6 were defined for overexpression constructs and heterologously expressed in *Pichia pastoris* in this doctoral thesis in order to investigate the carbohydrate-binding properties and functions of the LysM motifs. For the first overexpression construct the complete protein, consisting of six LysMs, was chosen, which is called TAL6₆ from here on in this thesis. The second overexpression construct was a truncated version of the TAL6 protein that consisted only of the four LysM motifs that are highly similar to each other and match the consensus pattern of LysM motifs in the PFAM database more closely (see below for details). Accordingly, this expression construct is called TAL6₄ from here on in this thesis. The purpose of this thesis was to characterize the LysM motifs and to elucidate their function.

4.1.1 Characteristics of TAL6

TAL6 is a protein found in *T. atroviride* (protein ID: 297859).

The amino acid sequence, as well as the DNA sequence of the coding region of TAL6, can be found in the appendix (see Appendix 6.1.1.2).

Compute pI/Mw is a tool that allows the computation of the theoretical pI (isoelectric point) and Mw (molecular weight) of proteins. Using the online tool Compute pI/MW, available on the ExPASy site and listed in the proteomic tools (<http://expasy.org/tools/>), the theoretical pI and the MW of TAL6 were calculated as shown in Table 53.

Table 53: Characteristics of TAL6

Molecular mass	78.7 kDa
Number of amino acids	746
Theoretical pI	5.13
OD₂₈₀	1.35

TAL6 consists of six lysin motifs (LysMs), four of which are highly similar to each other, but do not share this similarity with the other two modules [63]. This finding was verified by performing an amino acid (aa) pattern analysis using the online protein sequence analysis tool InterProScan (<http://www.ebi.ac.uk/Tools/InterProScan/>). InterProScan is a tool that

combines different protein signature recognition methods native to the InterPro member databases into one resource with look up of corresponding InterPro and GO annotation [87].

The TAL6 aa-analysis based on known domains, modules and motives is shown in Fig. 14.

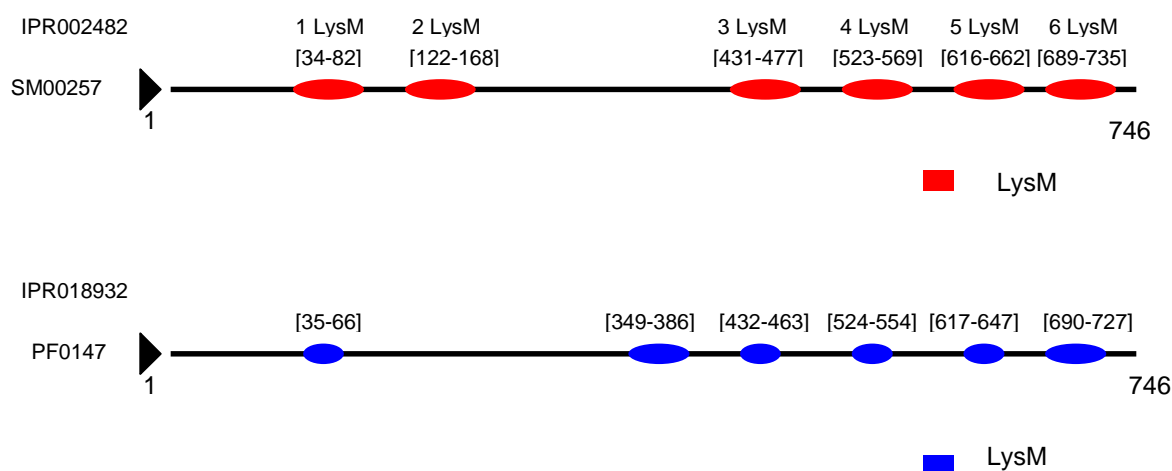


Fig. 14: Result of the *in silico* analysis using the online protein sequence analysis tool InterProScan. The numbers indicate aa residues, which are named from 1 LysM till 6 LysM.

In Fig. 14 the result of the *in silico* analysis of TAL6, using the available online protein sequence aligning tool InterProScan, is shown. InterProScan matches were found within two databases. The first result identified TAL6 according to the accession number IPR002482 using the SMART (simple modular architecture research tool) database as a lysin motif (LysM) with the SMART accession number SM00257. The description indicates that ‘this domain is approximately 40-residues long and is found in a variety of enzymes involved in bacterial cell wall degradation. This domain may have a general peptidoglycan binding function’ [88].

PFAM, the second database, is a database of protein domain families represented as (1) multiple alignments and as (2) HMM profiles. The second database interprets TAL6 as a peptidoglycan-binding lysin domain using the accession number IPR018392. Whereas the SMART database is able to distinguish between the motifs and cluster them into 4 motifs of very high similarity, PFAM is not able to detect a motif in the region from amino acids 100-200 aa. The LysM motifs detected with the PFAM consensus pattern are of different sizes, indicating that not the full-length motif is detected in all cases, whereas the SMART database indicates the LysM motifs of TAL6 are the same size.

These results showed that the LysM motifs are variable and do partly not match the current consensus pattern well. This could on one hand indicate that fungal LysM motifs are in general different from other, so far reported LysM motifs and on the other hand this might also possibly imply different properties and functions of these LysM motifs. Therefore, the aa-sequences of the LysM motifs were compared by multiple sequence alignment (Fig. 15). The aa-residues, which had been found using the SMART database were named 1 LysM- 6 LysM, accordingly, as is illustrated in Fig 14.

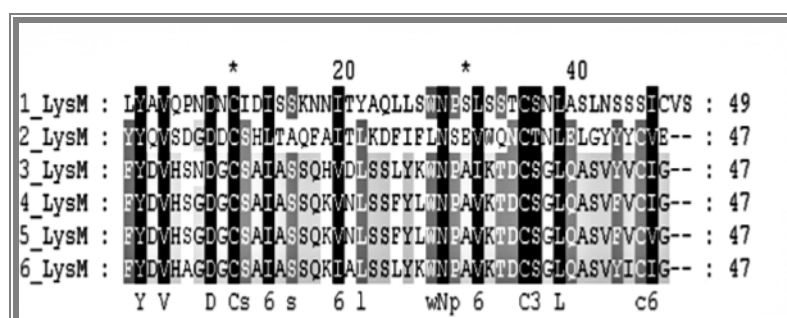


Fig. 15: The multiple sequence alignment done with the program GeneDoc of the 6 LysM motifs indicates that the first two LysM motifs are highly variable whereas the last 4 LysM motifs show high similarity.

The result of the multiple sequence alignment of the 6LysM motifs correlates very well with the aa-pattern of TAL6 found with the SMART database using InterProScan.

4.1.2 Characteristics of the overexpression constructs of TAL6₆ and TAL6₄

In order to analyze the difference between TAL6₆ and TAL6₄ (aa-sequences can be found in the appendix, section 6.1.3.2 and 6.1.4.2), cassettes for the expression of the respective genes in *P. pastoris* were created to be further able to investigate the function and role of the protein with either 6 LysM or 4 LysM motifs. A His-tag was added to the C-terminus of the protein in order to facilitate protein purification and detection. The details of the expression vectors are shown in the Material and Methods, the expression cassettes can be seen below (Fig. 16 and Fig. 17).

4. Results

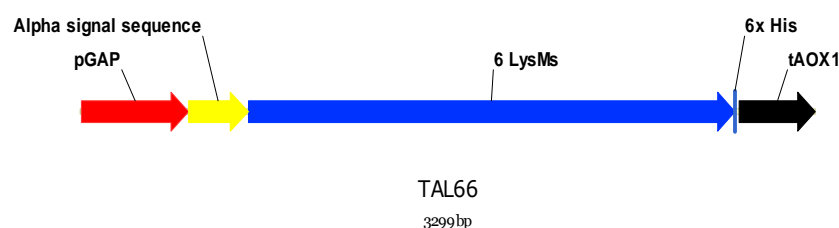


Fig. 16: Schematic illustration of the expression cassette used for expressing the 6LysMs of TAL6 in *Pichia pastoris*.

pGAP: promoter derived from the *P. pastoris* glyceraldehyde-3-phosphate dehydrogenase gene
 Alpha signal sequence: alpha mating type signal sequence for secreted protein expression
 6xHis: polyhistidine tag to allow for purification and detection of the expressed protein
 tAOX1: fungal transcription terminator.

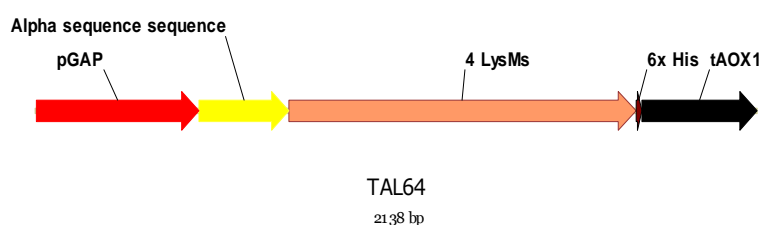


Fig. 17: Schematic illustration of the expression cassette used for expressing the 4LysMs of TAL6 in *P. pastoris*.

pGAP: promoter derived from the *P. pastoris* glyceraldehyde-3-phosphate dehydrogenase gene
 Alpha signal sequence: alpha mating type signal sequence for secreted protein expression
 6xHis: polyhistidine tag to allow for purification and detection of the expressed protein
 tAOX1: fungal transcription terminator.

Using the online tool Compute pI /MW available on the ExPASy site

(<http://expasy.org/tools/>) the theoretical pI and the MW of the secreted TAL6₆ and TAL6₄

including the His- tag were calculated. Results of this *in silico* analysis are shown in Table 54 and Table 55, respectively.

Table 54: Characteristics of the secreted TAL6₆ including the His Tag

Molecular mass	77.7 kDa
Number of amino acids	736
Theoretical pI	5.49
OD₂₈₀	1.35

Table 55: Characteristics of the secreted TAL6₄ including the His Tag

Molecular mass	36.2 kDa
Number of amino acids	349
Theoretical pI	8.72
OD ₂₈₀	0.964

The molecular mass and the theoretical pI were calculated using the above mentioned online available tool Compute pI/MW.

4.2 Overexpression of TAL6₆ and TAL6₄

4.2.1 Overexpression in *Pichia pastoris*

P. pastoris was used in this thesis as a protein expression host and is a well-established organism for high-level protein expression either for intracellular or secreted proteins. It uses an eukaryotic protein synthesis pathway allowing the optimal expression of foreign proteins [89]. *P. pastoris* is a favored organism for biotech applications because the organism can produce secreted protein in milligram-to-gram quantities but still allows for ease of downstream processing due to low-level production of endogenous proteins. For secretion of foreign proteins, a signal sequence is necessary to target the protein to the secretory pathway. In this thesis the expression vectors were constructed to contain the *Saccharomyces cerevisiae* α -factor prepro signal sequence, which is the most frequently used signal sequence.

As *tal6₆* contains introns, cDNA was used for the construction of the expression cassettes. The construction of the expression cassettes, as well as their transformation into *P. pastoris*, is described in Materials and Methods (3.3.2.2) and the primer pairs used are listed in Table 27 in Materials and Methods.

The first attempt to overexpress TAL6₆ and TAL6₄ in *P. pastoris* was carried out with the AOX1 promoter. The AOX1 promoter is a methanol inducible promoter, derived from the alcohol oxidase I gene that is uniquely suited for the controlled expression of foreign genes. This promoter can be induced by addition of methanol. While it is known that in *P. pastoris* two genes code for *aox*, namely *aox1* and *aox2*, only the *aox1* gene triggers the alcohol oxidase activity in the cell, which leads to a tightly regulated expression up to high levels. For the expression of heterologous proteins in *P. pastoris* with the AOX1 promoter a commercial kit (EasySelect™ *Pichia* Expression Kit; Invitrogen) is available. Construction of the

overexpression vectors and cultivation of *P. pastoris* following the supplier's instructions did not lead to high levels of expression.

As a transcript analysis of the two domains revealed low expression (data not shown) the promoter was exchanged with the GAP promoter, which is a promoter derived from the glyceraldehyde-3-phosphate dehydrogenase gene of *P. pastoris*. The GAP promoter is a constitutive promoter and when grown on glucose can achieve a higher protein level than the AOX1 promoter [90].

Positive colonies were identified using colony PCR amplification of the *tal6₆* and the *tal6₄* fragment, 2193 bp and 1030 bp, respectively, as shown in Fig. 18. For the colony PCR, the following oligomers were used to amplify *tal6₆*: 6LysM-Fw 5'-GTA CCT GCA GCA TCA AAG CTA GGC GTA CCC-3' and 6LysM-Rv 5'-GTA CGC GGC CGC TCC TGT AAC ACG AGC AGC G-3'. For amplifying *tal6₄* the forward primer was 4LysM-Fw 5'-GTA CCT GCA GAC AGC ATC CCA TCT ATT TCG C-3' and the reverse primer was 4LysM-Rv 5'-GTA CTC TAG AGC TCC TGT AAC ACG AGC AGC GG-3'.

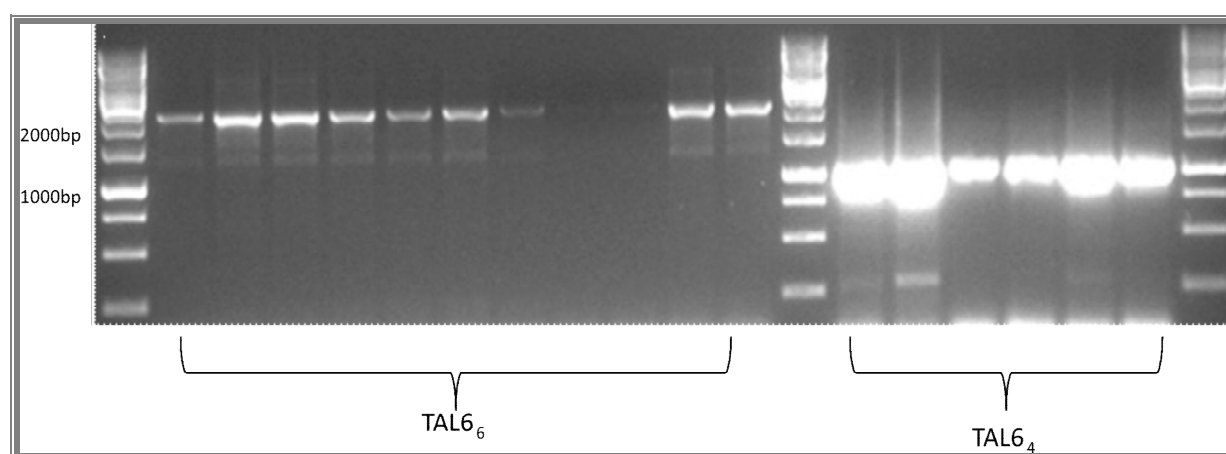


Fig. 18: Results of the colony PCR, which had been used to identify colonies, which have been inserted the *tal6₆* and *tal6₄* gene. 2 µl of the PCR reaction was loaded on the gel.

By doing a reverse transcription polymerase chain reaction (RT-PCR) the expression of TAL6₆ and TAL6₄ using the GAP promoter was analyzed. As can be seen (Fig. 19) a constitutive expression level over 48 hours was achieved.

4. Results

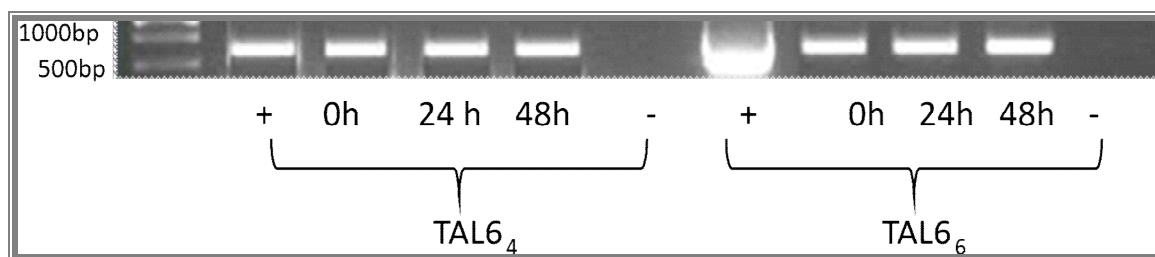


Fig. 19: RT- PCR showing the expression of TAL6₄ (515 bp) and TAL6₆ (557 bp) in a shake flask culture over 48 hours. The GAP promoter has been used. Cultivation conditions were carried out as described in Material and Methods.

In order to increase the protein secretion levels, various parameters during the expression in *P. pastoris* were analyzed and varied. This included different growth media that were used for cultivation of the TAL6₆ and TAL6₄ overexpression strains. Hohenblum et al. [90] showed that a variation of the medium composition can have pronounced effects on protein production levels even when constitutive promoters are used. We therefore compared TAL6₆ and TAL6₄ protein secretion levels in a buffered minimal medium (recommended in the EasySelet™ *Pichia* Expression Kit; from Invitrogen) with glucose as carbon source with a complex medium Yeast Extract Peptone Dextrose (YPD), where 20 g/L glucose were added every 24 hours

The expression was monitored for 72 hours. SDS- Page and Western Blotting of the TAL6₆ grown under these different conditions showed that YPD medium, with additional glucose doses (every 24 hours 20 g/L glucose) led to improved protein expression rates of TAL6₆ and TAL6₄ in comparison to buffered minimal medium.

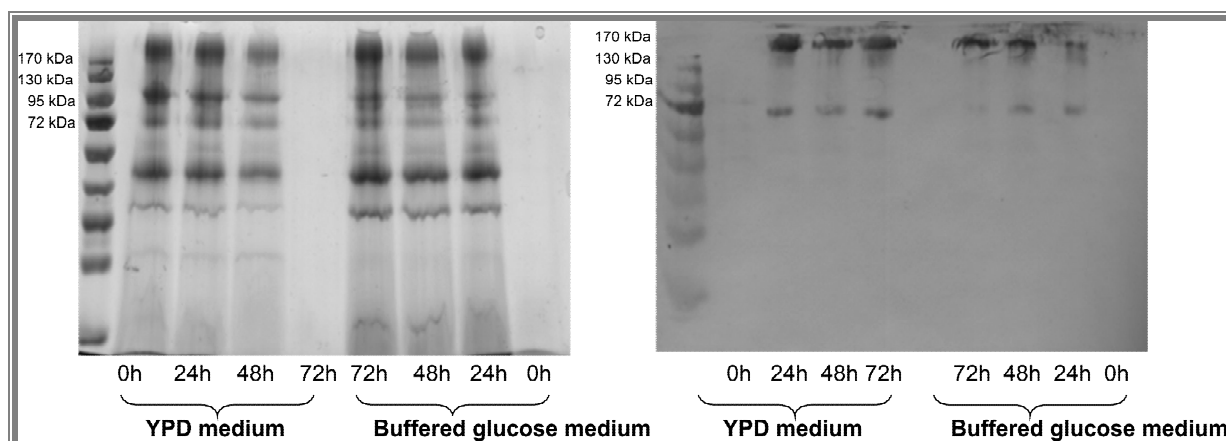


Fig. 20: Comparison of the expression of TAL6₆ in two different media. On the left side the result of the SDS- Page is shown and on the right side the appropriate Western blot is illustrated.

As illustrated in Fig. 20 the expression reached best results when growing in YPD medium using the constitutive GAP promoter. According to Western blot analysis the optimal time

point for harvesting was 24 hours as at this time point the protein expression yielded already high levels.

In order to verify if the two protein domains TAL6₆ and TAL6₄ are secreted proteins and do not stay attached to the fungal cell wall or trapped inside the cells, proteins were extracted from the biomass as described in Material and Methods (3.7) and treated with different chaotropic detergents and further were investigated by SDS- Page and Western blot.

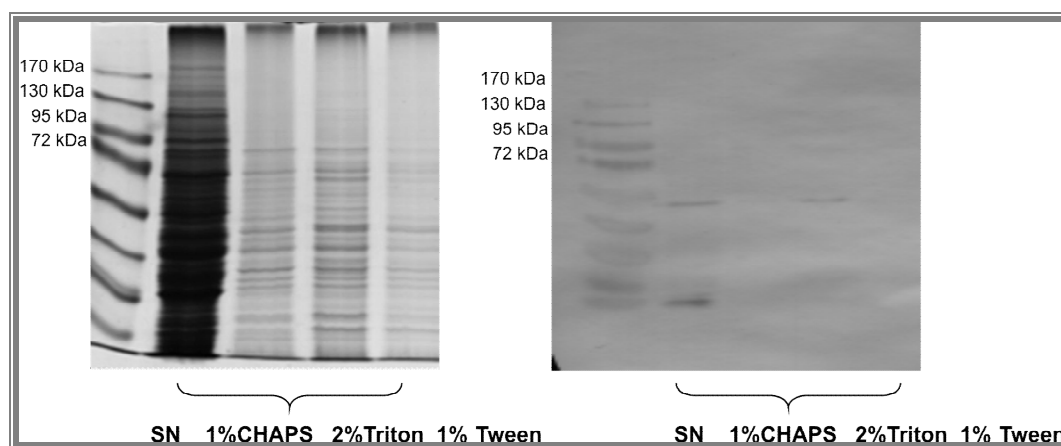


Fig. 21: Result of the analysis if TAL6₆ and TAL6₄ are secreted proteins. 5 µg were loaded on the SDS- Page (left). SN is the untreated supernatant (intracellular, soluble proteins) of the disrupted cells. 1 % (v/v), Triton, 1 % (w/v) Tween, 2 % (v/v) CHAPS are chaotropic detergents, which were sequentially added to the cell debris to extract attached proteins.

Illustrated in Fig. 21 it was verified that all of the produced TAL6₆ and TAL6₄ proteins are indeed secreted. Different chaotropic detergents namely 1 % (v/v) Triton, 2 % (w/v) CHAPS, 1 % (v/v) Tween were added to the mechanically cell disrupted cell debris. Western blot analysis did not show any significant signals that would indicate the presence of major amounts of TAL6₆ or for TAL6₄ inside the cells or attached to the cell wall.

In order to decide which concentrations give best signals for SDS- Page and Western blot analysis different concentrations of the proteins and different methods of downstream processing, namely concentration of the proteins in Amicon Ultra centrifugal filter units Ultra-15, MWCO 50 kDa (see Material and Methods 3.6) and concentration and afterwards chloroform/ methanol precipitation (see Material and Methods 3.8.1) have been conducted and analyzed (Fig. 22).

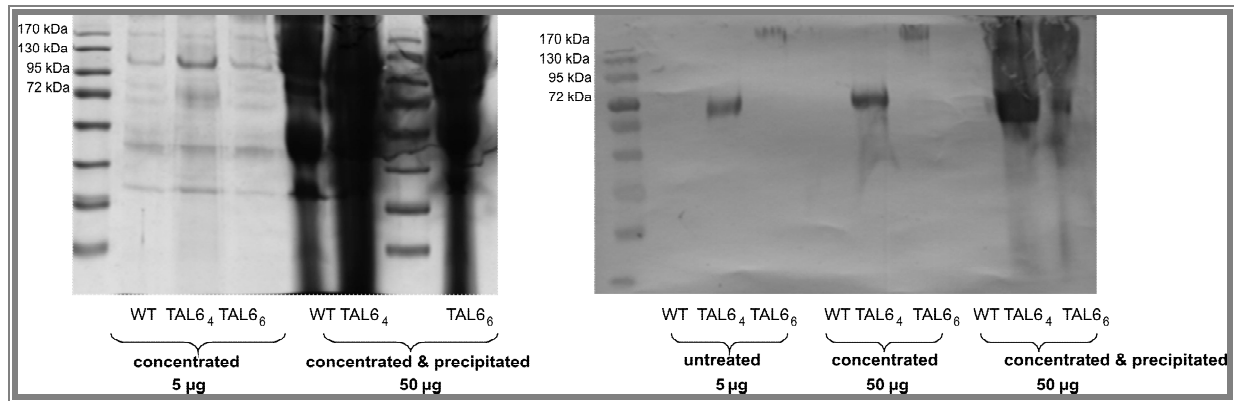


Fig. 22: Result of the analysis which concentration and downstream processing is optimal for SDS- Page (left) and Western blot (right).

TAL6₆ and TAL6₄ were best analyzed according to the above result by using concentrations in the range of 5 µg untreated or concentrated in Amicon Ultra centrifugal filter units Ultra-15, MWCO 50 kDa.

4.2.2 Overexpression of TAL6₆ in *Trichoderma reesei*

The expression of the TAL6₆ and TAL6₄ did not give high protein yields and molecular mass of the obtained proteins was significantly higher than their expected sizes (~130 kDa for TAL6₆ and ~72 kDa for TAL6₄). Therefore, overexpression of the proteins was also performed in *T. reesei*, in order to compare the expression levels and the molecular mass of the obtained proteins between *T. reesei* and *P. pastoris*.

T. reesei is a commonly host, if a protein shall be expressed in a filamentous fungus and has high protein secretion capacities. Since it is closely related to *T. atroviride* it was of interest to find out if the expression of the two proteins works better in *T. reesei*. Further, since Western analysis of TAL6₆ in *P. pastoris* showed protein bands with high molecular mass, which could be due to hyperglycosylation, we were interested to test whether the expression of TAL6 in *T. reesei* yields protein with a molecular mass that is closer to the expected size. As can be seen in Fig. 23 the expression of TAL6₆ in *T. reesei* resulted in signals with even higher molecular weight than shown in *P. pastoris*. We concluded from these results that the protein is glycosylated and/or a dimer and/or attached to cell wall fragments of *T. reesei*. However, since these results were similar to those obtained from expression in *P. pastoris*, we concluded that this is rather a feature of the protein TAL6 and not an artifact from the heterologous expression. The signals of TAL6₆ expressed in *T. reesei* were also very weak

and only an expression after 24 hours was detectable (Fig. 23). Therefore it was decided to continue the expression in *P. pastoris* because it gave better protein yields.

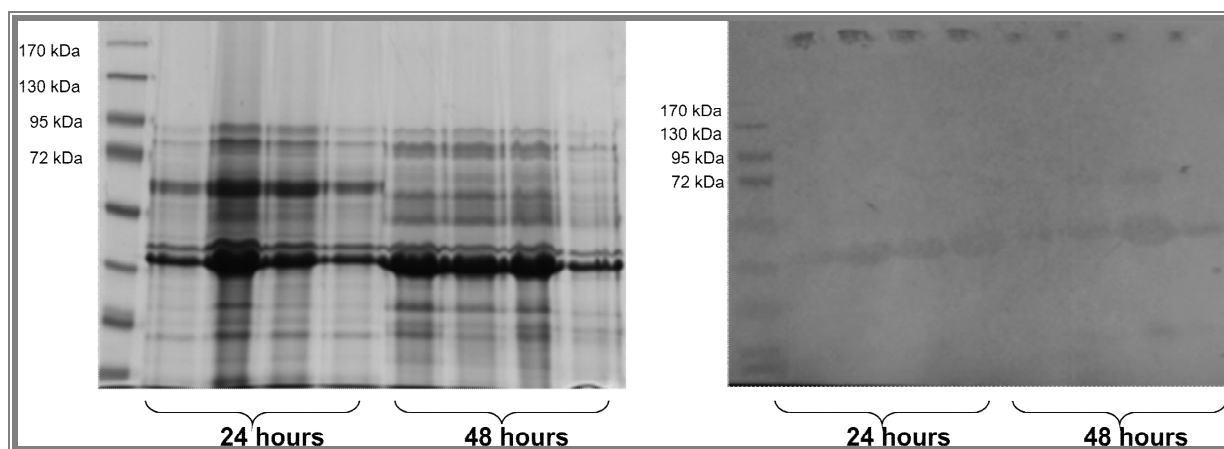


Fig. 23: Expression of TAL6₆ in *T. reesei* investigated for 24 h and 48 h. SDS- Page (left) and Western blot (right). The protein was concentrated using the Amicon Ultra centrifugal filter units Ultra-15, MWCO 50 kDa and 5 µg of the protein was then loaded on the gel.

4.3 Fermentation of TAL6₆ and TAL6₄

Fermentation of TAL6₆ and TAL6₄ was performed in a batch culture or discontinuous process. The fermentation process starts with the inoculation of the media and ends at a certain time point, when all of the substrate has been taken up.

The fermentation was performed as described in Material and Methods (3.5). Interestingly, the fermentation could only be performed using the complex YPD medium. A further approach using a minimal medium (BSM) resulted in no expression of the protein respectively in a degraded protein. 100 mL of the preculture were used to seed the medium in the bioreactor (schematic illustration can be seen in Fig. 24). The end of the batch was indicated by a sharp decrease of CO₂ in the offgas. Afterwards, a pulse of 500 mL 4- fold concentrated YPD media containing 80 g/L glucose was carried out to further increase the biomass concentration and concomitantly the product content. As soon as the concentration of CO₂ decreased the culture was fed with a solution composed of 4- fold concentrated YPD media containing 80 g/L glucose. The fermentation was carried out for about 72 hours. Then the protein broth was centrifuged in a RC-3B centrifuge (Sorvall Instruments) for 2 hours at 10000 g.

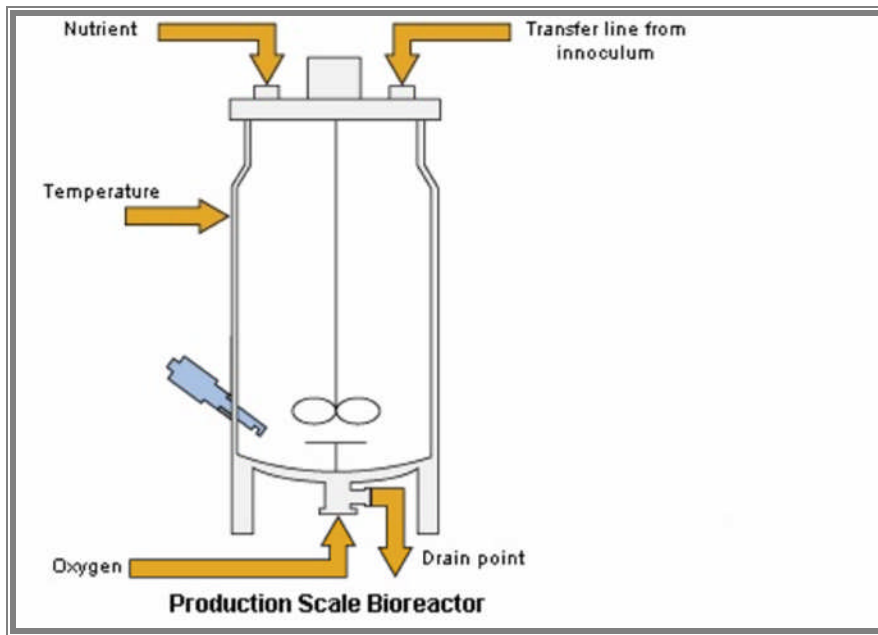


Fig. 24: Schematic illustration of a fermenter.

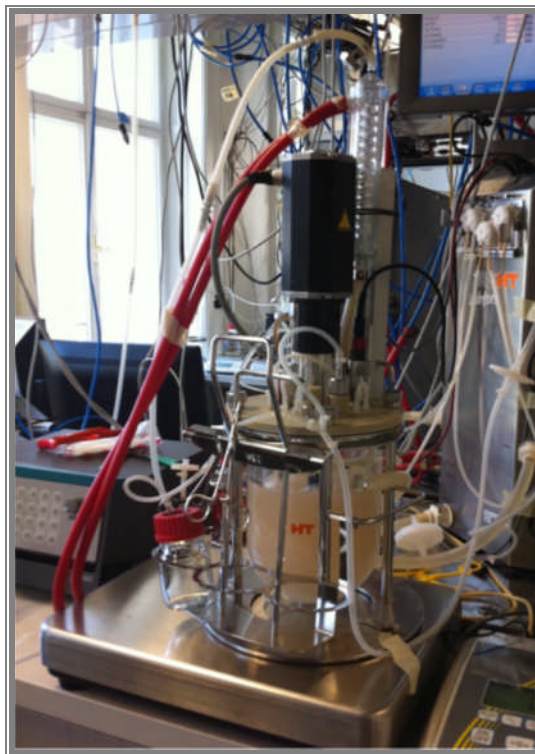


Fig. 25: Fermenter of the Institute of Chemical Engineering at Vienna University of Technology.

Although the expression conditions had been optimized in advance, by comparing the inducible AOX1 promoter with the constitutive GAP promoter and of course by comparing the expression system of *T. reesei* to *P. pastoris*, it was difficult to express TAL6₆ and TAL6₄. The expression did not yield in high levels of protein product and only the complex YPD medium lead to successful protein expression, when inducing the process with 4- fold concentrated YPD Medium with 80 g/L glucose. Western blot analysis of the expression of TAL6₆ in YPD medium and of TAL6₄ in a minimal medium BSM revealed that only in the YPD medium an expression of the LysMs of *T. atroviride* was possible (Fig. 26).

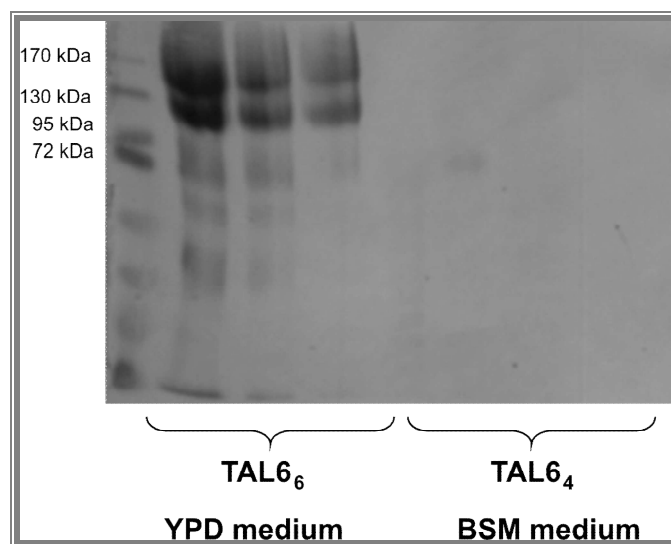


Fig. 26: Comparison of the complex medium with the minimal medium BSM. TAL6₆ was grown in complex medium whereas TAL6₄ was grown in BSM medium. Only in the complex medium the expression of the protein was possible.

4.4 Large scale purification of TAL6₆ and TAL6₄

The purification of the proteins was performed using the ÄKTATM purifier (Amersham Pharmacia Biotech, NY, USA) as described in Material and Methods (3.6).

For the fermentation of the proteins the YPD medium had been used and the pulse for induction of the promoter was 4- fold concentrated YPD medium with 80 g/L glucose. Prior to the purification the sugar and also the salts had to be removed from the produced viscous supernatant. This was done by buffer- changing the supernatant with 20 mM Tris HCl puffer, pH 7.5.

4. Results

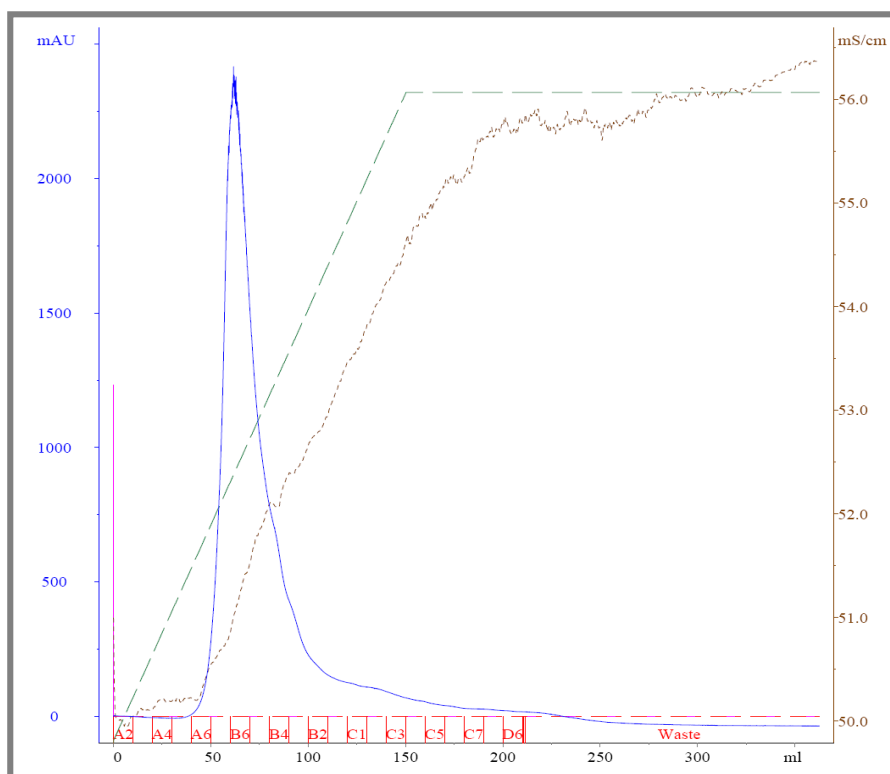
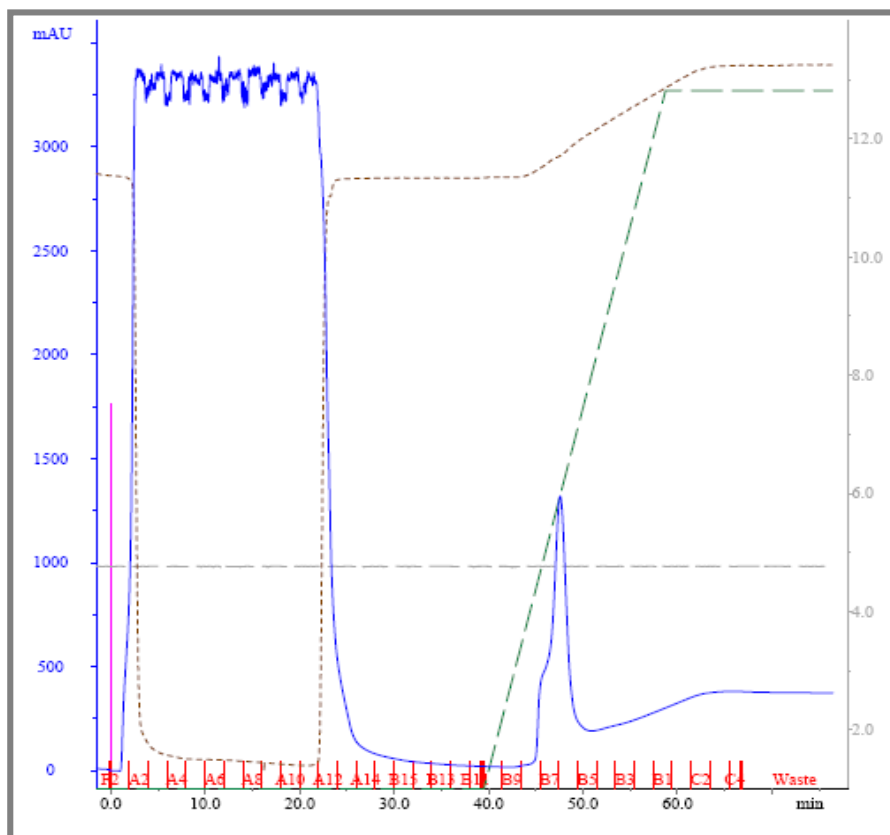


Fig. 27: Chromatogram of TAL6₆ using the affinity chromatography in combination with the HiScale 16 column.



4. Results

The blue line represents the fractions measured at 280 nm. The absorption maxima of a protein emerge at 280 nm, and give evidence of the binding of a protein. The peak which could be obtained during the purification of the TAL6₄ is smaller than the peak which can be seen from the chromatogram of TAL6₆. This is due to the use of different columns and therefore different loading volumes for TAL6₆ and TAL6₄. TAL6₆ was first purified using the HiScale 16 column. After the purification of TAL6₆ with the HiScale 16 column it could be observed that the the column had been discharged, this was due to the complex medium. Thus, for the purification of TAL6₄ HisTrapTM HP columns with less loading capacity were used.

The fractions which resulted from a peak in the blue line were collected and further investigated and verified by SDS- Page and Western blotting.

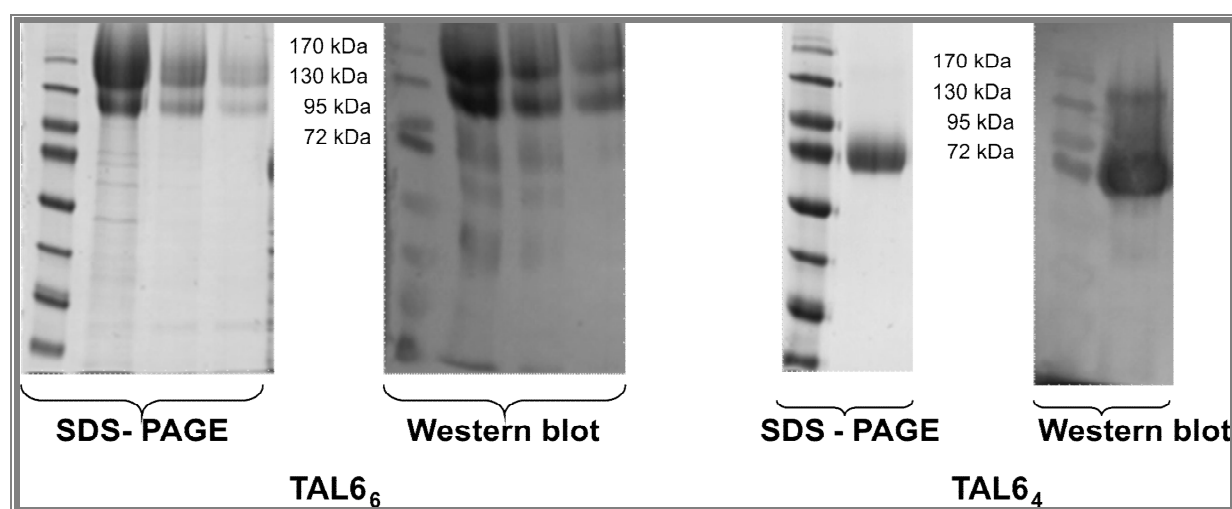


Fig. 29: Verification of TAL6₆ and TAL6₄ after purification. 5 µg of the proteins were loaded on the gels. Prior to loading on the gels the proteins have been concentrated by using the chloroform/ methanol precipitation.

It is shown that TAL6₆ appeared as a double band with a molecular mass of ~ 130 kDa of the upper stronger band and ~ 115- 120 kDa of the lower band on SDS-gels and Western blots. TAL6₄ only occurred as single band in the size of 72 kDa.

4.5 Characteristics of TAL6₆ and TAL6₄ according to *N*-glycosylation and 2D-Gel analysis

As the above findings were in contrast to the theoretical molecular weight obtained by the online available tool Compute pI/MW it was decided to further investigate if the change in the size of the molecular weight could be due to possible *N*-glycosylation or rather to dimerization.

4.5.1 *N*-glycosylation

A prediction of the *N*-glycosylation of the TAL6₆ and TAL6₄ was performed using the online available tool NetNGlyc available on the homepage of Center for Biological Sequence Analysis (CBS). This tool is able to predict the *N*-glycosylation of proteins according to *N*-glycosylation sequon, which is a consensus tripeptide, consisting of Asn-Xaa-Ser/Thr stretch (where Xaa is any amino acid except Proline), where the Asparagine is *N*-glycosylated. NetNGlyc attempts to distinguish glycosylated sequons from non-glycosylated ones. Any potential crossing the default threshold of 0.5 represents a predicted glycosylated site and a jury agreement column indicates how many of the nine networks support the prediction.

4.5.1.1 *N*-glycosylation prediction results for TAL6₄

DSIPSISPTGIITPTPTQSGMVSNCKFYDVHSNDGCSAIASSQHVDLSSLYKWNPAIKTDCSGLQASVYVCIGILTTS	80
STTSKLPTTTSKPSTTSKPPTGIITPTPTQSGMVKNCKFYDVHSGDGCASAIASSQKV NLS SFYLWNPVKTDCSGLQAS	160
VFVCIGITLTTSMSTTSKLPTTTSKPSTTSKPPTGIITPTPTQNGMVKNCKFYDVHSGDGCASAIASSQKV NLS SFYLWN	240
PAVKTDCSGLQASVFVCVGTATTTAAGITPTPTPTQSGMVSGCNKFYDVHAGDGCASAIASSQKIALSSLYKWNPAVKTDC	320
SGLQASVYICIGVGNAAAARVTGHHHHHH	

Fig. 30: Protein sequence of TAL6₄ with marked *N*- glycosylated amino acids.

In the sequence output of TAL6₄ above, Asn-Xaa-Ser/Thr sequons are highlighted in blue, and *N*-glycosylated Asparagines are red.

(Threshold=0.5)					
SeqName	Position	Potential	Jury agreement	N-Glyc result	
Sequence	139 NLSS	0.6962	(9/9)	++	
Sequence	232 NLSS	0.6536	(9/9)	++	

Fig. 31: Result of the jury agreement for TAL6₄.

4. Results

Interestingly TAL6₄ only exhibits two *N*-glycosylation sites. This predicted result was supported by nine of nine networks (Fig. 31).

4.5.1.2 *N*-glycosylation prediction results for TAL6₆

SKLGVPQPAQRDQVNCQLYAVQPNDNCIDISSKN	80
ATDIATTTAPVPSPTLDQTTSRCAKYYQVSDGDDCSHLTAQFAITLKDFIFLNSEVWQ	160
PGYLPATTTKPF	240
WNPSLGNDSGSSGSLSGAEASQVASSIAIPTTAPSSITNLYTYPCTVAANISYCVALVSSTGALPTNTAPPGPASGEI	320
SNCTAWFAPEAYDTCKSILDIFEMSFANFYKMNPSVGPDCSGLAVGTNYCVSTYPNGEDPNDDWDGDDSIPTGIIT	400
PTPTQSGMVSNCKNFYDVHSNDGCSAIASSQHVLDSSLYKWNPAIKTDCSGLQASVYVCIGILTSMSTTSKLPSTTSKP	480
STTSKPPTGIITPTPTQSGMVKNCKNFYDVHSGDGCSAIASSQKVNLSFYLWNPVAVKTDCSGLQASVFCIGTLTTSMS	560
TTTSKLPSTTSKPSTTSKPPTGIITPTPTQNGMVKNCKNFYDVHSGDGCSAIASSQKVNLSFYLWNPVAVKTDCSGLQAS	640
VFVVCVGTATTTAAGITPTPTPTQSGMVSGCNKFYDVHAGDGCSAIASSQKIALSSLYKWNPAVKTDCSGLQASVYICIGV	720
GNAAAAARVTGHHHHHH	

Fig. 32: Protein sequence of TAL6₆ with marked *N*-glycosylated amino acids.

In the sequence output of TAL6₆ above, Asn-Xaa-Ser/Thr sequons are highlighted in blue, and *N*-glycosylated Asparagines are red.

(Threshold=0.5)					
SeqName	Position	Potential	Jury agreement	N-Glyc result	
Sequence	35 NITY	0.6288	(8/9)	+	
Sequence	45 NPSL	0.6584	(8/9)	+	WARNING: PRO-X1.
Sequence	59 NSSS	0.6978	(9/9)	++	
Sequence	139 NCTN	0.5914	(8/9)	+	
Sequence	173 NQTS	0.6554	(8/9)	+	
Sequence	193 NSSV	0.6277	(8/9)	+	
Sequence	201 NGTR	0.6657	(9/9)	++	
Sequence	215 NLTE	0.5303	(6/9)	+	
Sequence	242 NPSL	0.6263	(6/9)	+	WARNING: PRO-X1.
Sequence	254 NLSG	0.6228	(9/9)	++	
Sequence	291 NISY	0.6808	(9/9)	++	
Sequence	322 NCTA	0.6173	(7/9)	+	
Sequence	353 NPSV	0.4637	(5/9)	-	
Sequence	526 NLSS	0.6361	(9/9)	++	
Sequence	619 NLSS	0.6134	(9/9)	++	

Fig. 33: Result of the jury agreement for TAL6₆.

In the case of TAL6₆ the prediction displayed a total of 15 *N*-glycosylation of which 6 (at position 59, 201, 254, 291, 526 and 619) predictions were according to nine of nine networks (Fig. 33).

4.5.2 Deglycosylation of TAL6₆ and TAL6₄

To further verify these findings the proteins were enzymatically deglycosylated. TAL6₆ and TAL6₄ were deglycosylated using Endo H (New England Biolabs) and α -Mannosidase from *Canavalia ensiformis* (Jack bean) (Sigma- Aldrich Chemie GmbH, Germany) enzymes. The results (Fig. 34) showed that the size of TAL6₄ was reduced to 60 kDa, whereas TAL6₆ still appeared as bands of approximately 130 kDa and 95 kDa and 60 kDa. These data indicate that TAL6₄ was present as monomer since its predicted size is 36.2 kDa and therefore 60 kDa is below the size for a dimer, but the protein was still not fully deglycosylated using Endo H and α -Mannosidase enzyme. For TAL6₆ the results were less clear because a reduction in size could also be observed, which indicated also a glycosylated protein.

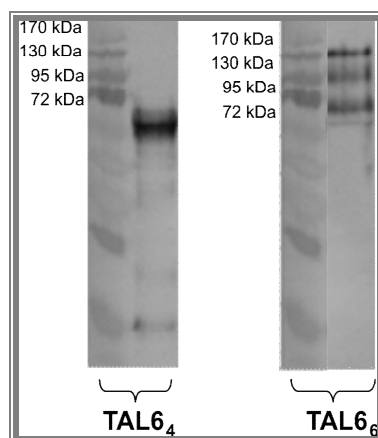


Fig. 34: Western blot of deglycosylated TAL6₆ and TAL6₄. His- tagged proteins were detected. Investigating the TAL6₆ and TAL6₄ only one concentration, 5 μ g, was used.

4.5.3 2D-Gel electrophoresis of TAL6₆ and TAL6₄

2D-Gel electrophoresis is a method, which separates the proteins in two consecutive steps. The first step is the separation according to the isoelectric point (pI) of the proteins and in the second step the proteins are separated according to their molecular weight. For the 2D-gel electrophoresis 50 μ g of each protein and a pH from 3-10 for isoelectric focusing were used. The result of the 2D-gel electrophoresis of TAL6₆ and TAL6₄ is in accordance to the findings of previous investigations (Table 54 and Table 55). The theoretical pI of TAL6₆ is calculated to be 5.49 and the theoretical pI of TAL6₄ is 8.72 according to the online tool Compute pI/MW. Results of TAL6₆ with 2D-gel electrophoresis indicated a pI in the range of 5.4- 6.1 for the ~ 130 kDa band and 7.1- 7.7 for the ~ 115- 120 kDa band and for TAL6₄ a single band

4. Results

of 72 kDa on SDS-gels was found for which a pI in the range of 8.0- 9.1 could be measured. The proteins appeared as several spots (protein trains), which can be seen on the 2D-gel (Fig. 35 and 36), which is in agreement with the findings of the enzymatic deglycosylation assays that showed that the proteins are glycosylated.

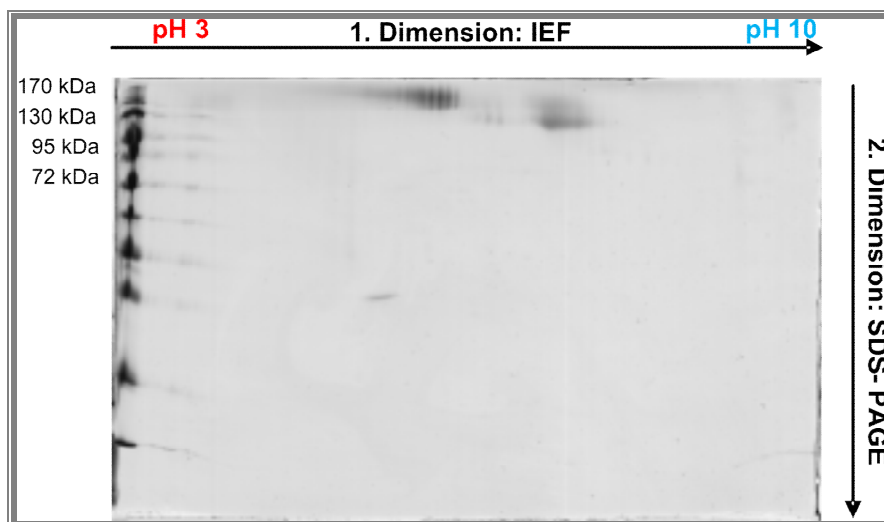


Fig. 35: 2D-gel electrophoresis of TAL6₆.

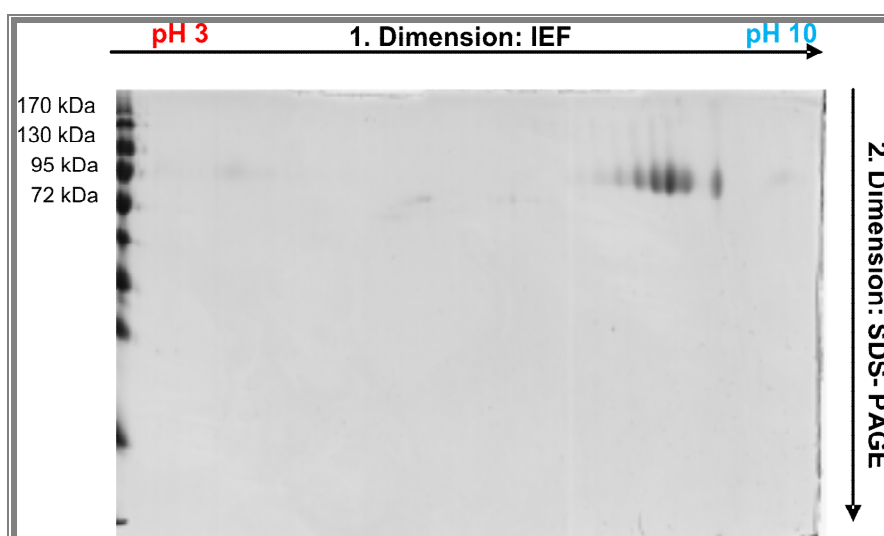


Fig. 36: 2D-gel electrophoresis of TAL6₄.

4.6 Carbohydrate-binding assays

Binding assays of TAL6₆ and TAL6₄ were performed to test if these proteins are able to bind to chitinous carbon sources and if so, investigate differences in binding specificities toward these carbon sources. For this purpose pull-down assays were carried out and protein was detected either unbound in the supernatant (SN) or bound to the carbon source, from which it was released by boiling with SDS-containing buffer.

For these experiments different types of chitin (chitin beads, colloidal chitin and chitin from crab shells fine and crude), cell walls of *T. atroviride* and related species as well as the plant pathogenic fungi, *Botrytis cinerea* and *Rhizoctonia solani*, and cellulose were used.

Prior to the implementation of the binding assay different buffer systems were tested in order to find a suitable buffer and pH in which the proteins are stable during the duration of the binding assay (Fig. 37). The chosen buffer system for the binding assays was 20 mM Tris-HCl buffer pH 7.5. Preparation of the cell walls and the binding assays were carried out as described in the Material and Methods chapter. 2.6 pmol of TAL6₆ and 5.5 pmol of TAL6₄ were used (200 µg of each protein).

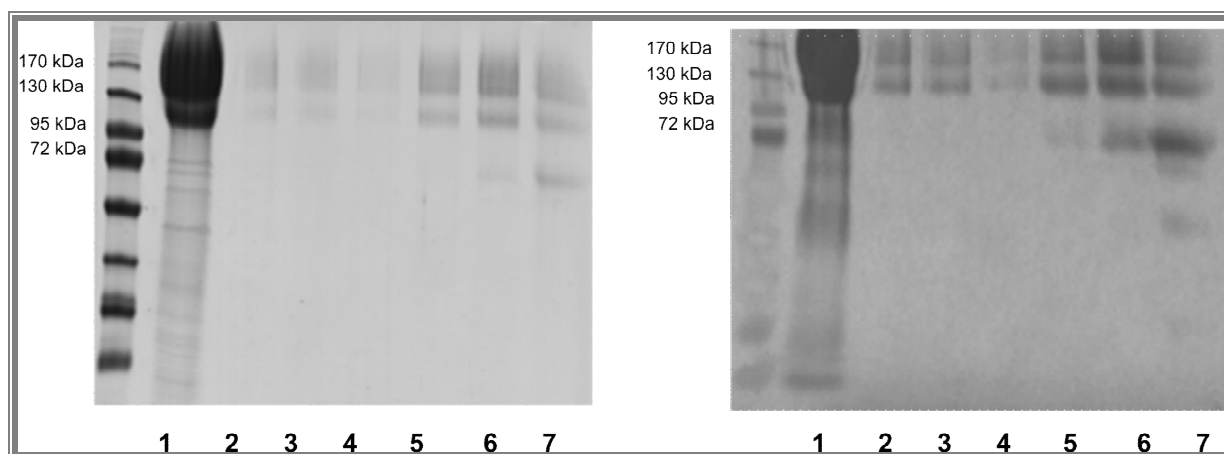


Fig. 37: SDS- Page (left) and Western Blot (right) of the supernatant of TAL6₆ treated with different buffer systems. After four hours of incubation bound proteins were boiled with SDS-containing buffer in order to be released. A description of the lanes is given in the text.

Description of the samples, which were loaded (Fig. 37):

- 1: Control (TAL6₆ untreated)
- 2: unbound TAL6₆ in Tris HCl/ NaCl pH 7.0
- 3: unbound TAL6₆ in Tris- HCl pH 7.5
- 4: unbound TAL6₆ in NaAc pH 5.4

5: bound TAL6₆ in Tris HCl/ NaCl pH 7.0

6: bound TAL6₆ in Tris- HCl pH 7.5

7: bound TAL6₆ in NaAc pH 5.4

After the right buffer system for the binding assays had been successfully identified carbohydrate-binding assays were conducted starting with TAL6₆.

4.6.1 Carbohydrate-binding results for TAL6₆

In the following the results of the binding assays using different carbon sources, chitin beads, *B. cinerea*, *R. solani*, and *T. atroviride* are illustrated.

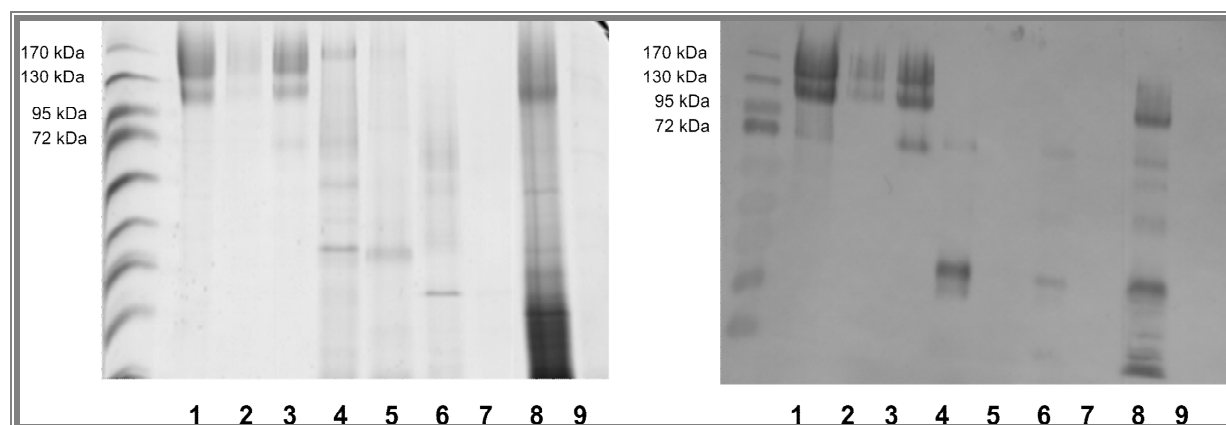


Fig. 38: SDS- Page (left) and Western Blot (right) of bound and unbound TAL6₆ treated with different carbon sources. After four hours of incubation bound proteins were boiled with SDS-containing buffer in order to be released. Description of the samples is given in the text below.

Description of the samples which were loaded (Fig. 38):

1: Control (TAL6₆ untreated)

2: unbound TAL6₆ after incubation with chitin beads

3: bound TAL6₆ to chitin beads

4: unbound TAL6₆ after incubation with the cell walls of *B. cinerea*

5: bound TAL6₆ to the cell walls of *B. cinerea*

6: unbound TAL6₆ after incubation with the cell walls of *R. solani*

7: bound TAL6₆ to the cell walls of *R. solani*

8: unbound TAL6₆ after incubation with the cell walls of *T. atroviride*

9: bound TAL6₆ to the cell walls of *T.atroviride*

TAL6₆ was found to be able to bind to chitin beads, but not to cell walls of *T. atroviride*, or to *R. solani* and *B. cinerea*.

4. Results

These findings were rather surprising, as TAL6₆ had been expected to bind to various chitinous substrates.

Since protein degradation was observed in the binding assays with cell walls, for the next binding assay cell walls of *B. cinerea*, *R. solani* and *T. atroviride* were autoclaved prior to use in order to inactivate proteases and enhance thereby the accessibility of these carbon sources for binding. Additionally binding to colloidal chitin was investigated.

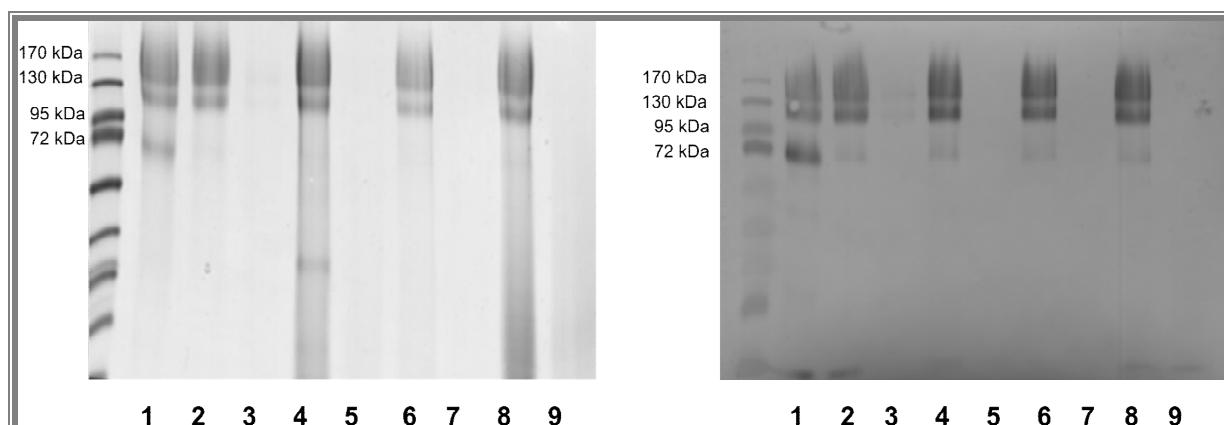


Fig. 39: SDS- Page (left) and Western Blot (right) of bound and unbound TAL6₆ treated with different carbon sources. After four hours of incubation bound proteins were boiled with SDS-containing buffer in order to be released. Description of the samples is given in the text below.

Description of the samples, which were loaded (Fig. 39):

- 1: bound TAL6₆ after incubation with NaAc buffer pH 5.4
- 2: unbound TAL6₆ after incubation with colloidal chitin
- 3: bound TAL6₆ to colloidal chitin
- 4: unbound TAL6₆ after incubation with the autoclaved cell walls of *B. cinerea*
- 5: bound TAL6₆ to the autoclaved cell walls of *B. cinerea*
- 6: unbound TAL6₆ after incubation with the autoclaved cell walls of *R. solani*
- 7: bound TAL6₆ to the autoclaved cell walls of *R. solani*
- 8: unbound TAL6₆ after incubation with the autoclaved cell walls of *T. atroviride*
- 9: bound TAL6₆ to the autoclaved cell walls of *T. atroviride*

No binding of TAL6₆ to colloidal chitin or to the heat treated cell walls was detectable. The only thing to mention is the degradation of TAL6₆, which is initiated when the protein is incubated in NaAc buffer pH 5.4.

In the next experiment the binding behavior to chitin flakes with variable size was investigated and also to cellulose. As cellulose is a carbon source which is in contrast to chitin not acetylated it was interesting to find out if a binding activity is exhibited by TAL6₆ toward cellulose.

4. Results

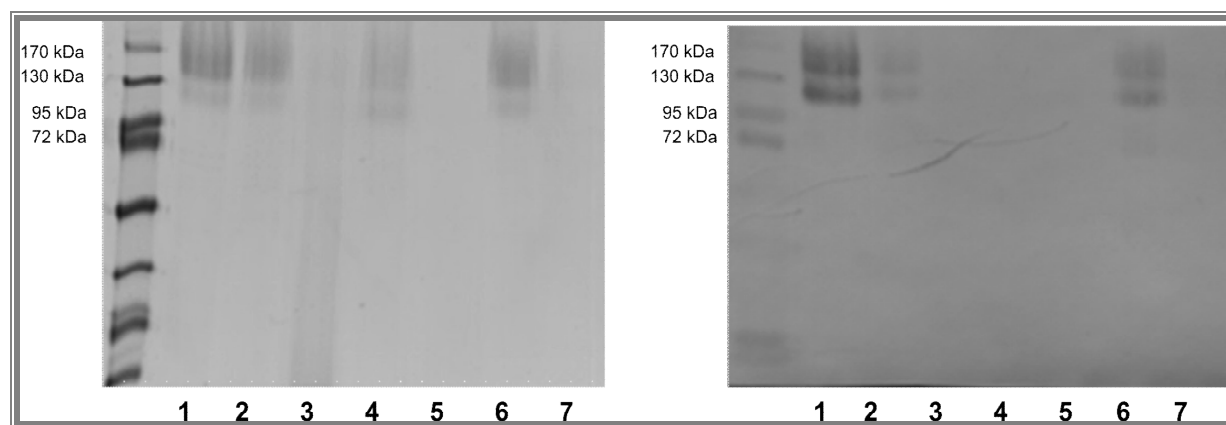


Fig. 40: SDS- Page (left) and Western Blot (right) of bound and unbound TAL6₆ treated with different carbon sources. After four hours of incubation bound proteins were boiled with SDS-containing buffer in order to be released. Description of the samples is given in the text below.

Description of the samples which were loaded (Fig. 40):

- 1: Control (TAL6₆ untreated)
- 2: unbound TAL6₆ after incubation with flaked crab shells fine
- 3: bound TAL6₆ to flaked crab shells fine
- 4: unbound TAL6₆ after incubation with the flaked crab shells harsh
- 5: bound TAL6₆ to flaked crab shells harsh
- 6: unbound TAL6₆ after incubation with cellulose
- 7: bound TAL6₆ to cellulose

No binding of TAL6₆ to flaked chitin or to cellulose was observable (Fig. 40).

The next binding investigation was done with *T. reesei* cell walls, which had been harvested after different time points (24 h and 48 h, respectively), in order to obtain cell walls with a slightly varying composition and accessibility of the different cell wall carbohydrates.

4. Results

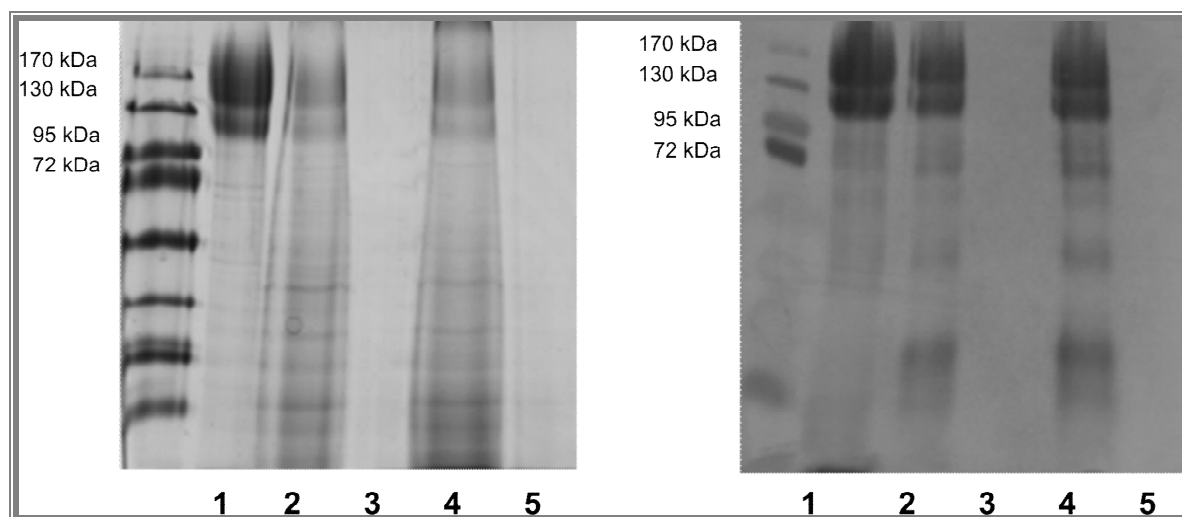


Fig. 41: SDS- Page (left) and Western Blot (right) of bound and unbound TAL6₆ treated with different carbon sources. After four hours of incubation bound proteins were boiled with SDS-containing buffer in order to be released. Description of the samples is given in the text below.

Description of the samples which were loaded (Fig. 41):

- 1: Control (TAL6₆ untreated)
- 2: unbound TAL6₆ after incubation with cell walls of *T. reesei* (harvested after 24 hours)
- 3: bound TAL6₆ to the cell walls of *T. reesei* (harvested after 24 hours)
- 4: unbound TAL6₆ after incubation with cell walls of *T. reesei* (harvested after 48 hours)
- 5: bound TAL6₆ to the cell walls of *T. reesei* (harvested after 48 hours)

As also binding to cell walls of *T. reesei* was not successful for TAL6₆ it was investigated if a positive effect on binding could be observable if the accessibility of the cell walls of *T. atroviride* was improved by performing an alkaline treatment of them (Material and Methods).

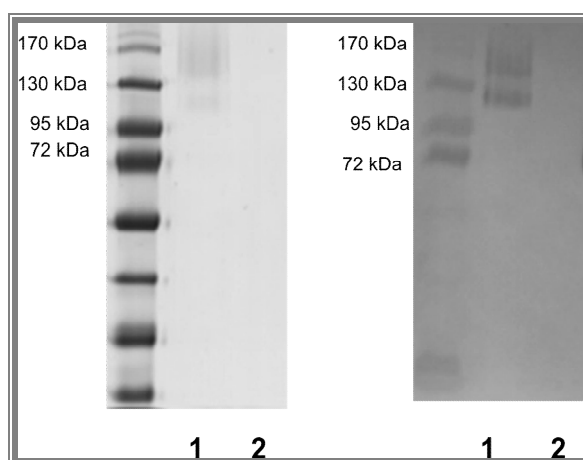


Fig. 42: SDS- Page (left) and Western Blot (right) of bound and unbound TAL6₆ treated with different carbon sources. After four hours of incubation bound proteins were boiled with SDS-containing buffer in order to be released. Description of the samples is given in the text below.

Description of the samples, which were loaded (Fig. 42):

1: unbound TAL6₆ after incubation with the alkaline treated cell walls of *T. atroviride*

2: bound TAL6₆ to the alkaline treated cell walls of *T. atroviride*

According to the findings of the binding assays (Fig. 38- 42) a summary is given to which carbon sources TAL6₆ is able to bind to. The TAL6₆ domain can only bind to chitin beads. Chitin beads (New England Biolabs) consist of pure chitin and are not interfering with an active matrix. The manufacturing contains a reacylation step based on purified chitosan.

Binding to	YES	NO
<i>Trichoderma atroviride</i> CW		x
alkaline treated <i>Trichoderma atroviride</i> CW		x
<i>Trichoderma reesei</i> CW		x
<i>Botrytis cinerea</i> CW		x
<i>Rhizoctonia solani</i> CW		x
Chitin Beads	x	
Flaked chitin fine		x
Flaked chitin crude		x
Cellulose		x
Colloidal chitin		x

Fig. 43: Summary of the binding characteristics of TAL6₆ to different carbon sources. Tal6₆ exhibits only binding activity for chitin beads, but not for cell walls (CW) of different fungi or for cellulose.

4.6.2 Carbohydrate-binding results for TAL6₄

Exactly the same conditions were maintained to investigate the binding behavior of TAL6₄. In the following figures cell wall binding studies of TAL6₄ are illustrated.

First binding capability of TAL6₄ to cell walls of *T. atroviride*, to cell walls of *T. atroviride* which have been autoclaved and to cell walls of *B. cinerea* has been investigated.

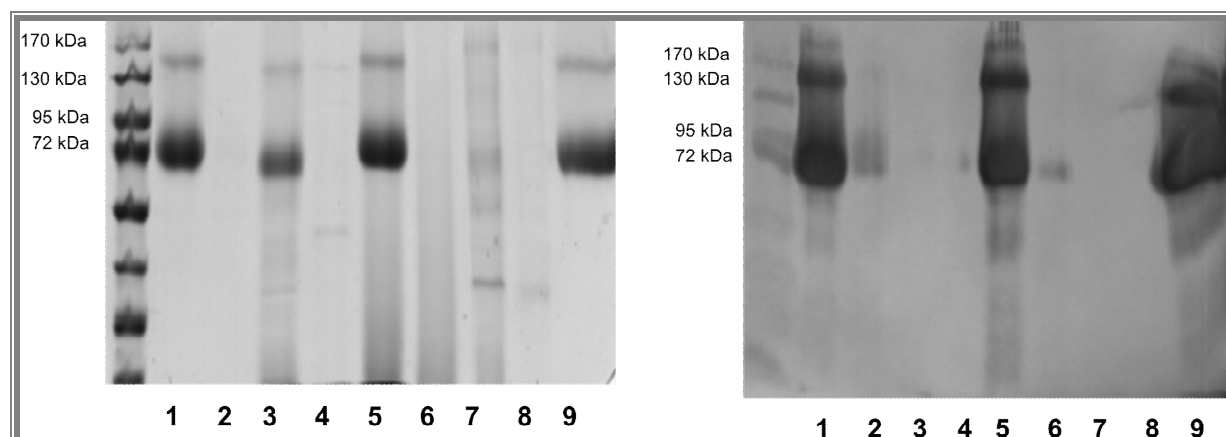


Fig. 44: SDS- Page (left) and Western Blot (right) of the supernatant of TAL6₄ treated with different carbon sources. After four hours of incubation bound proteins were boiled with SDS-containing buffer in order to be released. Description of the samples is given in the text below.

Description of the samples which were loaded (Fig. 44):

- 1: unbound TAL6₄ after incubation with cellulose
- 2: bound TAL6₄ to cellulose
- 3: unbound TAL6₄ after incubation with cell walls of *T. atroviride*
- 4: bound TAL6₄ to the cell walls of *T. atroviride*
- 5: unbound TAL6₄ after incubation with the autoclaved cell walls of *T. atroviride*
- 6: bound TAL6₄ to the autoclaved cell walls of *T. atroviride*
- 7: unbound TAL6₄ after incubation with the cell walls of *B. cinerea*
- 8: bound TAL6₄ to the cell walls of *B. cinerea*
- 9: bound TAL6₄ after incubation with the NaAc buffer pH 5.4

No binding affinity to the cell walls of *T. atroviride* or to the heat treated cell walls of *T. atroviride* was observable for TAL6₄. TAL6₄ is also not able to bind to cell walls of *B. cinerea*.

4. Results

Further the binding ability of TAL6₄ to heat pretreated cell walls of *B. cinerea* and *R. solani* as well as the binding behavior to untreated cell walls of *R. solani* was tested.

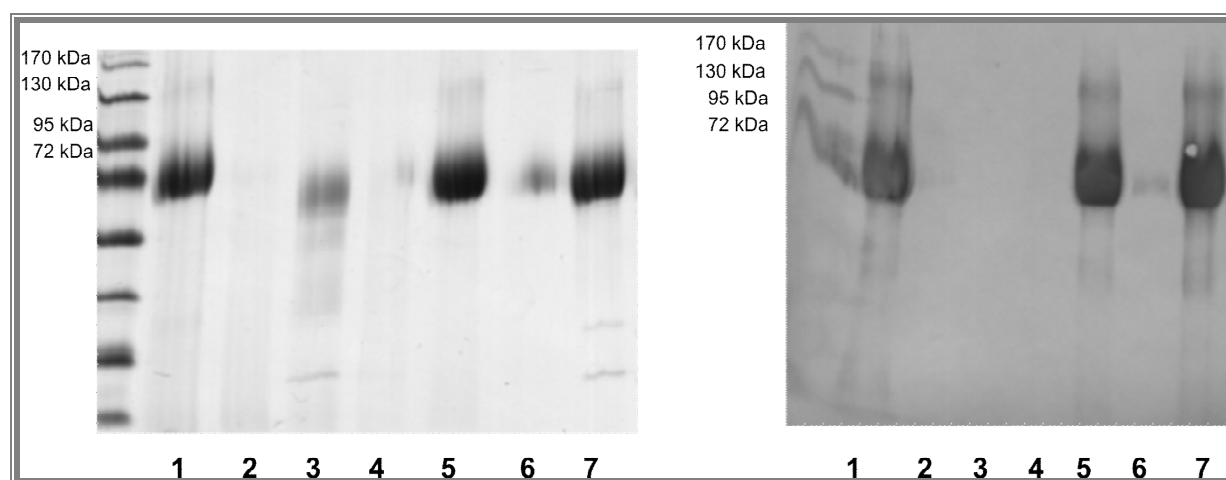


Fig. 45: SDS- Page (left) and Western Blot (right) of the supernatant of TAL6₄ treated with different carbon sources. After four hours of incubation bound proteins were boiled with SDS-containing buffer in order to be released. Description of the samples is given in the text below.

Description of the samples, which were loaded (Fig. 45):

- 1: unbound TAL6₄ after incubation with the autoclaved cell walls of *B. cinerea*
- 2: bound TAL6₄ to the autoclaved cell walls of *B. cinerea*
- 3: unbound TAL6₄ after incubation with cell walls of *R. solani*
- 4: bound TAL6₄ to the cell walls of *R. solani*
- 5: unbound TAL6₄ after incubation with the autoclaved cell walls of *R. solani*
- 6: bound TAL6₄ to the autoclaved cell walls of *R. solani*
- 7: Control (TAL6₄ untreated)

No binding to any of the cell walls, which have been used in this experiment, was detectable for TAL6₄. As a positive control an untreated sample of TAL6₄ was loaded on the gel as well. Next thing we wanted to investigate was the binding ability of TAL6₄ to chitin beads, for which the binding behavior of TAL6₆ was positive. Further we wanted to examine if a binding for TAL6₄ is possible to flaked chitin with different sizes as well as to colloidal chitin (Fig. 46).

4. Results

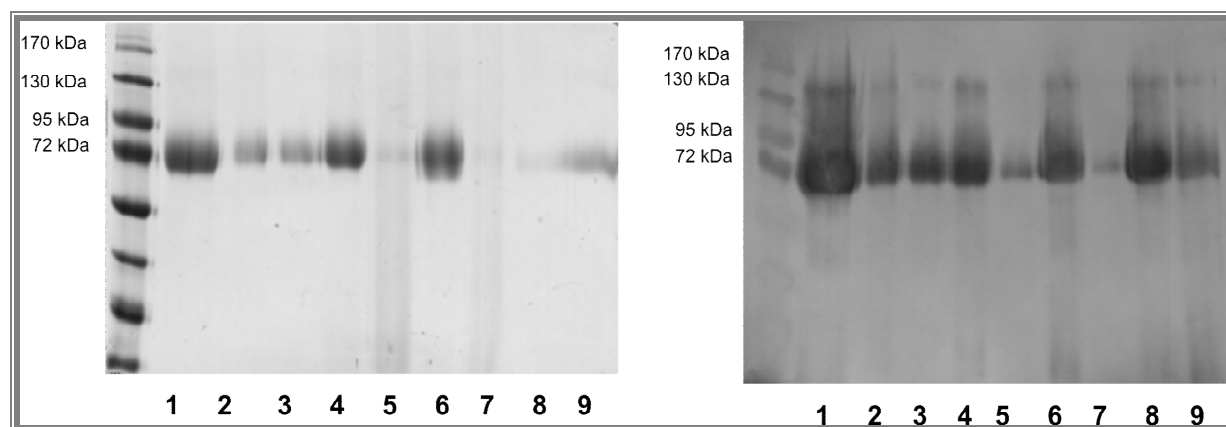


Fig. 46: SDS- Page (left) and Western Blot (right) of the supernatant of TAL6₄ treated with different carbon sources. After four hours of incubation bound proteins were boiled with SDS-containing buffer in order to be released. Description of the samples is given in the text below.

Description of the samples, which were loaded (Fig. 46):

- 1: Control (TAL6₄ untreated)
- 2: unbound TAL6₄ after incubation with chitin beads
- 3: bound TAL6₄ to chitin beads
- 4: unbound TAL6₄ after incubation with flaked crab shells fine
- 5: bound TAL6₄ to flaked crab shells fine
- 6: unbound TAL6₄ after incubation with flaked crab shells harsh
- 7: bound TAL6₄ to flaked crab shells harsh
- 8: unbound TAL6₄ after incubation with colloidal chitin
- 9: bound TAL6₄ to colloidal chitin

The results indicated binding activity of TAL6₄ for chitin beads as well as for colloidal chitin.

Binding to colloidal chitin could not be observed for TAL6₆.

Last thing we wanted to examine was the binding behavior of TAL6₄ to the cell walls of *T. atroviride*, which had been alkaline treated before to extract the chitin-glucan fraction of the cell walls (Fig. 47).

4. Results

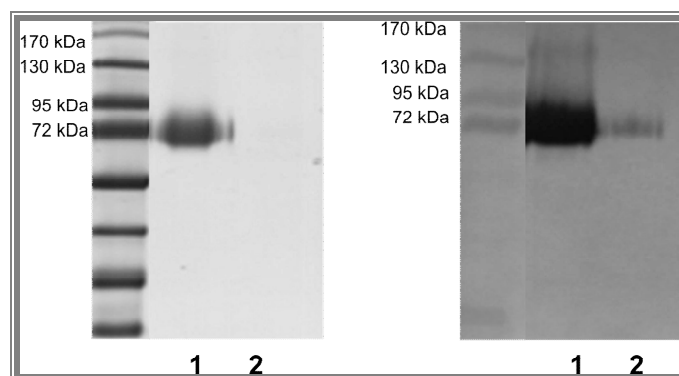


Fig. 47: SDS- Page (left) and Western Blot (right) of the supernatant of TAL6₄ treated with cell walls of *T. atroviride*, which had been alkaline treated before to extract the chitin-glucan fraction of the cell walls. After four hours of incubation bound proteins were boiled with SDS-containing buffer in order to be released. Description of the samples is given in the text below

Description of the samples, which were loaded (Fig. 47):

- 1: unbound TAL6₄ after incubation with the alkaline treated cell walls of *T. atroviride*
- 2: bound TAL6₄ to the alkaline treated cell walls of *T. atroviride*

According to the findings of the binding assays (Fig. 44- 47) a summary is given to which carbon sources TAL6₄ is able to bind to. The TAL6₄ domain binds to colloidal chitin and to chitin beads (Fig. 48).

Binding to	YES	NO
<i>Trichoderma atroviride</i> CW		X
alkaline treated <i>Trichoderma atroviride</i> CW		X
<i>Trichoderma reesei</i> CW		X
<i>Botrytis cinerea</i> CW		X
<i>Rhizoctonia solani</i> CW		X
Chitin Beads	X	
Flaked chitin fine		X
Flaked chitin crude		X
Cellulose		X
Colloidal chitin	X	

Fig. 48: Summary of the binding characteristics of TAL6₄ to different carbon sources. TAL6₄ exhibits binding activity for chitin beads and colloidal chitin, but not for cell walls (CW) of different fungi or for cellulose.

4.7 Effect on spore germination of TAL6₆ and TAL6₄

Although the Tal6₆ and TAL6₄ proteins did not bind to fungal cell walls in the pull-down assays, it was tested whether they have an effect on fungal growth. For several *Trichoderma* chitinases it was already shown that they can inhibit spore germination of host fungi, but the subgroup C chitinase gene *tac6* was shown to be expressed during hyphal network formation, which suggests a role of this protein in self-cell wall remodeling. Since the *tal6* gene is genomically adjacent to *tac6*, we were interested in testing whether TAL6 has an effect on spore germination of *T. atroviride* or other fungi, alone or in combination with a chitinase mix.

For the imaging experiment spore solutions of *T. atroviride*, *T. reesei*, *A. niger* and *N. crassa* were prepared and the experiment was carried out as described in Material and Methods. Samples were examined on an inverted Nikon TE300microscope by using differential interference contrast optics and imaged with a Nikon DXM1200F digital camera.

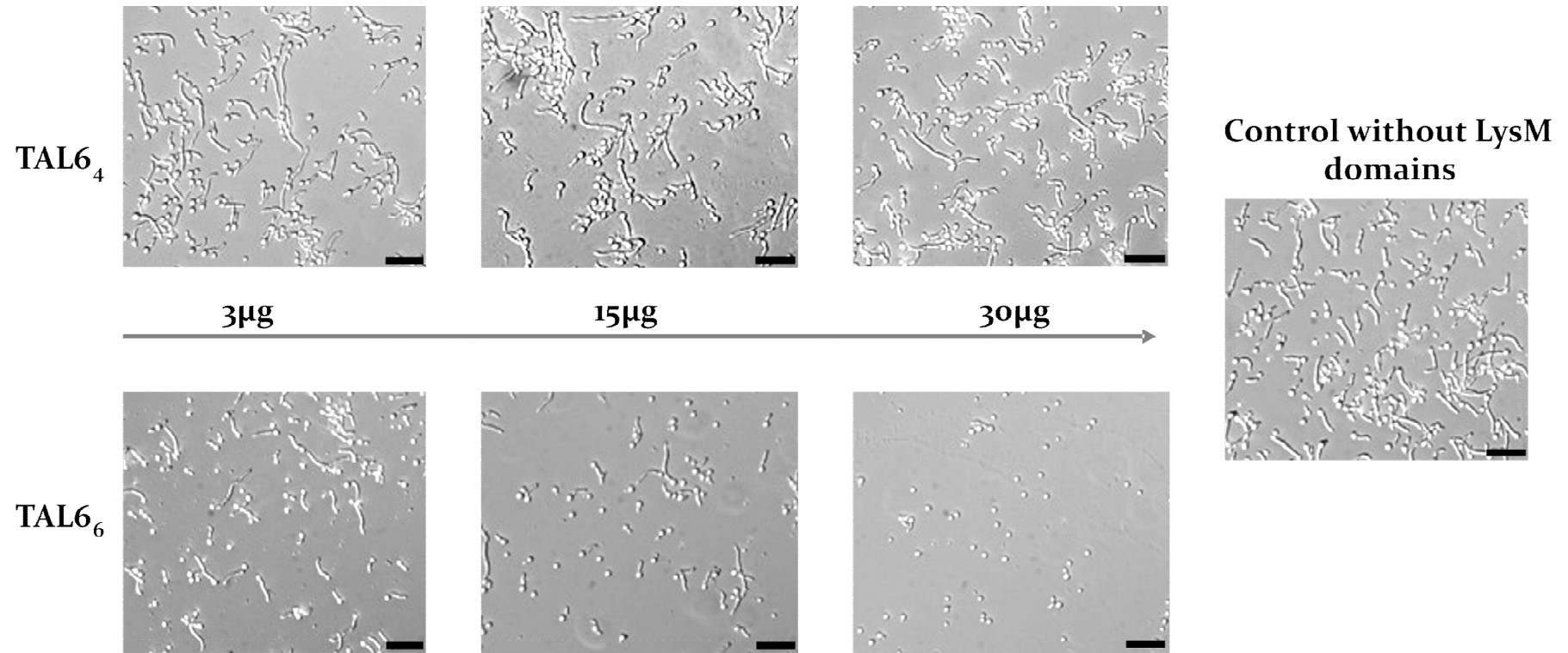


Fig. 49: Effect on spore germination of *T. atroviride* caused by TAL6₆ and TAL6₄, which were added to the spore solution. Control represents the germination of the *T. atroviride* spores in potato dextrose broth at 28 °C for 15 hours. Scale bars = 200 μm.

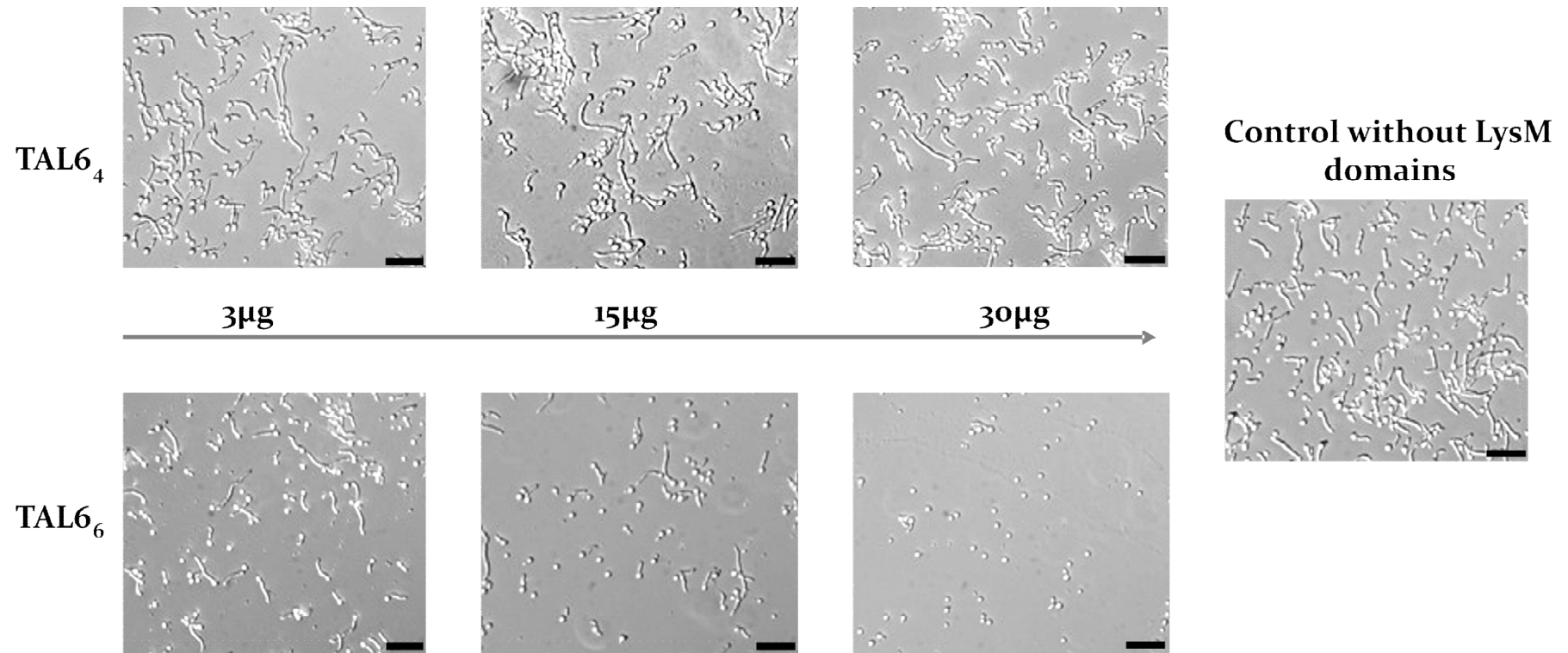


Fig. 50: Effect on spore germination of *T. atroviride* caused by TAL6₆ and TAL6₄, which were added to the spore solution incubated in potato dextrose broth at 28 °C for 15 h. 33 % of the medium were replaced with a chitinolytic *T. atroviride* enzyme mix in 20 mM Tris- HCl (pH 8.0) buffer or buffer alone (control). Scale bars= 200 μm.

TAL6₆ shows a strong effect on the spore germination, whereas TAL6₄ does not show an effect on the germination rate of spores. There is no difference between the growth behavior of the spores, where different amounts of TAL6₄ had been added and the control. Ungerminated spores (11.2%) and spores showing hyphal growing indicated a quite normal growing development under this incubation conditions for *T. atroviride*.

In contrast to TAL6₄, TAL6₆ inhibits the spore germination of *T. atroviride*. While some hyphal forms can be detected at concentrations of 3 µg and 15 µg of added TAL6₆, this growth development vanished at a concentration of 30 µg. Only ungerminated spores (97%) can be detected using this concentration of TAL6₆ (Fig. 49).

Further, it was investigated if an enzyme mix containing chitinolytic enzymes from the autolytic phase of *T. atroviride* cultures have an impact on spore germination (Fig. 50). The findings revealed that this was not the case for *T. atroviride*. Spore germination and impaired hyphal growth could be detected to the same extent as can be seen in Fig. 49, whereas the chitinolytic enzyme mix by itself did not influence spore germination of *T. atroviride*. Thus, spore germination of *T. atroviride* is not inhibited when incubating in a *T. atroviride* chitinase containing media.

In the case of *T. reesei* a strong impact on spore germination efficiency was also detected upon addition of TAL6₆ (Fig. 51): spore germination started to be inhibited even at the lowest concentration of TAL6₆ (3 µg) and additionally aggregation of the spores was observed at higher protein concentrations, which is indicative of extremely unfavourable conditions in this species. There was no effect of the spore germination caused by different concentrations of TAL6₄ (8.4 % of ungerminated spores). At high and at low levels of TAL6₄ concentrations the spore germination was almost the same compared to the control.

Different germination behavior was observed when adding an enzyme mixture containing chitinolytic enzymes from the autolytic phase of *T. atroviride* cultures. No spore germination occurred in the control as well as in the samples that contained different concentrations of TAL6₆ and TAL6₄ (Fig. 52). This effect correlates very well with recent findings, demonstrating that chitinases of *T. atroviride* can distinguish very well between self and non self cell walls [91].

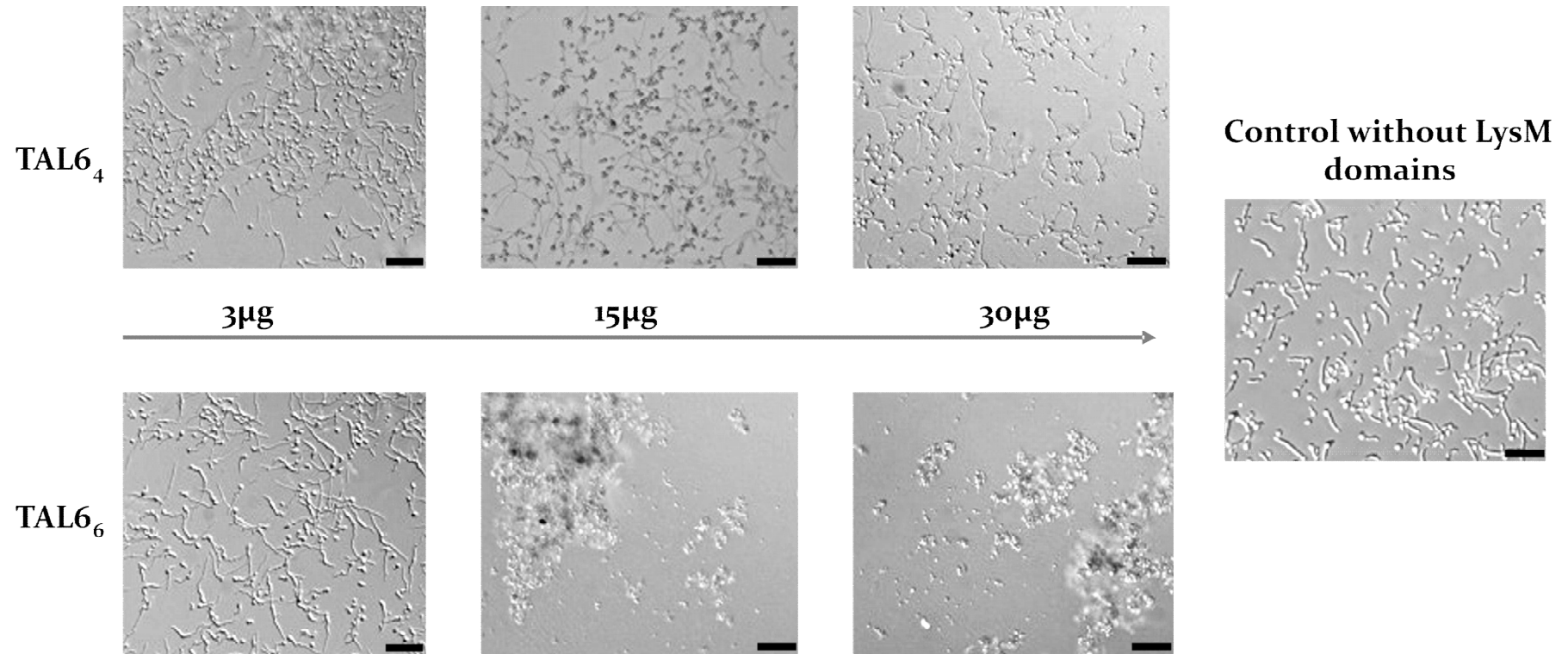


Fig. 51: Effect on spore germination of *T. reesei* caused by TAL6₆ and TAL6₄, which were added to the spore solution. Control represents the germination of the *T. reesei* spores in potato dextrose broth at 28 °C for 15 hours. Scale bars = 400 μm.

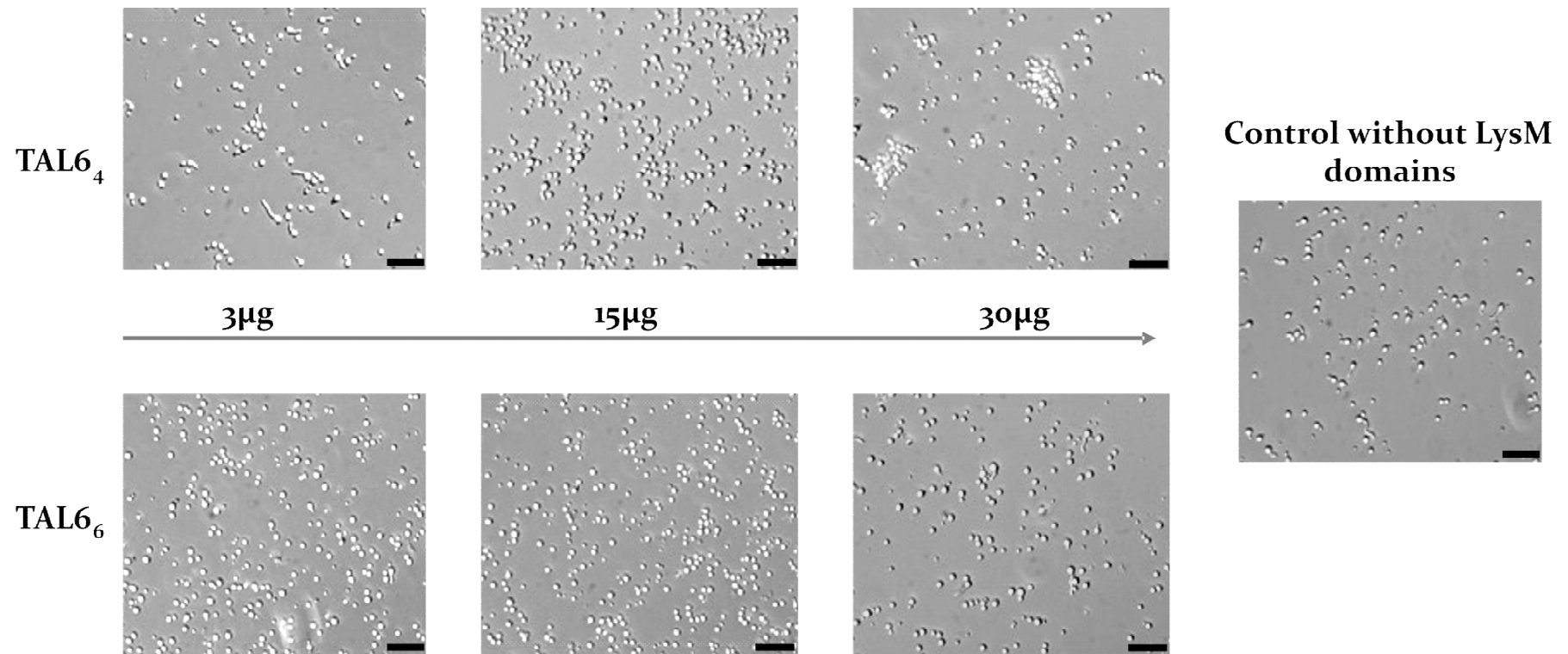


Fig. 52: Effect on spore germination of *T. reesei* caused by TAL6₆ and TAL6₄, which were added to the spore solution incubated in potato dextrose broth at 28 °C for 15 h. 33 % of the medium were replaced with a chitinolytic *T. atroviride* enzyme mix in 20 mM Tris-HCl (pH 8.0) buffer or buffer alone (control). Scale bars = 200 μm.

The finding that a chitinolytic enzyme mix is detrimental for spore germination was also found in assays with other fungal species, as can be seen in the first two pictures of the following figures (Fig. 53, Fig. 54). Germination was completely inhibited in *A. niger* and *N. crassa* upon incubation with a chitinolytic enzyme mix of *T. atroviride*.

In Fig. 53 and Fig. 54 the effect on spore germination of *A. niger* and *N. crassa* caused by a high concentration of TAL6₆ and TAL6₄ is also shown. In both cases the spore germination is not influenced by these two proteins (ungerminated spores of *A. niger* treated with TAL6₆ exhibit a percentage of 2.3 % and in the case of the treatment with TAL6₄ almost every spore was germinated; for the spores of *N. crassa* 5.8 % remained ungerminated when treated with TAL6₆ and when treated with TAL6₄ 2.3 % of the spores were not germinating as can be seen by comparing the samples to the control. Interestingly TAL6₆ does not inhibit the hyphal development of *A. niger* and *N. crassa*. However, in both cases the effect of spore germination is inhibited when the spores are exposed to a mixture of *T. atroviride* enzymes.

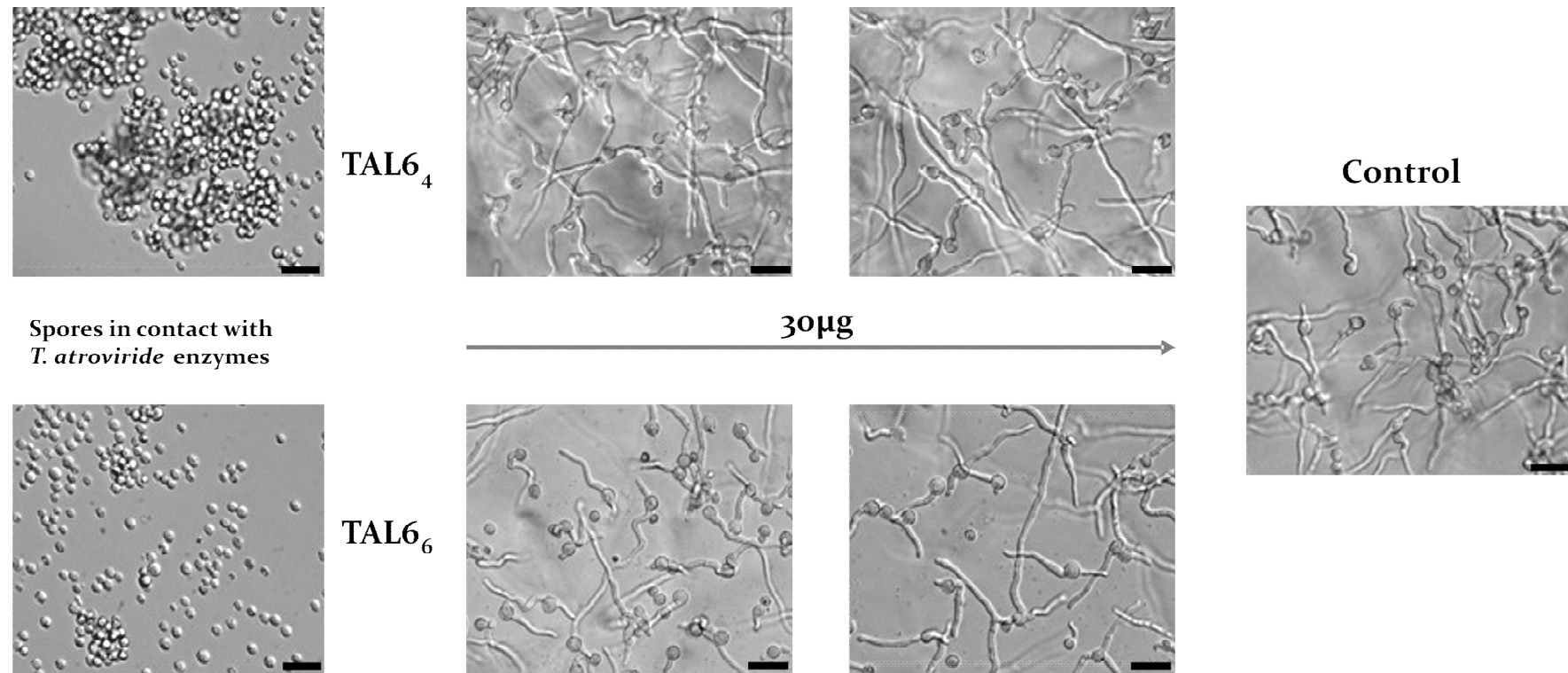


Fig. 53: Effect on spore germination of *A. niger* caused by TAL6₆ and TAL6₄, which were added to the spore solution incubated in potato dextrose broth at 28 °C for 15 h. The first two pictures show the effect on spore germination of *A. niger* caused by the replacement of 33 % medium with a chitinolytic *T. atroviride* enzyme mix in 20 mM Tris- HCl (pH 8.0) buffer or buffer alone (control). Scale bars = 100 µm.

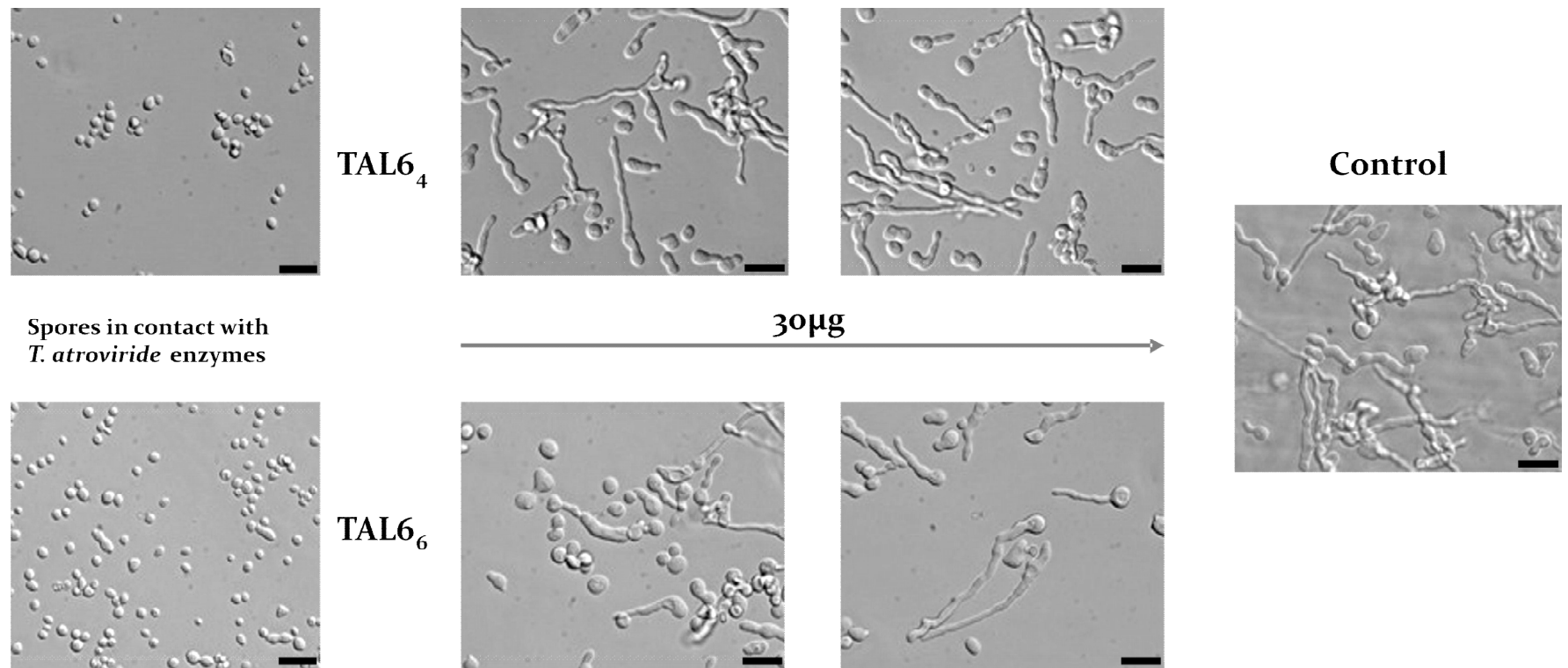


Fig. 54: Effect on spore germination of *N. crassa* caused by TAL₆₆ and TAL₆₄, which were added to the spore solution incubated in potato dextrose broth at 25 °C for 8 h. The first two pictures show the effect on spore germination of *A. niger* caused by the replacement of 33 % of the medium with a chitinolytic *T. atroviride* enzyme mix in 20 mM Tris-HCl (pH 8.0) buffer or buffer alone (control). Scale bars = 100 µm.

4. Results

A summary of the effects of TAL6₆ and TAL6₄ on the spore germination of *T. atroviride*, *T. reesei*, *A. niger* and *N. crassa* is given in Table 56. The numbers indicate the percentages of ungerminated spores of the respective fungus when treated with the proteins alone and when treated with a combination of proteins and chitinolytic enzyme mix of *T. atroviride*.

Table 56: Summary of the results obtained by investigating the effect on spore germination of TAL6₆ and TAL6₄

	TAL6 ₆	TAL6 ₄	TAL6 ₆ + chitinolytic enzyme mix	TAL6 ₄ + chitinolytic enzyme mix
<i>T. atroviride</i>	97%	11.2 %	97%	11.2%
<i>T. reesei</i>	97%	8.4%	99%	99%
<i>A. niger</i>	2.3%	1.0%	99%	99%
<i>N. crassa</i>	5.8%	2.3%	99%	99%

When incubating TAL6₆ with a spore solution of *T. atroviride*, a strong effect on spore germination could be observed. Compared to the control, 97% of the spores remained ungerminated. In contrast to that TAL6₄ did not show a strong effect on the spore germination. Only 11.2% remained ungerminated. Almost the same effect appeared by incubating the proteins with a spore solution of *T. reesei*. TAL6₆ showed again an inhibiting effect on spore germination. Almost no effect on spore germination could be observed by incubating TAL6₆ and TAL6₄ to spore solutions of *A. niger* and *N. crassa*. That means that the effect was only restricted to *T. atroviride*.

In the other experiments a chitinolytic enzyme mix of *T. atroviride* was additionally added to the spore solutions. Again TAL6₆ showed an inhibiting effect on spore germination and again TAL6₄ showed almost no effect on spore germination of *T. atroviride*, although a chitinolytic enzyme mix had been added.

This effect could not be observed for *T. reesei*, *A. niger* and *N. crassa*. Regardless of which LysM motif had been chosen for incubation, the spores remained to 99 % ungerminated. This suggests that the chitinolytic enzyme mix of *T. atroviride* is accountable for the inhibiting effect on spore germination.

4.8 EPL proteins of *T. atroviride*

4.8.1 Overview of EPL proteins of *T. atroviride* and other members of the cerato-platanin family

The genome of *T. atroviride* contains three genes that encode proteins belonging to the cerato-platanin family, named EPLs (eliciting plant response-like proteins) [78]. Members of the cerato-platanin family have been implied in various functions including cell wall coating and protection and have been demonstrated to act as elicitors of plant defense responses [74]. However, their primary functions in fungal growth and development are not understood yet. EPL1 is a small protein containing four cysteine residues that form disulfide bridges and was identified to be the major secreted protein of *T. atroviride* on glucose [78]. The orthologue of *T. atroviride* EPL1 in the fungus *T. virens* is SM1.

EPL1 and SM1 have high sequence similarity, both occur as monomer and as a dimer.

To analyze the biological functions of EPLs in *Trichoderma atroviride* knockout strains have been created to characterize these proteins in more detail.

All three *Trichoderma* species for which complete genome sequences are available, namely *T. reesei*, *T. virens* and *T. atroviride*, have each three genes encoding cerato-platanin proteins. In this thesis we wanted to investigate the function of EPL proteins of *T. atroviride*. This should further serve as a basis to understand better the roles of CPPs in fungi.

4.8.2 Characterization of EPL proteins of *T. atroviride*

EPL proteins are highly conserved according to their aa-sequence and exhibit 4 cysteine residues, which enable them to form two disulfide bonds. Using the tool Compute pI/MW online available on the ExPASy site (<http://expasy.org/tools/>) the isoelectric point (pI) and the molecular weight (MW) of the mature proteins (without signal sequence) was calculated, shown in Fig. 55.

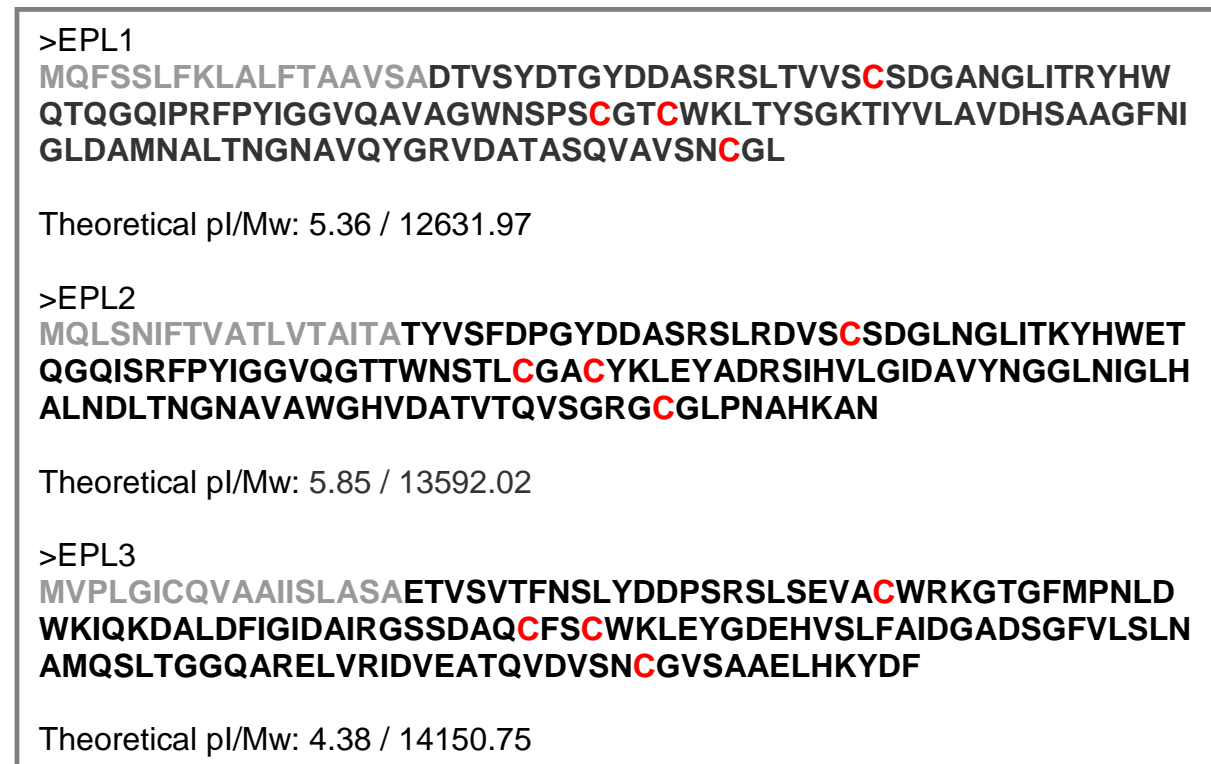


Fig. 55: Characteristic data of the EPL proteins of *T. atroviride*. Each amino acid sequence is illustrated as well as the isoelectric point and the molecular weight. The cysteine residues are shown in red and the signal sequence is shown in grey.

The red colored cysteine residues show a pattern, they are much conserved among the sequences of the EPL proteins. EPL1 and EPL2 are showing similar cysteine pattern: the first conserved motif [**CSDGL**] appears in EPL1 and EPL2, in the second motif [**CGT**] (shown for EPL1) EPL2 contains an A in stead of a T. The third cysteine pattern is [**CGL**], which is the same in EPL1 and EPL2, whereas EPL3 contains also the [**CG**]. Analysis of available EST sequences in the genome database of *T. atroviride* only yielded hits for *epl1*, which showed that it contains UTR's in the length of 144 bp in the upstream region and in the downstream region in the length of 262 bp.

4. Results

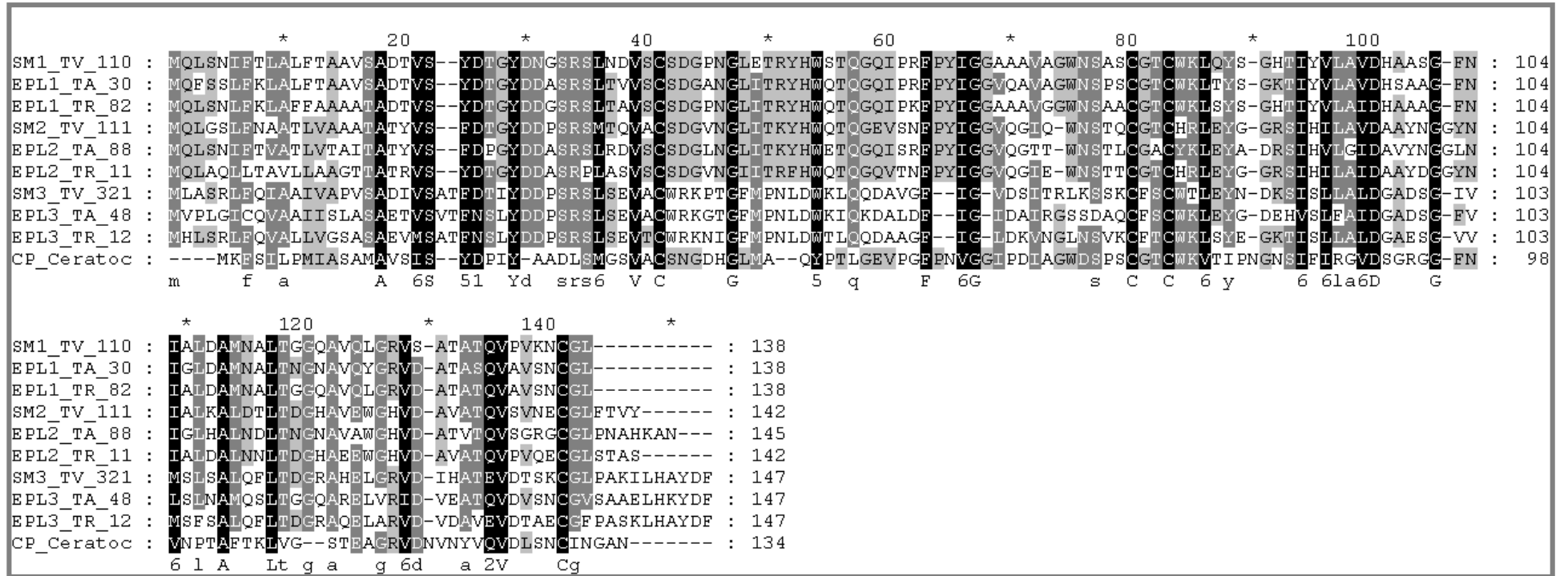


Fig. 56: Alignment of the three EPLs of *T. atroviride* with their orthologues in *T. vires* and *T. reesei* as well as the cerato-platanin protein of *C. platani* using the program GeneDoc.

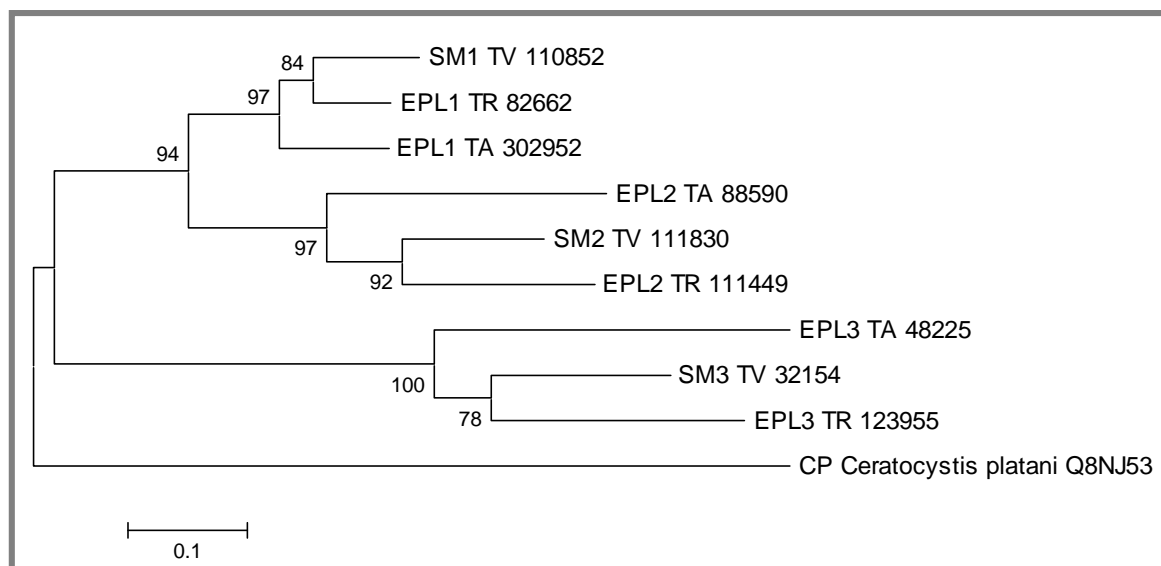


Fig. 57: Phylogeny of the EPL proteins of *T. atroviride* (TA) and its orthologues in *T. vires* (TV) and *T. reesei* (TR) as well as the CP of *C. platani*. The proteins containing their signal peptide were used for phylogenetic analysis using Neighbor joining analysis. The bar marker indicates the genetic distance, which is proportional to the number of amino acid substitutions. Protein names are followed by an abbreviation for the organisms and the protein ID number, except for CP of *C. platani*, where the UniProtKB number is given.

An alignment (Fig. 56) of the EPL proteins of *T. atroviride* and its orthologues in *T. vires* and *T. reesei* as well as the Cerato-platanin protein (CP) of *Ceratocystis platani* was performed using GeneDoc and a phylogenetic analysis was performed by using the Neighbor-Joining algorithm in the program Mega3.1 (Fig. 57). All branches exhibit high bootstrap percentages, which indicate that all of the observed clades reflect a phylogenetic history. Taken together, it can be concluded that EPL1 and EPL2 of *T. atroviride* and its orthologues in *T. vires* and *T. reesei* are more closely related to each other than compared to EPL3 of *T. atroviride* and its orthologues in *T. vires* and *T. reesei*. CP of *Ceratocystis platani* exhibits the highest distance to all of the other proteins.

4.8.3 Construction of the *epl* deletion cassettes

4.8.3.1 Construction of the *epl1* deletion cassette

For the construction of the *epl1* expression vector, where the *epl1* expression cassette could be obtained by PCR amplification, a promoter fragment in the size of 960 bp was amplified from the genomic DNA of *T. atroviride* P1 using the following oligos: *epl1amdSProm_Fw*: 5'-TAT CGA TAC CGT CGA CGC TGC TAG CAA GAA GAA CT-3' and *epl1amdSProm_Rv*: 5'-TAC TCA AGA CGT CGA CAA GCT GAG TAG TAG TGA AGC GAA-3' and also a

terminator fragment (1100 bp) was amplified using the following oligos: *ep11amdSTerm_Fw*: 5'-CTC AAC CAT GGT ACC GAC CAT TAT GGA ATT GCA TCG-3' and *ep11amdSTerm_Rv*: 5'-GGG CGA ATT GGG TAC CAC AGT CGT CGA TGT AAG T-3'. The promoter fragment was recombined with the cut vector according to the supplied manual of the In-Fusion Advantage PCR Cloning Kit w/Cloning Enhancer (Eubio, Austria) and transformed into *E. coli* one Shot TOP10 Chemically Competent cells (Invitrogen) and selected for ampicillin resistance. To verify positive colonies a restriction digest was carried out with *SalI*. Positive colonies were digested with *Acc65I* and recombined with the terminator fragment using again the In-Fusion Advantage PCR Cloning Kit w/Cloning Enhancer (Eubio, Austria).

The *ep11* expression cassette (5924 bp) was obtained by PCR amplifying the cassette using the oligos: *ep11amdSProm_Fw*: 5'-TAT CGA TAC CGT CGA CGC TGC TAG CAA GAA GAA CT-3' and *ep11amdSTerm_Rv*: 5'-GGG CGA ATT GGG TAC CAC AGT CGT CGA TGT AAG T-3' according to the supplied manual of the Roche Expand Long Template PCR System (Roche, Austria). Further details of the deletion cassettes of *ep11* are described in Material and Methods (3.4.3.1).

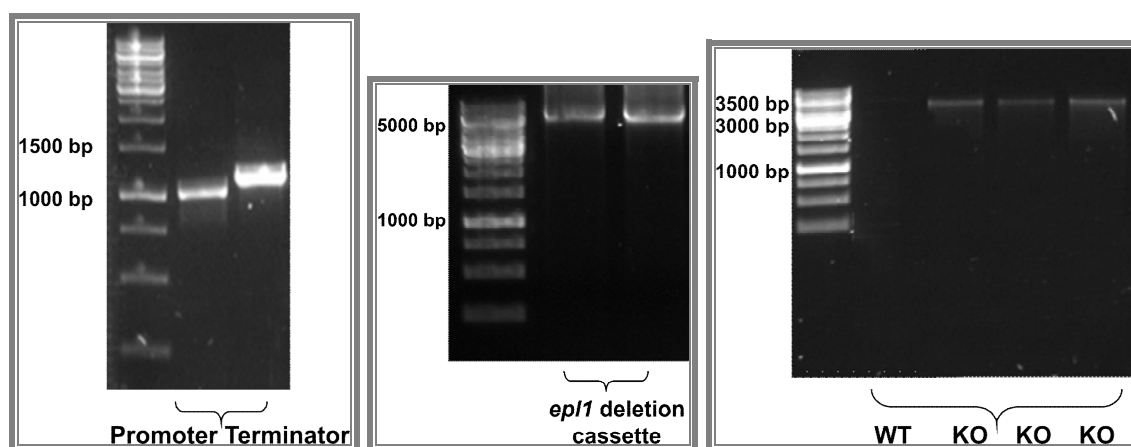


Fig. 58: Agarose gel analysis of the promoter and the terminator of the *ep11* deletion cassette (left), the complete *ep11* deletion cassette (5924 bp) (middle) and the screened KO's of *ep11* (3756 bp) (right).

The transformation of *ep11* deletion cassette into *Trichoderma atroviride* P1 is described in Material and Methods. DNA of putative positive colonies was isolated and identified positive by PCR amplification using the following oligos: *ep11 trafo-check_Fw*: 5'-ACA TCC TAC TCG TAC ATG CA-3' and *amds RV*: 5'-CCA GAG CTC GTT CAT GTT AAC AGC-3' for the verification of an *ep11*-knockout (3756 bp).

4.8.3.2 Construction of the *epl2* deletion cassette

The *epl2* deletion cassette (3878 bp) was obtained by PCR amplifying the cassette from the pJHepl2 vector, which had been created by Jasmin Hauzenberger (Bachelor thesis of Jasmin Hauzenberger: ‘Construction of gene knock-out vectors for *Trichoderma atroviride*’).

Following oligos were used: *epl2*HindIII_Fw: 5'-GTACAA GCT TGC TGG CTG TCA ACT GCA TGT C-3' and *epl2*SpeI_Rv: 5'-GTA CAC TAG TTT TCC ATG TGC TCG ACT TAC G-3'. Further details of the deletion cassettes of *epl2* are described in Material and Methods (3.4.3.2).

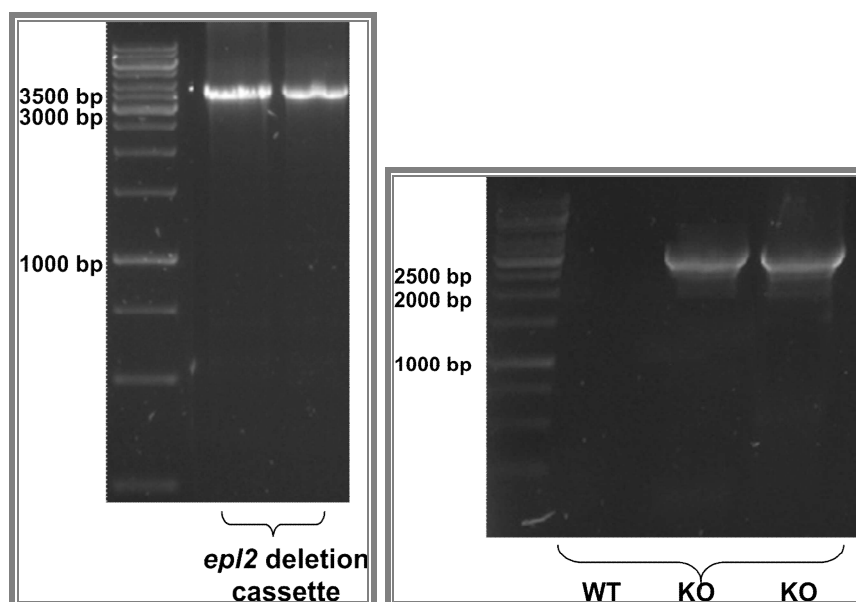


Fig. 59: The completed *epl2* deletion cassette (3878 bp) is shown on the left and the screened KO's of *epl2* are shown on the right. 2 μ L of DNA were loaded on the gels.

The transformation of the *epl2* deletion cassette into *Trichoderma atroviride* P1 is described in Material and Methods. Verification of an *epl2*-knockout was done by using the oligos: *hphSG_Fw*: 5'-CGC AAG GAA TCG GTC AAT AC-3' and *epl2trafo-check_Rv*: 5'-ATC CTG CTG TTA CGG CCT G-3' resulting in a size of 2517 bp demonstrating a positive result.

Analysis of the morphological phenotype of the knockouts in comparison to the WT reflects no differences in growth behavior (Fig. 60).

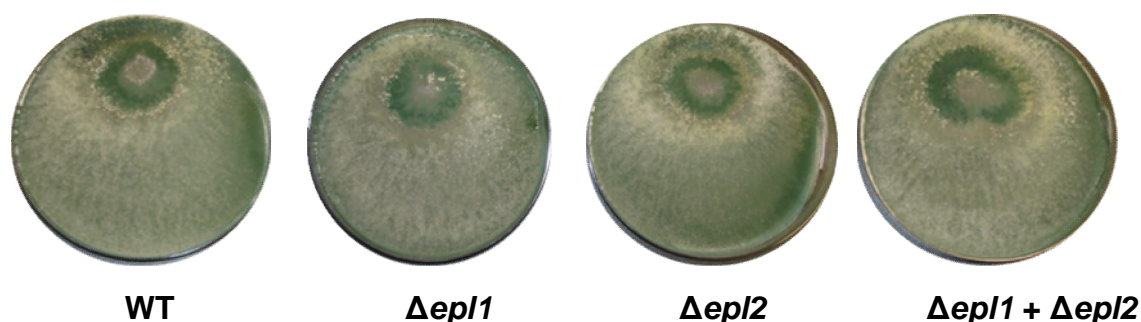


Fig. 60: Morphological analysis of the knockout strains of *epl1* and *epl2* and the double knockout of *epl1* and *epl2*. Strains were grown on PDA at 28 °C w/o light over days.

4.8.4 Binding assay of EPL1

Based on NMR modeling data an *N*-acetylglucosamine binding pocket was recently reported for the protein CP from *Ceratocystis platani* [92]. In order to verify experimentally whether cerato-platanin proteins are able to bind to chitinous carbon sources, carbohydrate binding studies with the protein EPL1 from *T. atroviride* were carried out in this thesis. The protein was detected either unbound in the supernatant (SN) or bound to the carbon source, from which it was released by boiling with SDS-containing buffer.

For these experiments different types of chitin (chitin beads, colloidal chitin and chitin from crab shells fine and crude) as well as cell walls of *T. atroviride* were used. After EPL1 was purified as described in [78], the protein was used for binding studies with pull-down assays using insoluble, chitinous carbon sources (Fig. 61).

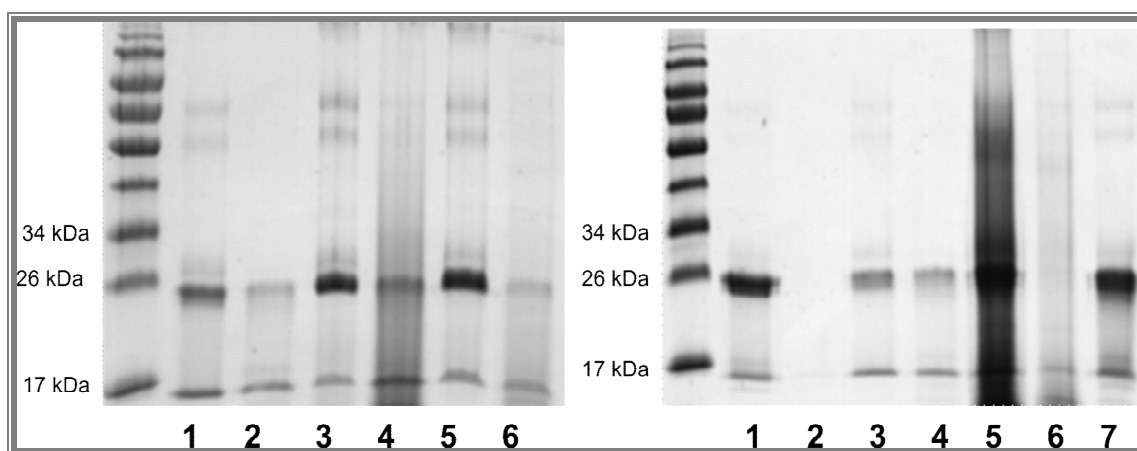


Fig. 61: SDS- Page of bound and unbound EPL1 treated with different carbon sources. After four hours of incubation bound EPL1 was boiled with SDS-containing buffer in order to be released. Description of the samples is given in the text below. 2.6 pmol of EPL1 were loaded.

Description of samples, which have been loaded (Fig. 61):

- 1: unbound EPL1 after incubation with colloidal chitin
- 2: bound EPL1 to colloidal chitin
- 3: unbound EPL1 after incubation with the flaked crab shells fine
- 4: bound EPL1 to flaked crab shells fine
- 5: unbound EPL1 after incubation with flaked crab shells harsh
- 6: bound EPL1 to flaked crab shells harsh
- 7: unbound EPL1 after incubation with chitin beads
- 8: bound EPL1 to chitin beads
- 9: unbound EPL1 after incubation with colloidal chitin
- 10: bound EPL1 to colloidal chitin
- 11: unbound EPL1 after incubation with cell walls of *T. atroviride*
- 12: bound EPL1 to the cells walls of *T. atroviride*
- 13: bound EPL1 after incubation with the NaAc buffer pH 5.4

EPL1 protein does not bind to the cell walls of *Trichoderma atroviride* and to chitin beads, but binds to flaked chitin fine and crude and to colloidal chitin. The result of the binding assay is summarized in Fig. 62.

Binding to	YES	NO
<i>Trichoderma atroviride</i> CW		x
Chitin Beads		x
Flaked chitin fine	x	
Flaked chitin crude	x	
Colloidal chitin	x	

Fig. 62: Result of the binding behavior of EPL1 to different carbon sources. EPL1 exhibit binding activity for colloidal chitin and flaked chitin crude and fine.

5. Discussion

5.1 LysM domains in eukaryotes and prokaryotes

The LysM motif is an ancient protein domain which was first described in bacteria binding to peptidoglycan of the cell wall [67] and later on was also discovered in plants as protein domain of a plant receptor-kinase binding to chitinous substrates [93]. In plants LysM motifs are part of a receptor-like kinase (RLK) and act as receptors for nodulation factors (Nod), thereby contributing to mediate symbiosis between plant and their symbiotic nitrogen-fixing bacteria [94]. Further, LysM motifs can also have other functions in plants and they have also been shown to be involved in defense signaling against fungal attacks [71]. Recently, a LysM domain of AcmA, a characterized autolysin of *Lactococcus lactis*, was reported to bind to eukaryotic cell walls, i.e. chitin and to the cell walls of the fungus *Psilocybe cubensis* [95], which refutes the hypothesis reported by Petutschnik that only eukaryotic LysM domains were able to bind to chitin [71].

In fungi, a fungal virulence factor, Ecp6, which contains three LysMs and do not contain any recognizable motif other than a varying number of LysMs was reported from the tomato pathogen *Cladosporium fulvum*. According to the classification assigned by de Jonge et al. [73] this fungal virulence factor belongs to Type A. Ecp6 was shown to dampen the defense response of tomato plants against the fungus *C. fulvum* by binding chitin-oligosaccharides and therefore preventing their recognition by the plants. This phenomenon could recently also be observed by LysM containing protein Slp1 of *Magnaporthe oryzae* [96, 97]. Over 4000 fungal LysM proteins can be found in public databases [73] but for the most part their function is still unknown. The amino acid sequences of fungal LysM domains are highly variable, which suggests that these proteins have different substrate binding abilities. Further LysM proteins such as those that were characterized in this thesis were detected in close proximity to subgroup C chitinases in the genomes of *Trichoderma* spp., which are reported to play a major role in mycoparasitism but also in cell wall remodeling. Thus, a supposed role for these domains could therefore be targeting of the chitinase to its correct place for hydrolysis [98].

5.2 TAL6₆ and TAL6₄ LysM domains of *Trichoderma atroviride*

5.2.1 Protein architecture of TAL6₆ and TAL6₄

In this thesis we were aiming to further unravel the function and the carbohydrate-binding specificities of LysM motifs in fungi in order to increase our understanding of chitin perception and degradation by fungi. We used the fungus *T. atroviride* as a model to study proteins with LysM domains. *T. atroviride* has 8 proteins with a total of 21 LysM motifs: (1) subgroup C chitinases that contain CBM18 and CBM50 (LysMs) and (2) LysM proteins, which contain a signal peptide sequence and are thus targeted to the secretory pathway, but contain no catalytic modules (Fig. 12). The genes encoding LysM proteins were recently shown to be exclusively located next to subgroup C chitinase genes in the genomes of *Trichoderma* spp. In this thesis we focused on TAL6, a protein that contains six LysM motifs. Its gene is located next to the subgroup C chitinase gene *tac6* on scaffold contig_17:997120-1000318 in the *T. atroviride* genome (<http://genome.jgi-psf.org/Triat2/Triat2.home.html>). Analysis of the LysM sequences of TAL6 showed that the 4 LysM motifs in the C-terminal regions of the proteins are highly similar to each other, whereas the two LysM motifs in the N-terminal region of the protein show a higher sequence variability and show less similarity to the LysM consensus pattern currently deposited in databases (e.g. SM00257, PF0147). Therefore, in this thesis we decided to overexpress and characterize a full-length version of TAL6 containing all six LysM motifs (TAL6₆) and a truncated version of TAL6 (TAL6₄) that consists only of the four strongly conserved LysM motifs from the C-terminal region of TAL6. Both proteins, designated TAL6₆ and TAL6₄, were heterologously expressed in *Pichia pastoris*.

5.2.2 Heterologous protein expression in *Pichia pastoris*

In this doctoral thesis two different constructs were created to be overexpressed (Fig. 16 and Fig. 17). The first construct contained all the six LysM motifs (TAL6₆) and the second construct contained only the 4 closely related LysM domains (TAL6₄). The aim was to detect possible differences in the carbohydrate-binding specificities and between these two protein versions. To be able to investigate the function of TAL6₄ and TAL6₆ it was necessary to produce the two protein domains in large quantities and in order to achieve this several parameters were optimized during this thesis. First, different promoters, signal peptide

sequences and growth media were tested for *P. pastoris*. Expression with the commercially available EasySelect™ Pichia Expression Kit, which uses the AOX1 promoter that can be induced with methanol, was not successful. Instead, we used the constitutive GAP promoter although it is reported that the methanol inducible alcohol oxidase 1 (AOX1) promoter is significantly stronger than the constitutive glyceraldehyde-3-phosphate dehydrogenase (GAP) promoter [99]. For protein secretion in *P. pastoris* the alpha signal sequence of *Saccharomyces cerevisiae* was used and a 6x His-Tag was added at the C-terminal ends of the proteins, which was useful for protein purification and detection. However, also with this promoter protein yields turned out to be rather low. Analysis of protein expression levels with different media showed that addition of a constant glucose concentration to the YPD medium resulted in an increase of expression levels, whereas buffered minimal media instead of complex YPD medium resulted in lower expression yields. Therefore, YPD medium with additional glucose were used to produce both proteins in higher yields in *P. pastoris*. Utilization of the GAP promoter and addition of glucose to the medium was also the means of choice for production of human trypsinogen in *P. pastoris* [90]. In order to obtain sufficient protein for detailed biochemical analysis, batch fermentations in 3 liter fermenters were carried out.

5.2.3 Protein characteristics of TAL6₆ and TAL6₄

The overexpressed, purified proteins TAL6₆ and TAL6₄ were characterized with respect to their protein parameters (MW, pI, glycosylation) and their carbohydrate-binding properties. Unpurified TAL6₆ appeared as a single band in the range of ~ 185 kDa, whereas purified TAL6₆ appeared always as a double band with a MW of ~ 130 kDa of the upper stronger band and ~ 115- 120 kDa of the lower band on SDS-gels and Western blots. In contrast to that TAL6₄ always occurred only as single band in the size of 72 kDa. Since the theoretical MW of TAL6₆ is 77.7 kDa and TAL6₄ is 36.2 kDa, the proteins were subjected to enzymatic deglycosylation using the enzymes Endo H and α -mannosidase. The results (Fig. 34) showed that the size of TAL6₄ was reduced to 60 kDa, and the double band of TAL6₆ was reduced to 130 kDa and 95 kDa. These data indicate that both proteins are present as monomers and are strongly glycosylated and that the glycans were not fully removed by enzymatic deglycosylation. The used enzymes Endo H and α -mannosidase specifically target the *N*-acetylglucosamine and mannose residues of *N*-linked glycans, but the protein might still contain *O*-linked sugars. However, a dimer of TAL6₄ would have at least 72.6 kDa (2 x 36.2)

kDa, and since the size of the deglycosylated TAL6₄ proteins was 55 kDa it can be concluded that TAL6₄ was present as a monomer. Similarly for TAL6₆ the size of the upper band after enzymatic deglycosylation is ~ 130 kDa which is smaller than the size of a potential dimer. The reason why double bands were observed for TAL6₆ is not entirely clear, but it is possible that TAL6₆ is a rather instable protein. *In silico* analysis of predicted *N*-glycosylation of TAL6₆ and TAL6₄ conducted with the online tool NetNGlyc, available on the homepage of Center for Biological Sequence Analysis (CBS) (www.cbs.dtu.dk/services), predicted many potential *N*-glycosylation sites for TAL6₆, but only few for TAL6₄. *N*-glycosylation is known to occur on asparagine-residues within stretches of Asn-Xaa-Ser/Thr (where Xaa is any amino acid except proline). TAL6₄ has two *N*-glycosylation sites at positions 139 and 232. In the case of TAL6₆ the prediction displayed a total of 13 *N*-glycosylation sites (positions 35, 59, 139, 173, 193, 201, 215, 254, 291, 322, 353, 526 and 619). As a next step, the pIs of the proteins were determined with 2D-gel electrophoresis, which consists of isoelectric focusing as a first step, and a SDS-PAGE gel as second step. Analysis of TAL6₆ with 2D-gel electrophoresis revealed a pI in the range of 5.4- 6.1 for the ~ 130 kDa band and 7.1- 7.7 for the ~ 115- 120 kDa band. In contrast to that, the TAL6₄ protein showed a single band of 72 kDa on SDS-gels and had a pI in the range of 8.0- 9.1 as observed in 2D-gel electrophoresis. The multiple spots ('trains') that were observed for both bands of the TAL6₆ protein as well as the TAL6₄ protein) are indicative for glycosylated proteins. This also supports the finding that both proteins are strongly glycosylated. Although the band of TAL6₄ illustrated in Fig. 36 indicates also for a glycosylated product according to the train of spots this finding does not correlated with the outcome of the few *N*-glycosylation sites, suggesting that these proteins are additionally *O*-glycosylated. In order to elucidate this in more detail, chemical deglycosylation and analysis of the glycan moieties would be necessary. Further, N-terminal sequencing of both TAL6₆ bands would aid in characterization of this protein in more detail. Since the proteins were detected by Western-blotting using an anti- His tag antibody which binds to the C-terminus of the protein it can be excluded that the overexpressed TAL6 proteins are processed at their C-terminus. It should be emphasized that the overexpression of TAL6₆ in *T. reesei* also resulted in a band with high molecular weight (~ 250 kDa, Fig. 23), suggesting that this protein is also strongly glycosylated in *Trichoderma* and therefore probably also in its native organism *T. atroviride*. Glycosylation is commonly observed for fungal proteins and could also in the case of TAL6 be important for stability of the protein and is may the relevant factor regarding the main function of this protein.

5.2.4 Carbohydrate-binding properties of TAL6₆ and TAL6₄

So far, only two LysM proteins have been described from fungi: Ecp6 of the plant pathogenic fungus *Cladosporium fulvum* and Slp1 of *Magnaporthe oryzae* [96] [97]. Slp1 and Ecp6 are both from plant pathogenic fungi and highly specific chitin binding LysM effectors that prevent chitin-triggered immunity in their plant hosts.

However, LysM proteins can also be found in non-pathogenic fungi e.g. the saprothrophs *Neurospora crassa* and *T. reesei* or the mycoparasites *T. atroviride* and *T. virens*. It is not clear yet what carbohydrate-binding specificities and functions LysM proteins have in these fungi. The gene encoding the *T. atroviride* protein TAL6 is in the genome next to the subgroup C chitinase encoding gene *tac6*, which was shown to be expressed during hyphal network formation of *T. atroviride*. The genes are 1000 bp distant from each other and share their 5' regions, which would point to a possible transcriptional coregulation of *tal6* and *tac6*. This was also experimentally confirmed by Gruber et al. [86].

In order to investigate the biological function of TAL6 its carbohydrate-binding properties were analyzed. The heterologously expressed proteins TAL6₆ and TAL6₄ were used for binding assays with several insoluble chitinous carbon sources. The following carbon sources were used: chitin beads, flaked chitin from shrimps, fungal cell walls of *T. atroviride*, *T. reesei*, *Botrytis cinerea* and *Rhizoctonia solani* and cellulose (Avicel). Interestingly, for the full-length protein TAL6₆ we were only able to detect binding to chitin beads in our assays, but not to any of the other tested forms of chitin or fungal cell walls. Fungal cell walls were also subjected to alkaline treatment of the cell walls in order to extract the alkali-insoluble fraction of the cell walls, which consists of β -1,3- glucans and chitin. Further, fungal cell walls were also subjected to thermal treatment prior to the binding assay in order to inactivate cell wall bound proteases and ensure optimal accessibility of these carbon sources (Fig.42). The results for TAL6₄ were similar, but in addition to the observed binding to chitin beads, also binding to colloidal chitin was observed (Fig. 48).

A possible explanation for the different binding behavior of TAL6₆ and TAL6₄ could be the properties of the various chitin preparations, in particular the degree of acetylation. Chitin can be characterized according to the extent of acetylation as well as according to the grade of polymerization. Per definition chitin exhibits an acetylation degree of 50 % and more, below 50 % the acetylation degree accounts for chitosan. Chitin beads (New England Biolabs) are fine chitin particles (50- 250 μ m) and consist of pure chitin. Their manufacturing process

contains a reacylation step based on purified chitosan. The deacetylation degree of the chitin beads were spectrochemically measured as found to reach 18 % [100]. Various chitinous materials were also examined, with 8 % found for colloidal chitin (PCI, Japan) and 22 % found for chitin flakes. According to these values one could expect that the binding to reprecipitated (colloidal) chitin should work best as it is further reported that colloidal chitin exhibits a high swelling ability and due to the surface area of the fluffy cotton like structure is able to account for an enhanced reactivity [101]. In this thesis only TAL6₄ was able to bind to the colloidal chitin, although it was estimated that both domains were able to bind to colloidal chitin. The colloidal chitin used in this thesis was prepared according to the protocol of Roberts et al. [85], but its specific properties including the deacetylation degree were not determined and it could be possible that the deacetylation degree was higher than was measured for the colloidal chitin used in the study of Wang et al. [100].

A further explanation could be the number of the available LysM motifs. We assume that the number of LysM motifs necessary for optimal binding to a specific substrate is predetermined. According to findings of Ohnuma et al. [69], who worked on LysM motifs from *Pteris pyukyensis* chitinase A using differential scanning calorimetry, isothermal titration calorimetry, and NMR spectroscopy, reported that by extrapolating their data the stoichiometry of lysine motifs and bound carbohydrates is 1:1. Thus, TAL6₆ should bind to more substrates than TAL6₄ according to the number of LysM motifs. However this is not the case as TAL6₆ shows binding affinity only to chitin.

Further, the accessibility and the aa-sequence variability of the LysM motifs could be a reason for the binding results. According to the findings achieved by the *in silico* analysis using the online available tool InterProScan, TAL6₄ represents a cluster of four strongly conserved LysM motifs representing a lower aa-sequence variability than the two additional motifs found in TAL6₆. It has been suggested that protein sequence variability may reflect diversity in substrate binding [63]. In this thesis it turned out that TAL6₆ exhibited only binding behavior for chitin beads among the tested carbon sources. Maybe the additional two LysM motifs have different substrate binding specificities and perturb binding to chitin of the other four conserved LysM motifs.

With respect to binding to oligosaccharides, the affinity of TAL6₄ and TAL6₆ for different soluble chitin-oligosaccharides was determined by isothermal titration calorimetry (ITC; Seidl et al, unpublished results). No binding behavior could be observed investigating the binding activity for (GlcNac)₃, (GlcNac)₅ and (GlcNac)₆. Low affinity for short chain chitin-oligosaccharides was reported for Avr4, a fungal avirulence protein containing an invertebrate

chitin-binding domain (CBM 14), which protects fungal cell walls against hydrolysis by plant chitinases by binding to chitin, whereas in contrast to that Ecp6 was shown to preferentially bind to short chitin-oligosaccharides. TAL6₆ and TAL6₄ were also used for a glycan array analysis carried out by the Consortium for Functional Glycomics (USA, Seidl et al., unpublished results). Also in this experiment no binding to any of the 611 oligosaccharide targets was detected. Although this glycan array is rather optimized for human glycan targets, it was conspicuous that no binding to any of the 611 targets, including *N*-acetylglucosamine oligosaccharides, was detected. However, these results confirm the findings from the ITC analysis and suggest that TAL6 preferentially binds to polymeric chitin. It remains to be elucidated whether TAL6 also shows binding to any chitin-derivatives that can be found in fungal cell walls. It has been described for *Aspergillus fumigatus* that the chitin in its cell wall is covalently cross-linked to β -1,3- glycan by a β -1,4- linkage [47]. However, it can be argued that we were not able to detect binding to fungal cell walls in our pull-down assays and thus the main biological carbohydrate-binding targets possibly still remain to be elucidated yet. In any case the results obtained in this thesis shed a completely new light on the carbohydrate-binding properties and thus functions of fungal LysM proteins.

5.2.5 Effect of TAL6₄ and TAL6₆ on spore germination in different fungi

Since the chitin-binding protein Avr4 has protective functions against chitinases, the question arose whether this concept could also be applied to TAL6₄ and TAL6₆, meaning that these two domains are responsible for protecting *T. atroviridis* hyphae against hydrolysis by its own chitinases? Further, it was investigated if an enzyme mix containing chitinolytic enzymes from the autolytic phase of *T. atroviride* cultures has a negative impact on spore germination and if so, are TAL6₄ and TAL6₆ able to enhance this effect?

Furthermore, we were interested in assessing if TAL6 alone has an effect on spore germination of fungi. This was tested by microscopical analysis of spore germination efficiency of different fungi, including *T. atroviride* itself and other fungi that can serve as preys for *T. atroviride* during mycoparasitism, i.e. *T. reesei*, *Botrytis cinerea*, *N. crassa* and *Aspergillus niger*.

Interestingly, when incubating TAL6₆ with a spore solution of *T. atroviride*, a strong effect on spore germination could be observed. Compared to the control, 97 % of the spores remained ungerminated. In contrast to that, with TAL6₄ germination behavior of *T. atroviride* was indistinguishable from the control. Similar effects for both proteins were detected for *T.*

reesei. In this case the effect of TAL6₆ was even more pronounced, whereas again TAL6₄ did not impair spore germination of *T. reesei*. When the same experiments were carried out with *A. niger* and *N. crassa*, surprisingly a high concentration of TAL6₄ and TAL6₆ showed in both cases that the spore germination was not influenced. These results showed clearly that TAL6 has a biological function which is not connected to mycoparasitism but is rather directed toward a self-regulatory effect during spore germination. The observed inhibition of germination was restricted to the genus *Trichoderma*, which suggests that there are specific events or signaling processes during spore germination in which TAL6 interferes.

In order to address the function of the TAL6 of *T. atroviride* it is necessary to look at it from a more general point of view. Spore germination is a biological process which is influenced and triggered by environmental conditions as well as by metabolic mechanisms. Water, oxygen, carbon dioxide, nutrients, temperature, pH and enzymes play an important role in the spore germination process [102] and several signaling molecules that influence germination efficiency have been reported [103].

TAL6₆ does inhibit the germination process of *T. atroviride* and *T. reesei* but does not inhibit the hyphal development of *A. niger* and *N. crassa* and therefore it must interfere with a molecule or pathway that is specific for *Trichoderma*. For the germination process to be initiated low molecular nutrients (amino acids, vitamins, C- sources) are able to trigger the spore to initiate the swelling process [104]. Taking into account the affinity of TAL6₆ for chitin beads it could be possible that TAL6₆ interferes with aspects of chitin synthesis or chitin remodeling during the early phases of spore germination. However, the fact that we did not detect binding of TAL6 to spores or fungal cell walls argues against a function of this type that directly acts at the fungal cell wall. Therefore, we think it is possible that TAL6 binds to a type of oligosaccharides that are fungal specific chitin-derivatives and acts as signaling molecule during germination. Our hypothesis is therefore that by binding of TAL6 to such a molecule it interferes the signaling processes that are responsible for the initiation of the spore germination process. Further, since the inhibitory effect on spore germination was only observed for TAL6₆ but not for TAL6₄, the data from this thesis show that the two LysM motifs that are more distantly related to the traditional LysM consensus pattern are essential for the biological function of TAL6.

Taking into account all hypotheses regarding the functional roles of TAL6₆ in the spore germination process it is assumable that TAL6₆ is able to bind to chitin-oligosaccharides, which impede signaling processes and hence prevent spore germination of *T. atroviride* and *T. reesei*.

Chitinases from *Trichoderma* spp. have been shown previously to inhibit spore germination of other fungi, e.g. *B. cinerea* [105]. In order to investigate whether the combination of TAL6 with chitinases has additive functions in the biological context of spore germination, experiments were conducted with the difference that an enzyme mixture containing chitinolytic enzymes from *T. atroviride* was added to the assay.

In the case of *T. atroviride* spore solution no difference to the already mentioned result could be investigated. The chitinase mixture did not influence spore germination in the absence of TAL6 proteins, whereas addition of TAL6₆ showed an impaired influence on the spore germination to the same extent as it did without the chitinase enzyme mixture. TAL6₄ showed no impact on the spore germination with and without chitinases.

In all other tested fungi, including *T. reesei*, the chitinases had a drastic effect on spore germination and spore germination was detectable even not in the control for all tested concentrations. The same result was achieved when adding the chitinolytic enzyme mixture to spore solutions of *A. niger* and *N. crassa*.

In summary, the characterization of TAL6 shows that the protein binds to polymeric chitin and impairs spore germination. While the chitin binding properties of the truncated version TAL6₄ are even slightly improved, the two LysM motifs present in the full-length version of the protein are essential for its biological function in inhibiting spore germination. The observed effects were restricted to *T. atroviride* and the closely related species *T. reesei*, but were not observed for the other tested ascomycetes. Therefore, the obtained results suggest that TAL6 is involved in the regulation of growth of *T. atroviride*. We assume that a possible role in mycoparasitism could be excluded; it could be rather possible that TAL6 has a specific role in auto-cell wall regulatory mechanisms and cell wall remodeling, as well as cell-cell communication. TAL6₄ showed no effect on spore germination, which suggests that the two N-terminal LysM motifs of TAL6₆, which are rather distantly related to the current PFAM consensus pattern motif for LysM motifs, are essential for the function of TAL6. This indicates that these two LysM motifs might have different carbohydrate-binding properties, which remain to be elucidated.

5.2.6 Carbohydrate-binding analysis of EPL1 (eliciting plant response-like protein)

Cysteine-rich cell wall proteins fulfill various functions connected to cell wall coating and cell wall protection. The protein EPL1 from *T. atroviride* belongs to the cerato-platanin protein family (CPPs) [78]. Members of the CPPs are small proteins, which share high sequence similarities, have four conserved cysteine residues that form disulfide bonds and are reported to act as phytotoxins, human allergens, pathogenesis-related proteins and further comprise activities in host fungus interactions [75]. They are also abundantly expressed in non-pathogenic fungi and EPL1 was shown to be strongly expressed and secreted into the medium in shake flask cultivations with glucose as carbon source at early time points. Therefore the question arises, what the primary function of CPPs is. To address this issue *T. atroviride* EPL1 was analyzed and its carbohydrate-binding properties were characterized in this thesis. EPL1 is a small non-glycosylated protein with four cysteine residues and can occur as a monomer and as a dimer [78]. A sequence alignment of the three amino acid sequences of the EPL proteins revealed that the sequences of EPL1 and EPL2 showed except for a few amino acids high similarity, whereas the amino acid sequence of EPL3 exhibits lower similarity to the sequences of EPL1 and EPL2, respectively. This finding correlates with the phylogenetic analysis that revealed that EPL3 and also an orthologous protein of *T. virens* showed the highest genetic distance to the other proteins, whereas EPL1 and EPL2 can be found grouped in one clade (Fig. 57).

CPPs in general, and this is also valid for EPL1 have no annotated carbohydrate-binding domains, but a recent NMR modeling study with cerato-platanin (CP) from *Ceratocystis platani* suggested that CP has a *N*-acetylglucosamine binding pocket. Recently the solution structure of CP of *Ceratocystis platani* was resolved by NMR spectroscopic measurements and further binding affinity of this protein could be highlighted. According to these findings the CP protein has a globular fold comprising 2 α -helices and 6 β -strands, together forming a 6-stranded double $\psi\beta$ -barrel, which is also found in *endo*-glucanases and in the defense protein barwin [92].

Binding modeling revealed that the region involved forms a flat and shallow groove on one face of the β -barrel which is suitable for sugar carbohydrate-binding. Furthermore, it could be concluded that all the residues involved in NAGs binding are among the most conserved ones in the CPP family.

The highly conserved residues, which are responsible for the interaction with NAGs are A19, D53, I49, N22, S4, V35 and V102.

In order to investigate the carbohydrate-binding properties of a CPP experimentally for the first time, purified EPL1 was subjected to carbohydrate-binding experiments.

The results of the carbohydrate-binding analysis revealed that EPL1 is able to bind to flaked chitin, in different sizes and to colloidal chitin but exhibited no binding affinity to chitin beads or to cell walls of *T. atroviride*. It is not clear yet what the biological function of this chitin-binding ability is. In the study on the NMR structure of CP of *C. platani* it was reported that the protein shows structural similarities to barwin-like *endoglucanases* and plant expansions [92]. Further Bacelli et al. [106] suggested that similarity of CP to expansins might indicate a role in the remodeling and enlargement of the cell wall. EPL1 is already produced at early growth stages of *T. atroviride* and the gene was found to be expressed in all tested growth conditions. This would also support a potential function of EPL1 in fungal growth. Further detailed analysis on the location of EPL1 in different types of fungal hyphae and various parts of the fungal colony will be necessary to elucidate this in more detail.

Beside the not yet fully understood function of CPPs in fungal growth, the involvement of these proteins in the induction of plant defense responses has been well documented for several fungal species. The orthologue of *T. atroviride* EPL1 in the fungus *T. virens* is SM1. This protein was shown to efficiently induce plant defense responses in cotton and in maize plants [79] [77]. *T. virens* SM1 is also produced in a monomeric and a dimeric form, but it was demonstrated that only the monomeric forms of SM1 and EPL1 are able to induce plant defense responses. EPL1 and SM1 have high sequence similarity, but SM1 is glycosylated and EPL1 is not. Further, EPL1 has two double oxidized tryptophane residues and this feature was shown to promote the aggregation of proteins. This is in agreement with the finding that EPL1 is predominantly present as a dimer (Fig. 61), whereas SM1 is mainly found as a monomer. In comparison to the monomeric forms the dimeric forms of both proteins were reported to be not glycosylated, which further led to the consumption that the glycosylation state may also be controlling the protein oligomerization [79].

In the past few years it was shown that several *Trichoderma* spp. are able to induce plant defense responses and enhance plant growth. A number of different elicitor proteins have already been described for these systems, ranging from CPPs and hydrophobins to xylanases and polygalacturonases. In the strain *T. virens* Gv29-8 the protein SM1 was shown to be a major component of this plant defense induction system. In the interaction of *T. virens sm1*

deletion strains with cotton cotyledons plant responses were strongly reduced, suggesting that in this system SM1 is of major importance for the crosstalk between the fungus and the plant. Since so many different types of elicitor proteins were already reported for *Trichoderma spp.*, it will be of interest to test the relevance of CPPs in *Trichoderma*-plant interactions with other *Trichoderma* species and strains in more detail. Further, the importance of the chitin-binding functions of CPPs for their capacity to elicit plant defense responses will also be an interesting topic for future studies.

In order to follow up on this aspect as well as the primary function of CPPs, single and double knockout strains of the two genes *epl1* and *epl2* were generated. Since no expression of *epl3* was detected under any of the tested growth conditions (Gruber and Seidl-Seiboth, unpublished results), we focused on the genes *epl1* and *epl2* for generation of the knockout strains.

Knockout strains of *T. virens* Gv29-8 *sm1* did not show a growth defect or morphological phenotype [77]. However, it is possible that one of the other CPPs, i.e. SM2 or SM3 complement for the lack of SM1. Further, the role of the cerato-platanin genes has not been studied in *T. atroviride* yet. Therefore, in this thesis single and double knockout strains of *epl1*, *epl1* and *epl1/epl2* were generated. The strains show no obvious growth phenotypes or morphological defects. Considering that for *epl1* and *epl2* strong gene expression can be detected under various growth conditions, this underlines that there are several aspects concerning fungal growth that are not fully understood yet. Therefore, further analysis of the knockout strains with respect to fungal growth and also in planta assays with these strains will help to elucidate the primary function of these genes as well as their capacity to elicit plant defense responses. Recently Bacelli et al. reported that the cerato-platanin gene *cp1* from the plant pathogenic fungus *Ceratocystis platani* is upregulated during chlamydospore formation [106]. However, there are no knockout strains available for *cp1*. The *T. atroviride epl*-knockout strains will greatly aid in learning more about the role of the cerato-platanin proteins in the fungal life cycle. Moreover, *T. virens* SM1 was shown to be a major effector of plant defense responses. Although *T. atroviride* EPL1 was less effective in inducing plant defense responses [77] in planta assays with the knockout strains will also increase our understanding of the crosstalk between *T. atroviride* and plants.

Studying the EPL2 protein of *T. atroviride* would be of great advantage to be able to further investigate the functions of the members of the cerato-platanin family. Knockout strains, which have been accomplished in this thesis, will contribute to unravel the role and functions

of these proteins and help to enlighten the secrets of the numerous applications of the fungus *T. atroviride*.

5.3 Concluding remarks

Trichoderma spp. belong to a genus of filamentous fungi that are used for numerous biotechnological applications. They are used for several industrial purposes e.g. the production of second-generation biofuels. Further, the applications of these fungi are not limited to industrial issues but they are also important for agricultural applications such as crop protection and are known as biocontrol species used in agricultural applications. *Trichoderma* spp. are thus important microorganisms in the fields of green and white biotechnology.

Since the agricultural industry started to increase their focus on biological crop protection in the past few years in order to improve the application of biopesticides, it will in the long term not only be important to select the optimal strains, but it will also be of utmost importance to understand the complexity of enzymes, secondary metabolites and other factors that participate in the crosstalk between the plant, plant-pathogenic fungi and plant-beneficial fungi and for that purpose *T. atroviride* is a good model organism.

As chitin degradation is an important step during mycoparasitism but also during cell wall remodeling and autolysis, it is obvious that a detailed understanding of the mechanisms and functions of chitinases and chitin-binding proteins are important. Considerable progress could be made during the last years concerning the investigations of chitinases in order to understand their pleiotropic roles in fungal colony development like hyphal growth and hyphal fusion, branching, cell wall remodeling and autolytic processes.

In this thesis first steps were made to elucidate the function of different types of chitin binding proteins. LysM proteins, members of CBM family 50, were analyzed in detail. Interestingly TAL6₆, a protein that contains 6 LysM motifs, was in this thesis shown to have a negative effect on spore germination only in *Trichoderma* spp., but not in other filamentous fungi. In contrast to that, for TAL6₄, a truncated version of TAL6 that contained only 4 LysM motifs, no effect was observed on *Trichoderma* spp. or on other fungi. The two proteins were also shown to differ in their binding behavior to different chitinous carbon sources.

In the context of the ability of *T. atroviride* to elicit plant defense responses, the elicitor protein EPL1, which is the major secreted protein of *T. atroviride* on glucose, was characterized. It was shown that EPL1 binds weakly to chitin and knockout strains of the genes *epl1* and *epl2* were created. A better understanding of the interactions and mechanisms

of the growth and development of *Trichoderma* spp. and its interaction with other organisms will aid in developing improved formulations for biocontrol agents. This will be important toward the existing demand for more ecological solutions with respect to crop protection to achieve a more environmentally friendly use of our natural resources in the future.

6. Appendix

6.1 Sequences

In the following the sequences, which were used in this thesis were demonstrated.

6.1.1 Sequences of *TAC6*, Prot ID: 348129, 174,8 kDa

6.1.1.1 cDNA sequence of *tac6* (JGI homepage)

```

1  ATGTTGTCGCCGAGGCCACGGCCACGGGTAAACATTTCCGCCATAACATTCACTGCCCTC 60
61  TTCACTTGTGTTTTATTCTGGCATCACCAGTCTTCGCCCTCGCTCAACATCTCCGTCAT 120
121 AGTAACCTTCACATAGAGCCAGTGCAACGCAGTGCAAATGATCAGGGTCTATCTCATCGA 180
181 CATCTATCATCTCGTTTTTCATGCAGCAATTATTGAGCATGAAACTTCGGTAGATACACCG 240
241 GCTGCGGGCCAGGGGAGACTATACATGCGGACCAAACAAGCCATGCTATAACGGAGCTTGC 300
301 TGTGGTGATAGCGGCTGGTGTGGTTTTGGCCCTACGTACTGTGGCAAGGGCTGCCAATCG 360
361 AACTGCAATGCTACAGCTGATTGCGGCCAGTTTTGCTCATAACCTGGATCCCCCTTGCCCT 420
421 CTGAACGTCTGTTGCTCTGAGTTTTGGCTTTTGCGGAACCTACTTCAGACTTTTGTGGCAAA 480
481 GGCTGCCAGTCTAACTGCCAGCAGCCCCAAGCCTTCCGGACCTTCCACAAATGTACAGCAA 540
541 AGGATTATTGGTTATTGGGAAGCCTGGAATTCTCAACACCCGTGTGGTACAATGGCTGTT 600
601 GGCGAGATTCCCGTTAATTATTTAACCACCTTAATATTGCTTTTGGATACATTAGCCAC 660
661 GACTTTTCGTATTACAAATATGGATGGAGTATCTTCAGATTTGTACCGCAATGTGGGTAAC 720
721 CTCAAAGCCAGAAATCCAAATCTCAAAATCGTCATCTCTTTGGGAGGATGGGCCTTCAG 780
781 GATCCTGGCCCTTGGCGCAGCGTTTTCCCTACAATGACGTCTTCGTCAGCAAATCGCGCG 840
841 ACATTCATTTCAGAATCTGCTAGGTTTTCTCTCAGAGTATGGCTACGATGGTGTGATTGG 900
901 GAATATCCCGGGGCGGACGATCGAGGTGGCAGTGACGCAGACGCTGCTAATTATGTTGCG 960
961 CTGTTGAAAGAGTTGCGAGCAGCTATAGCCAGCAGTGCCATAGTTACATTGTACATTT 1020
1021 ACAGCCCCAACATCGTATTGGTACTTGCGGCACTTTGACATTAAAAGCATGGCATCATAT 1080
1081 GTTGATTGGATCAATCTCATGTTCATATGACCTTCATGGGGTCTGGGATAGTACAAATCCA 1140
1141 ATAGGTTCCCAAGTTCTTGCTCACACTAATCTAACTGAGATTGACTTGGCTTTGGATTG 1200
1201 TTCTGGAGAGCTGAAATAGATCCATCCAACATTGTACTGGGTCTTGCCTTTTATGGTCGA 1260
1261 ACCTTCAACTTGAAGTCGTATCTTGTCTGGAAGCCTGGCTGTCCATTTGGAGGCCAGGA 1320
1321 GATGCGGGTCCGTGTACTGATACGGCAGGCATTTTGTTCATATCGAGAAATCCAGACGATA 1380
1381 CTTGATCAGACCGGTGCGGCTTCATATCTGGATAAAGAGGCCGCTGTGAGATACTTGGTA 1440
1441 TATGGTAACAACAGCTGGGTTTTCTTTGATGATGATATCACCTTCCAAGCAAAAATCGAT 1500
1501 TATGCCAGTAAGATAGGCCTTTCCGGCACTTATGGTTTTGGGCGGTTGATCTCGACGACAGC 1560
1561 AAAGTGAACGCCCTCAGAGCCATCTCAGGAGCCAGTGAGAGACTGGAGCTGATAGCGCC 1620
1621 TTTTCACTTGTTGATCTGAAGTATTTGTTCCCTCAGAAGACCTTCCATCCTCTGACTCA 1680
1681 CAGCCTTCATACGGCCTCGTCACATTTGGCAGTGGTGGGGATTTGCATGATGTTAGTCCC 1740
1741 GCATCTGGACCGTTTCGGCTTTTTTCTGGTTGCGGGAGACTCTCACGTTGTCACAAATCTG 1800
1801 AAGAAAAGGAAAGGTGAACCGGAACCATTTACCTTCTTGACTGTCTCTCAAATGTTTGA 1860
1861 GATCAGCCAGAAATATAAAGTTCAAAGCGCAAGAGTAACCTGTCTGAGCGATGACTTGGAA 1920
1921 GGCTGCTTCCGAATACTTGAACGTGGCGTTGAAGGAACCATTTGTTGAAATGCCGGACAAC 1980
1981 AGCTATTTCTCTGAATATCTCACCAGAGATATGCCAGACCAATCAGTACCTTTGGGCATC 2040
2041 AGAGACGGGATTCCCCCTTCTCCCGTATATGATTTTTTCGTTTGAATTTCAACCTTGGACTT 2100
2101 ATGCGCAGAGACTCAGACAACACGAGATTTTCGATTGGATTACTCTAACGTCCCCGGCTAT 2160
2161 TGGAACCATCTTGTCAACGCACCAGGCATACAATCTAGAGATTTGAACAATTTGGAGAGT 2220
2221 CGGTTCTTCGCTCCAACAACAGAAGATTGGAACACAGCATTTGAAACCATCGAATTCGAT 2280
2281 TGGTCTCCACAGACGCTACGCAGATTCAAGAAGATGTGAGCGCGCCGGTTTTCTGGCAG 2340
2341 TCCGCGGGCGACTGCTCTATAGGTAACCTTACCTATGCAGAAGGCTTTGGTGCAATTTGTT 2400
2401 CAAGGCAAGATTGATGCACAATTTTGGTTTGGTTTCTCTATGATTGCAACACTCAAGGAC 2460
2461 AACAAATTTGATGTTTCATCAAGCGCATGGCTTTCTCAAAGCAAGGGGGCAAACAGATCTA 2520
2521 ACATATGGCATTGGTGGCATTGGGGACATTGATATCTCTAAAGCAGGAAAAGGCAACCCA 2580
2581 GCCATTAGCGATGATAATCTCGTTAACCTAAAAGGGCATACAATCAATACTCCAAAATCT 2640
2641 GGGGGGAGGATTTTCGCTTAACCCATATTATCAACTCACTTATCAAATGGCCACTTTCAAT 2700
2701 GGGTCGACCGGTAACGATTTTGTGAAACAGTGTGGCTTCATTCAACGGACGGCTGACTACT 2760
2761 CGCATTATCACGGATCTTGGAGATTTTCAGGCAAACCTTTCCGCCTCCTGAAAATCTACCC 2820
2821 AATGAGGCGTACAATGACAAACGCCAGCAGAATAAAATATCTATTCTGAAAACGACATC 2880

```

2881 CTATACGGCACTTCTAATGACGGAGGCCACATTGCTATCGGTACTAATCTCATTTTGGG 2940
 2941 TTGAAGTTGGAATTTTTTGTCTTCGGTGACTTATTTCAGATGGGACTTTGATCTACCAAAG 3000
 3001 ATGAATCTGGTGTATAACACCATGGAAATCTTTACTTTCTCTCCAGGAAGTGCGGACCAC 3060
 3061 CCTGAATTTGCATGTTCTGACTACGAGGTCATCTTACAGTTTTTGGACTCAAGTACAAAT 3120
 3121 GTTTATCAAACAGTGGAAAAAGGAGAATCTCTTGGTTGGAATGATTCCAACGCCTTGACA 3180
 3181 GCAAATCTCGCATATGATCGACAAATACCCTCTCGAGGCCAAGTTTGCTACCCAGCAGCG 3240
 3241 GACAGTTCAAAAAACGCCGCGATATACACACCGCTGATAGCGGAAACCTATCACATGAG 3300
 3301 AAAACGGATATACCACTCGATCATATGTATCCGGATGCCGATTGCCTTGAATGCAAGAAG 3360
 3361 CAGTCTCTTGGTCCTCGAGGATTTCGGGCAGATTAACCCATGGCAATACAGCCCTTACTCC 3420
 3421 CCAGCGGAACCGAGCATTTATTTGTAGATGCTCAGGACCTCATCACATTTCGACAGCTCG 3480
 3481 AAACCTAAATTTGATTGTAGAGATTGTAGACTTGTTATGAAGAAGAGGTAAGCGAATGT 3540
 3541 TCGCGATGCGTTTTCTCTGGACGTTACGTGGCCCAATATGCTGGATATGTCTCCTTGCGAC 3600
 3601 ATTGACGTATGTGAACCGCTCACTGGCGCGTGGCTGGGCACCTCTTCCATTTCAAAAAAGA 3660
 3661 CAAGAAGACCTTTCTGAACTCAAATGCGAGATAATGAATGATACATTTGTTCGATGATGGA 3720
 3721 CAATCACTATCTCCACGGCAGCCTGCAAATCCGGTAATAAATAAACAAGAAGCGAATT 3780
 3781 TCGGTTTGCAAAGTCCCCTTTGGACTAAACGCGCCATACAACCTATCCATCATTTCGGGAA 3840
 3841 AACCCTAACACGCAGTGGGATGGAGGGAAATTTGATGCAGTATCGAGGTACTGGGGCAAC 3900
 3901 ACATCAGGAATTTGCCAAAGCTGGGCAGTAGGCAAGGTGCAGCCTGCGGACGTGACATAT 3960
 3961 ATACCCAATAGTCTCGGAGGGTACAATCGGCAAAGGTGCGCTTTATCAAACCGAGCACCCCT 4020
 4021 TTTGAGGCGCAGTTGATCAGCAACTTCTTTACCAATTGGCTGGACAAGGGCCGGTTAAAT 4080
 4081 GACCTGGACCAATTTGTCTACTCAACACCCAAGATGCCATGTGCCGTGACCAAGGCCTGG 4140
 4141 GTAAACAAGGTTGTCCCAGATTTCCAGATATTGCGTAACGGAGTGCTAGGGAGCGCAGCA 4200
 4201 TTTCTCAGCTTCTCTTGACAGAGCTGGGCAGTCAACAGCACCAGGACCGCCTCACCATT 4260
 4261 ATGCTCGCGAGGCTTAATGGGAGGAAAGGAAGAATGTTTCAAGGGCACAGAATTGTAATC 4320
 4321 GATGATAATTACAAATTGCAAACTCAGCAAGAACAGCTCTTAGTAGCAAAGGAAGTGGGC 4380
 4381 ATGATATTCAATTATTTCAACACAAAAGAAGTGTGGGATATGTTTTGCGCTTCATATGAG 4440
 4441 GCCATGTACGACCACATGGGTGCCTTCAATACTTTTACGCGCGACAGGGCCAAGCTGTC 4500
 4501 ACGATACCAGACTTACAAACCGAATGGGAAGAGTTTGTCCGGACTACTCTAGACAACATA 4560
 4561 GTGACTCGGAGTCTCACCCTTTTGACATGATGTACGAGAACAGACGTGCGGGTACCAGC 4620
 4621 TTTTTCAGTACTATATTTCCGATTGCATGGCTGTATAACAAATATTGGAACAGGGGTTTCG 4680
 4681 ATTAGGTTGACCGGAACGTGTCCGCATTTAGGCGCTACTAGAGTGTAG 4728

6.1.1.2 Protein sequence of TAC6

1MLSPRPRPRV NISAITFTAL FTCVLFLASP VFALAQHLRH SNLHIEPVQR SANDQGLSHR
 61HLSSRFHAAI IEHETSVDP AAGQGDYTCG PNKPCYNGAC CGDSGWCGFG PTYCGKGCQS
 121NCNATADCGQ FAHTPGSPCP LNVCCSEFGF CGTTSDFCGK GCQSNQCQPK PSGPSTNVQQ
 181RIIGYWEAWN SQHPCGTMAV GEIPVNYLTH LNIAGFYISH DFRITNMDGV SSDLYRNVGN
 241LKARNPNLKI VISLGGWAFS DPGPWRSVFP TMTSSSANRA TFIQNLGFL SEYGYDGVWD
 301EYPGADDRGG SDADAANYVA LLKELRAAIA SSGHSYIVTF TAPTSYWYLR HFDIKSMASY
 361VDWINLMSYD LHGVWDSTNP IGSQVLAHTN LTEIDLALDL FWRAEIDPSN IVLGLAFYGR
 421TFNLKSSSCW KPGCPFGGPG DAGPCTDTAG ILSYREIQT LDQTGAASYL DKEAAVRYLV
 481YGNNWSVSFD DDITFQAKID YASKIGLSGL MVWAVDLDDS KLNALRAISG ASGETGADSA
 541FSLVDLKYLF PSEDLPSSDS QPSYGLVTFG SGGDLHDVSP ASGPFGFFLV AGDSHVVTNL
 601KKRKGPEPEP TFLDCPSNVR DQPEHKVQSA RVTCLSDDL E GCFRILERV EGTIVEMPDN
 661SYFSEYLTRD MPDQSVPLGI RDGIPSPVY DFSFDFNLGL MRRSDNTRF RLDYSNVPGY
 721WNHLVNAPGI QSRDLNNLES RFFAPTTEW NTAFETIEFD WSPTDATQIQ EDVSAPVFWQ
 781SAGDCSIGNS TYAEGFGAFV QGKIDAQFWF GFSMIATLKD NKFDVHQAHG FLKARGQTDL
 841TYGIGGIGDI DISKAGKGNP AISDDNLVNL KGHTINTPKS GGRISLNPYY QLTYQMATFN
 901GSTGNDFENS VASFNGLRTT RIITDLGDFQ ANFPPEENLP NEAYNDKRQQ NKISIPENDI
 961LYGTSNDGGH IAIGNLIFG LKLEFFVFGD LFRWDFDLPK MNLVYNTMEI FTFSPGSADH
 1021PEFACSDYEV ILQFLDSSTN VYQTVEKGES LGWNDSNALT ANLAYDRQIP SRGQVCYPAA
 1081DSSKKRRDIH TADSGNLSHE KTDIPLDHMY PDADCLECKK QSLGPRGFGQ INPWQYSPYS
 1141PAEPSIYFVD AQDLITFDSS KPKFDCRDCQ TCYEEEVSEC CGCVSLDVTW PNMLDMSPCD
 1201IDVCEPLTGA WLGTSSISKR QEDLSELKCE IMNDTFVDDG QSLSPRQPAN PVINITKKRI
 1261SVCKVPFGLN APYNYPSPFE NPNTQWDGK FDAVSRYWGN TSGICQSWAV GKVQPADVTY
 1321IPNSLGGYNR QRSLYQTEHP FEAQLISNFF TNWLDKGRLN DLDQFVYSTP KMPCAVTKAW
 1381VNKVVPDFQI LRNGVLGSAA FPQLLLTELQ SQQHQRDLTI MLARLNGRKG RMFQGHRIVI
 1441DDNYKLQTQQ EQLLVAKEVG MIFNYFNTKE VWMFCASYE AMYDHMGAFN TFYARQGQAV
 1501TIPDLQTEWE EFVRTTLDNI VTRSLTAFDM MYENRRAGTS FFSTIFPIAW LYNKYWNRGS
 1561IRLTGTCPHL GATRV

6.1.2 Sequences of TAL6 Prot ID: 297859, 78kDa

6.1.2.1 cDNA sequence of *tal6* (JGI homepage)

```

1  ATGAAGCTGTAACTTTTCAGTCAACTCTTTTTCG 60
61  TGGGGATACAGGCATCAAAGCTAGGCGTACCCAGCCTGCGCAGAGAGATCAAGTCAATT 120
121  GCCAACTCTATGCCGTCCAGCCAAACGATAAAGTGCATTGATATCAGCAGCAAAAAATAATA 180
181  TCACCTACGCCCAACTGCTCTCTTGGGAATCCTTCACTCAGCTCTACATGCTCTAACCTTG 240
241  CGAGCTTGAAGTCAAGTAGCATCTGTGTGAGTAATCCTAAAGGCACATTTTCTATTTCAA 300
301  GTAATACCGTTGGGGCAACCGATATTGCTACTACAAGTCCAGTTCCATCTCCAACCT 360
361  TGGACCAGACAACATCTAGATGCGCAAAGTATTATCAAGTCTCTGACGGCGACGATTGCT 420
421  CCCACTTGACTGCACAATTTGCAATTACACTGAAGGATTTTCATCTTTTGAATTCTGAAG 480
481  TTTGGCAAAATTGCACAAATCTGGAATTGGGTTATTACTACTGCGTTGAGCCGGTTCGGAT 540
541  ACATCTCTACCTACCCAGGGTATTTACCTACGGCTACAACGAAACCATTTCAACCAAACTA 600
601  GTGCGACGTCTCTGCCATATGATGGGGATCCATGGGCCAGATTCTCTTCAAACCTCCTCAG 660
661  TGATACCTATTGCAAATGGCACACGCGTAGATTGTTATTCGTACGTCTATGTAAAGAACC 720
721  TCACGGAAAACCTATTTGTCAGATTGTTGGAATATGGCGAGCATGTATGAAATTACACGTG 780
781  AAGAGCTGGTACTATGGAATCCTTCCCTTGGCAATGATGGCTCTTCAGGGTCAAATCTCT 840
841  CAGGCGCTGAAGCTAGTCAAGTTGCATCATCGATAGCAATTCGACTACTGCTCCAAGCT 900
901  CAATCACCACCAATCTTTATACCTATCCGTTACAGTTGCCGCTAATATTTCTGACTGCG 960
961  TCGCCTTGCTTTCTTCGACTGGTGCTCTACCTACGAATACGGCACCCCGAGGCTCAGC 1020
1021  CTTCTGGAGAGATATCTAATTGTACGGCATGGTTTGCACCCGAAGCCTACGATACGTGCA 1080
1081  AATCAATCTTGGACATATTTGAGATGTCGTTTGCAAAACCTTCTACAAAATGAACCCCTCGG 1140
1141  TTGGCCCAGATTGCTCTGGCCTTGGCGTGGGAACGAACTATTGTGTATCAACGTATCCTA 1200
1201  ATGGTGAGGATCCGAATGATGATTGGGATGGAGACGACAGCATCCCATCTATTTTCGCCCA 1260
1261  CTGGAATTATAACGCCTACACCAACTCAGAGTGGCATGGTTAGTAATTGCAACAAATTTT 1320
1321  ACGACGTCCACTCCAACGATGGCTGTTTCAGCCATTGCAAGCAGCCAGCATGTCGATCTAA 1380
1381  GTTCTCTTTACAAATGGAACCCGGCCATTAAGACCGACTGCTCTGGTCTTCAAGCAAGTG 1440
1441  TTTACGTCTGCATCGGAATTTTAACGACATCCATGTCCACCACATCCAAACTGCCACCA 1500
1501  CTACGTCTAAGCCATCTACCACCTCCAAACCGCCCACTGGCATCACGACACCTACACCCA 1560
1561  CTCAAAGCGGTATGGTCAAGAACTGTAATAAAATTTTACGATGTGCACTCGGGAGACGGCT 1620
1621  GTTCGGCGATTGCAAGTAGCCAAAAGGTCAACCTTAGTTTCTATTCTACCTATGGAATCCAG 1680
1681  CTGTCAAGACGGATTGCTCTGGCCTTCAGGCCAGCGTATTTGTCTGTATCGGAACTTTAA 1740
1741  CGACATCCATGTCCACCACCACATCCAAACTACCCACCACTACATCTAAGCCATCTACTA 1800
1801  CCTCTAAACCACCACTGGCATTATAACACCTACACCACTCAAAACGGTATGGTCAAGA 1860
1861  ACTGTAATAAAATTTTACGATGTGCACTCGGGAGACGGCTGTTTCGGCGATTGCAAGCAGCC 1920
1921  AAAAGGTTAACCTCAGTTTCTTACCTATGGAATCCAGCTGTCAAGACGGATTGCTCTG 1980
1981  GTCTTCAGGCCAGCGTATTTGTCTGTGTTGGCAGCAGACAACTACAACAGCTGCCGGCA 2040
2041  TAACACCCCTACGCCACCCAGAGCGGCATGGTGAGCGGTTGTAACAAATTTCTACGACG 2100
2101  TCCACGCCGGGGATGGCTGTTCCGCAATTGCAAGCAGTCAAAAAATAGCTCTATCTTCGC 2160
2161  TGTATAAGTGAATCCGGCTGTGAAGACGGATTGCTCTGGCCTTCAAGCGAGTGTATACA 2220
2221  TATGCATCGGTGTGGGAAATGCTGCCGCTGCTCGTGTTACAGGATGA 2241

```

6.1.2.2 Protein sequence of TAL6

```

1MKLLTFSQLF FVGIQASKLG VPQPAQRDQV NCQLYAVQPN DNCIDISSKN NITYAQLLSW
61NPSLSSTCSN LASLNSSSIC VSNPKGTFSI SSNTVGATDI ATTTAPVPSP TLDQTTSRCA
121KYYQVSDGDD CSHLTAQFAI TLKDFIFLNS EVWQNCTNLE LGYYYCPEPV GYISTYPGYL
181PTATTKPFNQ TSATSLPYDG DPWARFSSNS SVIPIANGTR VDCYSYVYVK NLTENLFADC
241WNMASMYEIT REELVLWNPS LGNDGSSGSN LSGAEASQVA SSIAIPTTAP SSITTNLYTY
301PCTVAANISY CVALVSSTGA LPTNTAPPGP HASGEISNCT AWFAPAYDT CKSILDIFEM
361SFANFYKMNP SVGPDCSGLA VGTNYCVSTY PNGEDPNDDW DGDDSIPSIS PTGIITPTPT
421QSGMVSNCKN FYDVHSNDGC SAIASSQHVD LSSLYKWNPA IKTDCSGLQA SVYVCIGILT
481TSMSTTSKLP TTTSKPSTTS KPPTGITPT PTQSGMVKNC NKFYDVHSGD GCSAIASSQK
541VNLSSFYLWN PAVKTDCSGL QASVFVCIGT LTTSMTTTS KLPTTTSKPS TTSKPPTGII

```

601TPTPTQNGMV KNCNKFYDVH SGDGCSAIAS SQKVNLSSEFY LWNPAVKTDC SGLQASVFVC
 661VGTATTTTAA GITTPTPTQS GMVSGCNKFY DVHAGDGCSA IASSQKIALS SLYKWNPAVK
 701TDCSGLQASV YICIGVGNA AARVTG

6.1.3 Sequences of TAL₆, 77.7 kDa

6.1.3.1 cDNA sequence of the tal₆ including the His-tag

tcaaagctaggcgtacccagcctgcgagagagatcaagtcaattgccaaactctatgccgtccagccaaacgat
 aactgcattgatatcagcagcaaaaataatatcacctacgcccactgctctcttgggaatccttcactcagctct
 acatgctctaacttgcgagcttgaactcaagtagcatctgtgtcagtaatcctaaaggcacattttctatttca
 agtaataaccgttggggcaaccgatattgctactacaactgccccagttccatctccaaccttggaccagacaaca
 tctagatgcgcaagatattatcaagtctctgacggcgacgattgctcccacttgactgcacaatttgcaattaca
 ctgaaggatttcatcttttgaattctgaagtttggcaaaattgcacaaatctggaattgggttattactactgc
 gttgagccggctcggaatcatctctacctaaccagggtatttacctacggctacacgaaccattcaaccaaact
 agtgagcagctctctgcatatgatggggatccatgggacagattctcttcaaactcctcagtgatacctattgca
 aatggcacacgcgtagattgttattcgtacgtctatgtaagaacctcacggaaaacttatttgagattgttgg
 aatatggcgagcatgtatgaaattacacgtgaagagctggactatggaatccttcccttggcaatgatggctct
 tcagggtcaaactctctcaggcgctgaagctagtcaagttgcatcatcgatagcaattccgactactgctccaagc
 tcaatcaccaccaatctttatacctatccgtgtacagttgccgctaataatttctgactgcgtgccttgggttct
 tcgactgggtgctctacctaagaatacggcaccacccagggcctcacgcttctggagagatatctaattgtacggca
 tgggttgcacccgaagcctacgatacgtgcaaatcaatcttggacataatttgagatgtcgtttgcaaaacttctac
 aaaatgaaccctcggttggcccagattgctctggccttggcgtgggaacgaactattgtgtatcaacgatcct
 aatgggtgaggatccgaatgatgattgggatggagacgacagcatcccatctatttgcgccactggaattataacg
 cctacaccaactcagagtggttagtaattgcaacaaattttacgacgtccactccaacgatggctgttca
 gccattgcaagcagccagcatgtcgatctaagttctctttacaaatggaacccggccattaagaccgactgctct
 ggtcttcaagcaagtgtttacgtctgcatcggaattttaacgacatccatgtccaccacatccaaactgccacc
 actacgtctaagccatctaccacctccaaacccgcccactggcatcacgacacctacacccactcaaagcgggatg
 gtcaagaactgtaataaaattttacgatgtgcaactcgggagacggctgttcggcgattgcaagtagccaaaaggctc
 aaccttagttcattctacctaaggatccagctgtcaagacggattgctctggccttcaggccagcgtatttgtc
 tgtatcggaactttaacgacatccatgtccaccaccacatccaaactacccaccactacatctaagccatctact
 acctctaaccacccactggcattataacacctaaccacactcaaaacggatgggtcaagaactgtaataaaattt
 tacgatgtgcaactcgggagacggctgttcggcgattgcaagcagccaaaaggtaacctcattctaccta
 tggaaactcagctgtcgaagacggattgctctggcttccaggccagcgtatttgtctgtgtggcacagcgacaact
 acaacagctgccggcataacaacccctacgcccacccagagcggcatgggtgagcgggtgtaacaaattctacgac
 gtccacgcggggatggctgttccgcaattgcaagcagtcaaaaaataagctctatcttcgctgtataagtggaat
 ccggctgtgaagacggattgctctggccttcaagcagtgatatacatatgcacgggtgtgggaaatgctgccgct
 gctcgtgttacaggacatcatcatcatcatcat

6.1.3.2 Protein sequence of the secreted TAL₆ including the His-tag

1KLGVPQPAQR DQVNCQLYAV QPNDNCIDIS SKNNITYAQL LSWNPSLSST CSNLASLNSS
 61SICVSNPKGT FSISNTVGA TDIATTTAPV PSPTLDQTTT RAKYYQVSD GDDCSHLTAQ
 121FAITLKDFIF LNSEVWQNT NLELGYYYCV EPVGYISTYP GYLPTATTKP FNQTSATSLP
 181YDGDPPARFS SNSSVIPIAN GTRVDCYSYV YVKNLTENLF ADCWNMASMY EITREELVLW
 241NPISLGNDGSS GSNLSGAEAS QVASSIAIPT TAPSSITTNL YTPCTVAAN ISYCVLVSS
 301TGALPTNTAP PGPHASGEIS NCTAWFAPEA YDTCKSILDI FEMSFANFYK MNPSVGPDCS
 361GLAVGTNYCV STYPNGEDPN DDWDGDDSIP SISPTGIITP TPTQSGMVS CNKFDVHSN
 421DGCSAIASSQ HVDLSSLYKW NPAIKTDCSG LQASVYVCIG ILTSMSTTS KLPTTTSKPS
 481TTSKPPTGIT TPTPTQSGMV KNCNKFYDVH SGDGCSAIAS SQKVNLSSEFY LWNPAVKTDC
 541SGLQASVFVC IGTLTSMST TSKLPPTTS KPSTTSKPPT GIITPTPTQN GMVKNKCNKFY
 601DVHSGDGCSA IASSQKVNLS SFYLWNPVK TDCSGLQASV FVCVGTATTT TAAGITPTPT
 661TQSGMVSGCN KFYDVHAGDG CSAIASSQKI ALSSLYKWN AVKTDCSGLQ ASVYICIGVG
 721NAAARVTGH HHHHH

6.1.4 Sequences of TAL6₄ 36.2 kDa

6.1.4.1 cDNA sequence of tal6₄ including the His-tag

gacagcatcccatctatcttgcgcccactggaattataacgcctacaccaactcagagtgggcatgggttagtaattgc
aacaatttttacgacgtccactccaacgatggctgttcagccattgcaagcagccagcatgtcgatctaagttct
ctttacaaatggaacccggccattaagaccgactgctctggctcttcaagcaagtgtttacgtctgcatcggaatt
ttaacgacatccatgtccaccacatccaaactgcccaccactacgtctaagccatctaccacctccaaaccgccc
actggcatcacgacacctacaccactcaaagcgggtatgggtcaagaactgtaataaattttacgatgtgcactcg
ggagacggctgttcggcgattgcaagtagccaaaagggtcaaccttagttcattctacctatggaatccagctgtc
aagacggattgctctggccttcaggccagcgtatttgtctgtatcggaactttaacgacatccatgtccaccacc
acatccaaactaccaccactacatctaagccatctactacctctaaaccaccactggcattataaacacctaca
cccatcaaaacgggtatgggtcaagaactgtaataaattttacgatgtgcactcgggagacggctgttcggcgatt
gcaagcagccaaaagggttaacctcagttcattctacctatggaatccagctgtcaagacggattgctctggctctt
caggccagcgtatttgtctgtgttggtgacagcgacaactacaacagctgccggcataacaacccctacgcccacc
cagagcggcatgggtgagcgggttgtaacaaattctacgacgtccacgcccgggatggctgttccgcaattgcaagc
agtcaaaaaatagctctatcttcgctgtataagtggaaatccggctgtgaagacggattgctctggccttcaagcg
agtgtatacatatgcatcggtgtgggaaatgctgccgctgctcgtgttacaggacatcatcatcatcatcat

6.1.4.2 Protein sequence of the secreted TAL6₄ including the His-tag

1DSIPSISPTG	IITPTPTQSG	MVSNCNKFYD	VHSNDGCSAI	ASSQHVDLSS	LYKWNPAIKT
61DCSGLQASVY	VCIGILTTSM	STTSKLPSTT	SKPSTTSKPP	TGITTPTPTQ	SGMVKNCNKF
121YDVHSGDGCS	AIASSQKVN	SSFYLNPAV	KTDCSGLQAS	VFVCIGTLTT	SMSTTTSKLP
181TTTTSKPTTS	KPPTGIITPT	PTQNGMVKNC	NKFYDVHSGD	GCSAIASSQK	VNLSSFYLN
241PAVKTDCSGL	QASVFVCVGT	ATTTTAAGIT	TPTPTQSGMV	SGCNKFYDVH	AGDGCSAIAS
301SQKIALSSLY	KWNPAVKTDC	SGLQASVYIC	IGVGNAAAAR	VTGHHHHHH	

7. References

1. **Persoon, C.H.**, *Disposita Methodica Fungorum in Classes, Ordines, Familias et Genera*. Römer's Neues Magazin für die Botanik, Ziegler und Söhne, Zürich, 1974: p. 63-128.
2. **Bisby, G.R.**, *Trichoderma viride Pers ex Fries, and notes on Hypocrea*. Trans. Br. Mycol.Soc.23, 1939: p. 149-168.
3. **Kullnig, C.M., et al.**, *Confusion abounds over identities of Trichoderma biocontrol isolates*. . Mycology Res 105, 2001: p. 769-772.
4. **Rifai, M.A.**, *A revision of the genus Trichoderma*. . Mycol. Pap. 116, 1969: p. 1-56.
5. **Bissett, J.**, *A revision of the genus Trichoderma I- IV*. Canadian Journal of Botany, 1984-1992.
6. **Rehner, S.**, *Molecular systematics of the Hypocreale: A telemorph gene phylogeny and the status of their anamorphs*. Can. J. Bot.73 1995: p. 816-823.
7. **Tulasne, L.R.**, *Selecta fungorum carpologia 3*. 1865: p. 27- 35.
8. **Kubicek, C.P., M. Komon-Zelazowska, and I.S. Druzhinina**, *Fungal genus Hypocrea/Trichoderma: from barcodes to biodiversity*. Journal of Zhejiang University. Science. B, 2008. 9: p. 753-63.
9. **Martinez, D., et al.**, *Genome sequencing and analysis of the biomass-degrading fungus Trichoderma reesei (syn. Hypocrea jecorina)*. Nature biotechnology, 2008. 26: p. 553-60.
10. **Kubicek, C.P., et al.**, *Comparative genome sequence analysis underscores mycoparasitism as the ancestral life style of Trichoderma*. Genome biology, 2011. 12: p. R40.
11. **Druzhinina, I.S. & C.P. Kubicek**, *The first 100 Trichoderma species characterized by molecular data*. Mycoscience 47, 2006: p. 55-64.
12. **Druzhinina, I.S., et al.**, *Trichoderma: the genomics of opportunistic success*. Nature reviews. Microbiology, 2011. 9: p. 749-59.
13. **Harman, G.E., et al.**, *Trichoderma species--opportunistic, avirulent plant symbionts*. Nature reviews. Microbiology, 2004. 2: p. 43-56.
14. **Weindling, R.**, *Trichoderma lignorum as a parasite of other fungi*. Phytopathology 22, 1932: p. 837-845.
15. **Walsh, T.J., et al.**, *Infections due to emerging and uncommon medically important fungal pathogens*. Clinical microbiology and infection : the official publication of the

- European Society of Clinical Microbiology and Infectious Diseases, 2004. 10 Suppl 1: p. 48-66.
16. **Kredics, L., et al.**, *Molecular identification of Trichoderma species associated with Pleurotus ostreatus and natural substrates of the oyster mushroom*. FEMS microbiology letters, 2009. 300: p. 58-67.
 17. **Seaby, D.**, *Trichoderma as a weed mould or pathogen in mushroom cultivation*. in: Harmann, G.E.; Kubicek, C.P. (eds) *Trichoderma and Gliocladium*. Taylor and Francis, London, 1998: p. 267-288.
 18. **Sinden, J.H.**, *Nature and control of three mildew diseases of mushrooms in America*. Mushroom Sci. 2, 1953: p. 177-180.
 19. **Karsten, P.A.**, *Finlands mögelsvamper (Hyphomycetes fennici)*. Helsinki. 1892: p. 192.
 20. **Bissett, J.**, *A revision of the genus Trichoderma. III. Section Pachybasium*. Can. J. Bot. 69, 1991: p. 2372–2417.
 21. **Samuels, G.J., et al.**, *Trichoderma species associated with the green mold epidemic of commercially grown Agaricus bisporus*. Mycologia, 2002. 94: p. 146-70.
 22. **McBeath, J.H. et al.**, Sun, M., *Evaluation of Trichoderma atroviride in controlling Rhizoctonia solani under potato field conditions in Montana*. . Phytopathology 85, 1995: p. 1153.
 23. **Roberti, R. et al.**, *Evaluation of biological seed treatment of wheat for the control of seed-borne Fusarium culmorum*. J Plant Dis Prot 107, 2000: p. 484–493.
 24. **Lorito, M., et al.**, *Translational research on Trichoderma: from 'omics to the field*. Annual review of phytopathology, 2010. 48: p. 395-417.
 25. **Nicholson, G.M.**, *Fighting the global pest problem: preface to the special Toxicon issue on insecticidal toxins and their potential for insect pest control*. Toxicon : official journal of the International Society on Toxinology, 2007. 49: p. 413-22.
 26. **Council, E.F.I.**, *Die Grundlagen- Landwirtschaft*. 2006.
 27. **Attaran, A., et al.**, *Balancing risks on the backs of the poor*. Nature medicine, 2000. 6: p. 729-31.
 28. **Cook, R.J. & K.F. Baker**, *The nature and practice of biological control of plant pathogens*. American Phytopathological Society, St. Paul, NM, 1983.
 29. **Hoitink, H.A.J. et al.**, *Mechanisms of suppression of soilborne plant pathogens in compost- amendment substrates*. in: Hoitink, H.A.J; Keener, H.M., eds. *Science and*

- engineering of Composting. Design, Environmental, Microbiological and utilization Aspects. Worthington, OH: Renaissance, 1993: p. 601-621.
30. **Tuzun, S.K., et al.**, *Potential application of plant growth- promoting rhizobacteria to induce systemic disease resistance.* in : Reuveni, R.; ed. Novel Approaches to Integrated Pest Management. Boca Raton, FL: CRC Press, 1995: p. 115-117.
31. **Kloepper, J. et al.**, *Free- living bacterial inocula for enhancing crop productivity.* Trends Biotech 7, 1989: p. 39-43.
32. **Baker, R.G. et al.**, *Molecular strategies for biological control of fungal plant pathogens.* in: Reuveni, R.(ed) Novel approaches to integrated pest management. Lewis, CRC Press, Boca Raton, 369pp, 1995.
33. **Reithner, B. et al.**, *The G protein I subunit Tga1 of Trichoderma atroviride is involved in chitinase formation and differential production of antifungal metabolites.* Fungal Genet. Biol., 2004. 42: p. 749- 760.
34. **Matarese, F., et al.**, *Biocontrol of Fusarium head blight: interactions between Trichoderma and mycotoxigenic Fusarium.* Microbiology, 2012. 158: p. 98-106.
35. **Benitez, T., et al.**, *Biocontrol mechanisms of Trichoderma strains.* International microbiology : the official journal of the Spanish Society for Microbiology, 2004. 7: p. 249-60.
36. **Barnett, H.L. & F.L. Binder**, *The fungal host- parasite relationship.* Annu. Rev. Phytopathol 11, 1973: p. 273-292.
37. **Elad, Y. & I. Chet**, *Use of Trichoderma harzianum in combination or alternation with fungicides to control cucumber gray mould (Botrytis cinerea) under commercial greenhouse conditions.* Plant Pathol. 42, 1993: p. 324-332.
38. **Guetsky, R., et al.**, *Combining biocontrol agents to reduce the variability of biological control.* Phytopathology, 2001. 91: p. 621-7.
39. **Meyer, S.L. & D.P. Roberts**, *Combinations of biocontrol agents for management of plant-parasitic nematodes and soilborne plant-pathogenic fungi.* Journal of nematology, 2002. 34: p. 1-8.
40. **Berg, G.,** *Plant-microbe interactions promoting plant growth and health: perspectives for controlled use of microorganisms in agriculture.* Applied microbiology and biotechnology, 2009. 84: p. 11-8.
41. **Paulitz, T.C. & R.R. Belanger**, *Biological control in greenhouse systems.* Annual review of phytopathology, 2001. 39: p. 103-33.

42. **Freeman, Stanley et al.**, *Trichoderma biocontrol of Colletotrichum acutatum and Botrytis cinerea and survival in strawberry*. Eur. J. Plant Pathol. 110, 2004: p. 361-370.
43. **Fravel, D.R.**, *Commercial biocontrol products for use against soilborne crop disease*. USDA ARS Biocontrol of Plant Diseases Laboratory: Commercial Biocontrol Products [online], 2000.
44. **Weindling, R.**, *Studies on lethal principle effective in the parasitic action of Trichoderma lignorum on Rhizoctonia solani and other soil fungi*. Phytopathology 24, 1934.
45. **Bigirimana, J. et al.**, *Induction on systemic resistance on bean (Phaseolus vulgaris) by Trichoderma and Gliocladium*. Med. Fac. Landbouww. Univ. Gent, 1997. 62: p. 1001-1007.
46. **Harman, G.E.**, *Overview of Mechanisms and Uses of Trichoderma spp.* Phytopathology, 2006. 96: p. 190-4.
47. **Latge, J.P.**, *The cell wall: a carbohydrate armour for the fungal cell*. Molecular microbiology, 2007. 66: p. 279-90.
48. **Tharanathan, R.N. & F.S. Kittur**, *Chitin--the undisputed biomolecule of great potential*. Critical reviews in food science and nutrition, 2003. 43: p. 61-87.
49. **Aam, B.B., et al.**, *Production of chitooligosaccharides and their potential applications in medicine*. Marine drugs, 2010. 8: p. 1482-517.
50. **Campbell, J.A., et al.**, *A classification of nucleotide-diphospho-sugar glycosyltransferases based on amino acid sequence similarities*. The Biochemical journal, 1998. 329: p. 719.
51. **Markovich, N.A.**, *Lytic enzymes of Trichoderma and their role in plant defense from fungal diseases: a review*. Applied Biochemistry and Microbiology, 2003. 39:p 341-351.
52. **Ait-Lahsen, H., et al.**, *An antifungal exo-alpha-1,3-glucanase (AGN13.1) from the biocontrol fungus Trichoderma harzianum*. Applied and environmental microbiology, 2001. 67: p. 5833-9.
53. **Zimad, G. et al.**, *Effect of two isolates of Trichoderma harzianum on the activity of hydrolytic enzymes produced by Botrytis cinerea*. Physiological and Molecular Plant Pathology, 1998. 52: p. 127-137.

54. **Mendoza-Mendoza, A., et al.,** *Enhanced biocontrol activity of Trichoderma through inactivation of a mitogen-activated protein kinase*. Proceedings of the National Academy of Sciences of the United States of America, 2003. 100: p. 15965-70.
55. **Seidl, V., et al.,** *Transcriptomic response of the mycoparasitic fungus Trichoderma atroviride to the presence of a fungal prey*. BMC genomics, 2009. 10: p. 567.
56. **Suarez, B., et al.,** *Isolation and characterization of PRA1, a trypsin-like protease from the biocontrol agent Trichoderma harzianum CECT 2413 displaying nematocidal activity*. Applied microbiology and biotechnology, 2004. 65: p. 46-55.
57. **Lopez-Mondejar, R., et al.,** *The beta-N-acetylglucosaminidases NAG1 and NAG2 are essential for growth of Trichoderma atroviride on chitin*. The FEBS journal, 2009. 276: p. 5137-48.
58. **Neuhaus, J.-M. et al.,** *A revised nomenclature for chitinase genes*. Plant Molecular Biology Reporter, 1996. 14: p. 102-104.
59. **Fukamizo, T.,** *Chitinolytic enzymes: catalysis, substrate binding, and their application*. Current protein & peptide science, 2000. 1: p. 105-24.
60. **Seidl, V., et al.,** *A complete survey of Trichoderma chitinases reveals three distinct subgroups of family 18 chitinases*. The FEBS journal, 2005. 272: p. 5923-39.
61. **Seidl, V.,** *Chitinases of filamentous fungi: a large group of diverse proteins with multiple physiological functions*. The British Mycological Society, 2008.
62. **Horn, S.J., et al.,** *Endo/exo mechanism and processivity of family 18 chitinases produced by Serratia marcescens*. The FEBS journal, 2006. 273: p. 491-503.
63. **Gruber, S., et al.,** *Analysis of subgroup C of fungal chitinases containing chitin-binding and LysM modules in the mycoparasite Trichoderma atroviride*. Glycobiology, 2011. 21: p. 122-33.
64. **Karlsson, M. & J. Stenlid,** *Evolution of family 18 glycoside hydrolases: diversity, domain structures and phylogenetic relationships*. Journal of molecular microbiology and biotechnology, 2009. 16: p. 208-23.
65. **Boraston, A.B., et al.,** *Carbohydrate-binding modules: fine-tuning polysaccharide recognition*. The Biochemical journal, 2004. 382: p. 769-81.
66. **Garvey, K.J., et al.,** *Nucleotide sequence of Bacillus phage phi 29 genes 14 and 15: homology of gene 15 with other phage lysozymes*. Nucleic acids research, 1986. 14: p. 10001-8.
67. **Buist, G., et al.,** *LysM, a widely distributed protein motif for binding to (peptido)glycans*. Molecular microbiology, 2008. **68**: p. 838-47.

68. **Bateman, A. & M. Bycroft**, *The structure of a LysM domain from E. coli membrane-bound lytic murein transglycosylase D (MltD)*. Journal of molecular biology, 2000. 299: p. 1113-9.
69. **Ohnuma, T., et al.**, *LysM domains from Pteris ryukyuensis chitinase-A: a stability study and characterization of the chitin-binding site*. The Journal of biological chemistry, 2008. 283: p. 5178-87.
70. **Iizasa, E. et al.**, *Direct binding of a plant LysM receptor-like kinase, LysM RLK1/CERK1, to chitin in vitro*. The Journal of biological chemistry, 2010. 285: p. 2996-3004.
71. **Petutschnig, E.K., et al.**, *The lysin motif receptor-like kinase (LysM-RLK) CERK1 is a major chitin-binding protein in Arabidopsis thaliana and subject to chitin-induced phosphorylation*. The Journal of biological chemistry, 2010. 285: p. 28902-11.
72. **Ponting, C.P., et al.**, *Eukaryotic signalling domain homologues in archaea and bacteria. Ancient ancestry and horizontal gene transfer*. Journal of molecular biology, 1999. 289: p. 729-45.
73. **de Jonge, R. & B.P. Thomma**, *Fungal LysM effectors: extinguishers of host immunity?* Trends in microbiology, 2009. 17: p. 151-7.
74. **Pazzagli, L., et al.**, *Purification, characterization, and amino acid sequence of cerato-platanin, a new phytotoxic protein from Ceratocystis fimbriata f. sp. platani*. The Journal of biological chemistry, 1999. 274: p. 24959-64.
75. **Boddi, S., et al.**, *Cerato-platanin protein is located in the cell walls of ascospores, conidia and hyphae of Ceratocystis fimbriata f. sp. platani*. FEMS microbiology letters, 2004. 233: p. 341-6.
76. **Kubicek, C.P., et al.**, *Purifying selection and birth-and-death evolution in the class II hydrophobin gene families of the ascomycete Trichoderma/Hypocrea*. BMC evolutionary biology, 2008. 8: p. 4.
77. **Djonovic, S., et al.**, *Sml1, a proteinaceous elicitor secreted by the biocontrol fungus Trichoderma virens induces plant defense responses and systemic resistance*. Molecular plant-microbe interactions : MPMI, 2006. 19: p. 838-53.
78. **Seidl, V., et al.**, *Epl1, the major secreted protein of Hypocrea atroviridis on glucose, is a member of a strongly conserved protein family comprising plant defense response elicitors*. The FEBS journal, 2006. 273: p. 4346-59.

79. **Vargas, W.A., et al.**, *Dimerization controls the activity of fungal elicitors that trigger systemic resistance in plants*. The Journal of biological chemistry, 2008. 283: p. 19804-15.
80. **Lin-Cereghino, J., et al.**, *Condensed protocol for competent cell preparation and transformation of the methylotrophic yeast Pichia pastoris*. BioTechniques, 2005. 38: p. 44, 46, 48.
81. **Thor, D., et al.**, *Cloning and characterization of the Pichia pastoris MET2 gene as a selectable marker*. FEMS yeast research, 2005. 5: p. 935-42.
82. **Mandels, M. & R. ,Andreotti**, *Problems and challenges in the cellulose to cellulase fermentation*. Proc Biochem 1978. 13: p. 6-13.
83. **Wessel, D. et al.**, *A method for the quantitative recovery of protein in dilute solution in the presence of detergents and lipids*. Analytical Biochemistry, 1984. 138: p. 141-143.
84. **Sambrook, J. & D.W. Russell**, *SDS-Polyacrylamide Gel Electrophoresis of Proteins*. CSH protocols, 2006. 2006.
85. **Roberts. W. K. & Selitrennikoff, C. P**, *Plant and bacterial chitinases differ in antifungal activity*. J. Gen. Microbiol., 1988. 134: p. 169-176.
86. **Gruber, S. et al.**, *Differential regulation of orthologous chitinase genes in mycoparasitic Trichoderma species*. Applied and environmental microbiology, 2011. 77: p. 7217-26.
87. **Zdobnov, E.M. et al.**, *InterProScan-an integration platform for the signature-recognition methods in InterPro*. Bioinformatics, 2001. 17: p. 847-8.
88. **Joris, B., et al.**, *Modular design of the Enterococcus hirae muramidase-2 and Streptococcus faecalis autolysin*. FEMS microbiology letters, 1992. 70: p. 257-64.
89. **Cregg, J.M., et al.**, *Recombinant protein expression in Pichia pastoris*. Molecular biotechnology, 2000. 16: p. 23-52.
90. **Hohenblum, H. et al.**, *Effects on gene dosage, promoters, and substrates on unfolded protein stress of recombinant Pichia pastoris*. Wiley Periodicals, 2003. 10.
91. **Gruber, S. & V. Seidl-Seiboth**, *Self vs. non-self: Fungal cell wall degradation in Trichoderma*. Microbiology, 2011.
92. **de Oliveira, A.L., et al.**, *The structure of the elicitor Cerato-platanin (CP), the first member of the CP fungal protein family, reveals a double psibeta-barrel fold and carbohydrate binding*. The Journal of biological chemistry, 2011. 286: p. 17560-8.

93. **Knogge, W. & D. Scheel**, *LysM receptors recognize friend and foe*. Proceedings of the National Academy of Sciences of the United States of America, 2006. 103: p. 10829-30.
94. **Mulder, L., et al.**, *LysM domains of Medicago truncatula NFP protein involved in Nod factor perception. Glycosylation state, molecular modeling and docking of chitooligosaccharides and Nod factors*. Glycobiology, 2006. 16: p. 801-9.
95. **Ganesh Rham R. Visweswaran, et al.**, *A genetically engineered protein domain binding to bacterial murein, archaeal pseudomurein, and fungal chitin cell wall material*. Applied Microbiol Biotechnol, 2011.
96. **Mentlak, T.A., et al.**, *Effector-mediated suppression of chitin-triggered immunity by magnaporthe oryzae is necessary for rice blast disease*. The Plant cell, 2012. 24: p. 322-35.
97. **de Jonge, R., et al.**, *Conserved fungal LysM effector Ecp6 prevents chitin-triggered immunity in plants*. Science, 2010. 329: p. 953-5.
98. **Hartl, L. et al.**, *Fungal chitinases: diversity, mechanistic properties and biotechnological potential*. Applied microbiology and biotechnology, 2012. 93: p. 533-43.
99. **Cereghino, J.L. & J.M. Cregg**, *Heterologous protein expression in the methylotrophic yeast Pichia pastoris*. FEMS microbiology reviews, 2000. 24: p. 45-66.
100. **Wang, J.-Y. et al.**, *Immobilization of Cells with Surface- Displayed Chitin- Binding Domain*. Applied and environmental microbiology, 2005. 72: p. 927-931.
101. **Shimojoh, M.**, *Preparation and characteristics of reprecipitated chitin: a new morphological form easy to manipulate with versatile utility*. Polym. Bull., 2011. 67: p. 1435-1441.
102. **Gottlieb, D.**, *The physiology of spore germination in fungi*. 1950. XVI, No.5.
103. **Ugalde, U.**, *Autoregulatory signals in mycelial fungi*. Mycota I (Growth, Differentiation and Sexuality).
104. **Chitarra, G.S.**, *Doctoral thesis*. 2003.
105. **Woo, S.L. et al.**, *Disruption of the ech42 (Endochitinase- Encoding) Gene Affects Biocontrol Activity in Trichoderma harzianum P1*. The American Phytopathological Society, 1999. 12: p. 419-429.

106. **Bacelli, I.C. et al.**, *The expression of the cerato-platanin gene is related to hyphal growth and chlamydospores formation in Ceratocystis platani*. FEMS microbiology letters, 2011. 11.

CURRICULUM VITAE

Date of birth	30th of October, 1981
Place of birth	Graz, Austria
Nationality	Austrian

EDUCATION

Since October 2011	Marketing and Sales Coordinator (DSM Fine Chemicals)
October 2008-2011	PhD thesis at Vienna University of Technology
May 2007- May 2008	Institute of Gastroenterology, „Klinikum rechts der Isar“, Munich University of Technology
May 2007	Final examination (Dipl.-Ing. Technische Chemie)
April 2006- April 2007	Diploma thesis at the Institute of Molecular Biotechnology at Graz University of Technology Supervisor: Univ. Prof. Dr. Anton Glieder Industrial partner: Biocatalytics Project title: <i>Cloning and expression of novel cytochrome P450 enzymes</i>
2000-2006	Graz University of Technology, Faculty of technical chemistry

SCHOOLING

June 2000	Higher School Certificate
1992- 2000	Bundesgymnasium und Bundesrealgymnasium Seebachergasse, Graz Austria (secondary school)
1988- 1992	Volksschule Berliner Ring , Graz Austria (primary school)

List of publications

Research Paper:

Hartl, L., S. Zach, & V. Seidl-Seiboth, Fungal chitinases: diversity, mechanistic properties and biotechnological potential. *Applied microbiology and biotechnology*, **2012**. 93(2): p. 533-43.

Matthias Schittmayer, Anton Glieder, Michael K. Uhl, Andreas Winkler, Simone Zach, Jörg H. Schrittwieser, Wolfgang Kroutil, Peter Macheroux, Karl Gruber, Spiros Kambourakis, J. David Rozzell, Margit Winkler; Old Yellow Enzyme catalyzed dehydrogenation of saturated ketones. *Advanced Synthesis and Catalysis*, 2011. 353: p. 268-274.

Other scientific publications:

Posters:

VAAM 09- Molecular Biology of Fungi

27th- 30th of September 2009

Title: Development of a reusable selection marker system for multiple gene knockouts in *Trichoderma atroviride*

Author: Simone Zach, Christian P. Kubicek, Verena Seidl

Lisa Circle

16th of October 2006

Title: *Engineered Nitrilases and Cytochrome P450 Enzymes*

Author: Anton Glieder, Bianca Hecher, Hannelore Mandl, Matthias Schittmayer, Ulrike Schreiner, Mandy Vink, Simone Zach, David Rozzell

8th International Symposium on Cytochrome P450 Biodiversity and Biotechnology

July 23rd- 27th 2006

University of Wales Swansea

Medical School

Title: *The Mutein Database (muteindb)*

Author: Michael Guggemos, Gerhard Thallinger, Simone Zach, Vincent Rabin, Anton Glieder

Research Experience

II. Medical Department of the „Klinikum rechts der Isar“, Technical University Munich

During this internship I worked within the group of Dr. Florian Greten, who focused on investigating the role of the IKK/NF-kappaB signaling pathway with particular focus on tumorigenesis of different cell types in sporadic and colitis associated colon carcinoma. I was interested in the expression profiles of cytokines and growth factors of macrophages which are responsible for paracrine signal transduction during acute and chronic inflammation in a mouse model of colitis associated cancer. Therefore, I isolated and characterized bone marrow-, peritoneum- and intestinal mucosa derived macrophages from mice, which had a deletion of IKK β in myeloid cells (IKK $\beta^{\Delta mye}$) after an ex vivo stimulation.

In addition I was involved in the investigation of the role of macrophages in a mouse model of sporadic colon cancer.

Members of the project: 1

Supervisor: Dr. Florian Greten/ Institute of Gastroenterology

Period: May 2007 – May 2008

Lang Sumah CryoTech GmbH & Co KEG/ Institute of Biotechnology, Technical University Graz

This project was a cooperation work between the company CryoTech and the Institute of Biotechnology TU Graz. In the course of this project my task was to isolate and characterize unknown microbial DNA. Furthermore I developed different strategies to prevent objectionable microbial growth. That was a great challenge for me due to the non typical materials, which are used by the company and which had to be taken into account by creating different sterilizing methods.

Members of the project: 1

Supervisor: Univ. Prof. Dr. Walter Steiner/ Institute of Biotechnology

Cooperation Partner: Cryotech GmbH & Co KEG

Period: September- December 2006

Research Centre Applied Biocatalysis

During this project my task was to clone and purify a sulfite reductase of microbial origin. First I did an *in silico* screening of databases and then designed the primers for the sulfite reductase. For cloning I used a new vector system, which first had been created. Moreover I developed a strain to express the domain of the reductase in *E.coli*.

Members of the project: 3

Supervisor: Univ. Prof. Dr. Anton Glieder/ Institute of Molecular Biotechnology

Period: April – June 2006

Institute of Environmental Biotechnology, Technical University Graz

In this project I was involved in the investigation of different substrates used to react with several bacterial Laccases. A second task of this project was to create a continuous reactor, to ascertain that Laccases are spore- bound.

Members of the project: 4

Supervisor: Univ. Prof. Dr. Georg Gübitz/ Institute of Environmental Biotechnology

Period: September – October 2005

Danksagung

Mein Dank gilt Christian P. Kubicek, der mir dieses interessante Thema zur Verfügung gestellt hat und immer bereit war Hilfestellungen und nützliche Tipps zu geben.

Besonders herzlich möchte ich mich bei Verena Seidl-Seiboth bedanken, die mich während meiner Arbeit betreut und mir positive Denkanstöße gegeben hat.

Weiters möchte ich mich bei allen Institutsmitarbeitern für eine kollegiale Zeit bedanken.

Meinen Eltern, Gertrude und Walter Zach, widme ich diese Arbeit, denn ihnen gilt mein größter Dank.